

## ROBOTIC WALKING TRAINING DEVICE



Apr. 24<sup>th</sup>, 2020

Final Report – Tyler Team 4 (TYL4)

Team Members: Ryley Tharp, Will Clinton, Alex Craig, Heather McIntyre, Chris Whitton

Faculty Advisor: Dr. Chung Hyun Goh

Department of Mechanical Engineering

Sponsors: Department of Nursing and Health Sciences and Department of Health and kinesiology at UT Tyler

## Acknowledgements

The members of the Tyler Team 4 would like to thank Dr. Yong Tai Wang and Dr. X. Neil Dong for their support as sponsors and for their input and ideas on the designing of this project. We would also like to thank Dr. Chung Hyun Goh for being our advisor and guiding us in the right direction, providing valuable feedback and expertise. Lastly, we would like Ed Farina for all the help and advice given when we were working in the Fabrication Lab.

## Nomenclature

- S.C.I. - Spinal Cord Injury
- FES - Functional Electronic Stimulation
- RWTD. - Robotic Walking Training Device
- FEA - Finite Element Analysis
- FHCS - Flat Head Counter-Sunk
- O.D - Outer Diameter
- SHCS - Socket Head Cap Screw
- UHMW - Ultra High Molecular Weight
- PWM - Pulse Width Modulation
- VIN - Voltage In
- GND - Ground
- I/O - Input/Output
- Qty - Quantity
- PPU - Price Per Unit
- PPS-Pulses per second
- SOOW-S=Service Cord, OO=Oil resistant both inside insulation and outside jacket,  
W=weather/water resistance

## Executive Summary

Physical rehabilitation is a necessary step in regaining lower body function after a partial paralysis caused by a spinal cord injury (S.C.I) or a stroke. As such, patients undergo physical therapy guided by a physical therapist to help regain lower body function. Currently, this rehabilitation is predominantly conducted by suspending the patient in a harness over a treadmill or a floor while a physical therapist moves the lower limbs in a set trajectory. Thus, the focus of this project is to build and optimize a training device that uses linkages to accurately recreate the motion of the ankle and knee in a gait cycle, and to electrically stimulate the appropriate muscle groups that function for such movement with the goal of rehabilitation for individuals with minor spinal cord injuries or who are victims of a stroke.

This final report seeks to detail the design and material selected for the device. Contained herein are detailed calculations, feasibility analysis and renderings of the Robotic Walking Training Device (RWTD), as well as all the pertinent electronic components and selection criteria for all parts. Further details of the Functional Electronic Stimulator (FES) and waveforms typically used for therapeutic purposes. The budget, Bill of Materials, timeline, and test & evaluation plan among other documents are included. The goal of the team after presenting this final report is to demonstrate the RWTD is able to meet all specifications required by the sponsors.

# Table of Contents

Acknowledgements .....	i
Nomenclature .....	ii
Executive Summary .....	iii
Introduction.....	1
Requirements and Specifications .....	2
Constraints .....	3
Applicable Standards.....	4
Final Design .....	5
Safety .....	7
Motion Analysis .....	8
Final System .....	11
Scissor Lift.....	11
Arm Support.....	14
Leg Assembly.....	16
Electronics for the Leg Assembly.....	17
FES System.....	20
Electrotherapy Modulation .....	21
Final Design Calculation Results .....	25
Feasibility Analysis .....	26
Mechanical .....	26
Electrical .....	28
Risk Assessment.....	30
Failure Mode and Effects Analysis .....	32
Finite Element Analysis.....	33
Final Testing Results .....	35
Plan to Compare Simulation vs. Actual Testing Results .....	36
Bill of Materials .....	38
Budget.....	44
Economic feasibility.....	45
Target Market & Competition.....	45
Cost of Prototype.....	47
Cost of Mass Production.....	47
Flowcharts of Software.....	49

Electrical Design Flowchart .....	49
Program Flowchart .....	51
Final Acceptance Criteria .....	53
Timeline and Milestones.....	54
Discussion.....	55
Testing of Motors .....	55
Future Construction.....	55
Challenges.....	56
Recommendations .....	56
Conclusion .....	57
References.....	58
Appendix A.....	59
Appendix B.....	60
Appendix C.....	63
Appendix D.....	64
Appendix E.....	65
Appendix E1 .....	65
Appendix E.2 .....	67
Appendix E.3 .....	68
Appendix E.4 .....	69
Appendix E.5 .....	70
Appendix E.6 .....	71
Appendix E.7 .....	73
Appendix F .....	76
Appendix G.....	77
Appendix H.....	78
Appendix J.....	79
Appendix K.....	81
Appendix L .....	87
Appendix L.1 .....	88
Appendix L.2 .....	105
Appendix M.....	106
Appendix N.....	108
Appendix N.1 .....	108
Appendix N.2.....	111

Appendix N.3.....	121
Appendix N.4.....	125
Appendix O.....	139
Appendix P.....	142
Appendix Q.....	147
Appendix R.....	149

## Introduction

Two of the leading disabilities around the world are SCI and stroke. Approximately 795,000 people have a new or recurrent stroke annually, and it is estimated between 232,000 and 316,000 people have a SCI. Strokes and SCI can lead to paralysis of the lower limbs. More than 50% of people who have had a stroke have difficulty walking, while more than 90% of SCI patients lose their sensory and motor control of their lower limbs. To help patients who have these disabilities regain the function of walking unassisted, gait rehabilitation is performed. Currently, the predominant form of rehabilitation is suspending the patient in a harness over a treadmill or a floor while a robotic arm moves the lower limbs in a set trajectory. The key aspect of this design is the repetitiveness of the task but lacks muscular stimulation to provide neurological reinforcement. Furthermore, this method is physically taxing for therapists; to ease their labor input, Robotic Assisted Gait Rehabilitation systems have been produced. [1] To help provide muscular stimulation to provide neurological reinforcement a Functional Electrical Stimulation device can be used. The FES applies small electrical pulses to the muscles in the lower extremities that are affected by injuries to restore or improve muscular function. By applying these small electrical pulses, the pathways that have been disrupted or broken can be re-written allowing for the patient to use their muscles as they did before the injury occurred. [2]

Currently, a device does not exist that can accurately recreate the human gait path motion of the knee and ankle at the same time, as well as provide electric stimulation. The purpose of our project is to build and optimize a training device that accurately recreates the motion in a gait cycle with the goal of rehabilitation for individuals with minor spinal cord injuries or who are victims of a stroke. We will be using a combination of a mechanical movement to recreate the gait motion path of the ankle and knee and electrical stimulation to reinforce neurological pathways. An adjustable linkage system will be used to support the patient's legs, while a gear motor at each major joint will dictate the motion path. While the step is being taken, the FES will be used on the quadricep to stimulate the muscle in sync with the step, with future considerations for additional muscle groups. The combination of the RWTD and the FES will aid in rehabilitation at an accelerated rate than the utilization of the RWTD alone.



## Requirements and Specifications

Below is the table that lists the Requirements and specification for the RWTD device. The specifications were approved by the sponsors as seen in Appendix A.

Table 1. RWTD Requirements and Specifications.

Requirement	Validation Method	Metric
Reproduced natural gait path of knee and ankle within $\pm 10\%$	SolidWorks Motion to recreate path of the knee and the ankle using imported data from Vicon Motion Capture	N/A
Adjustable for varying leg lengths between 60-76 in.	Measure in SolidWorks Design to verify lengths are met	in.
Able to hold various body types between 120-300 lbs.	Perform FEA testing to verify device will hold 300 lbs.	lbs.
Electro-Stimulate thigh muscle in time with walking motion	Comparing the codes for both the motion path and the FES waves to verify they are timed correctly	secs.

## Constraints

Below is the table that lists the Constraints that the team encountered in the designing and building of the RWTD device.

Table 2. Constraints of the RWTD.

Constraints	
Type	Details
Funding	The project is limited to a budget of \$2000
Time	The device must be completed by April 20 <sup>th</sup> 2020
Production	Structural components will be fabricated in <u>          </u> and the University Fabrication Lab
Length	The length of the legs cannot be more than 76 in.
Materials	All materials used must be medical compatible
Weight	The weight of the legs must be less than 25 lbs.

## Applicable Standards

IEEE 1149.1-1990 JTAG, is a low-level interface designed to provide access to debugging facilities incorporated into an MCU or other logic device.

IEEE 1394- an interface standard for a serial bus for high-speed for high-speed communications and isochronous real-time data transfer.

IEEE 118.1-1990- Standard for Microcontroller System Serial Control Bus.

IEEE 1801-2013- Standard for Design and verification of Low-Power Integrated Circuits.

## Final Design

The Robotic Legs are mounted to an adjustable frame (scissor lift). The adjustable frame allows for the patient to easily enter the RWTD and be strapped into the device before it is moved into the necessary position. The robotic legs are adjustable to allow for the adjustability for patients of different heights. Adjustable arm supports are mounted to the sides of the frame and allow for adjustability for different sized patients. The arms also folded back to allow for easier access to enter the RWTD, then fold back down into position once the patient is in the device to allow for additional stability and support for the patient. The movement of the legs are driven by motors at each joint and a manufactured Pivot Pin. These motors are controlled by a central microcontroller which sends the programmed code to individual motor controllers. The motors contain integrated Hall encoders which provide pulse counts to individual microcontrollers, which in turn send these counts back to the central microcontroller where the program is checked, and the loop continues as dictated by the program code. The F.E.S is used in tandem with the robotic legs and sends pulses to corresponding thigh muscles when the muscle group would naturally be utilized. Foam padding is also utilized throughout the assembly to provide comfort, as well as provide minor natural flexion to facilitate a more accurate motion. A complete schematic of the device can be seen in Figure 1.

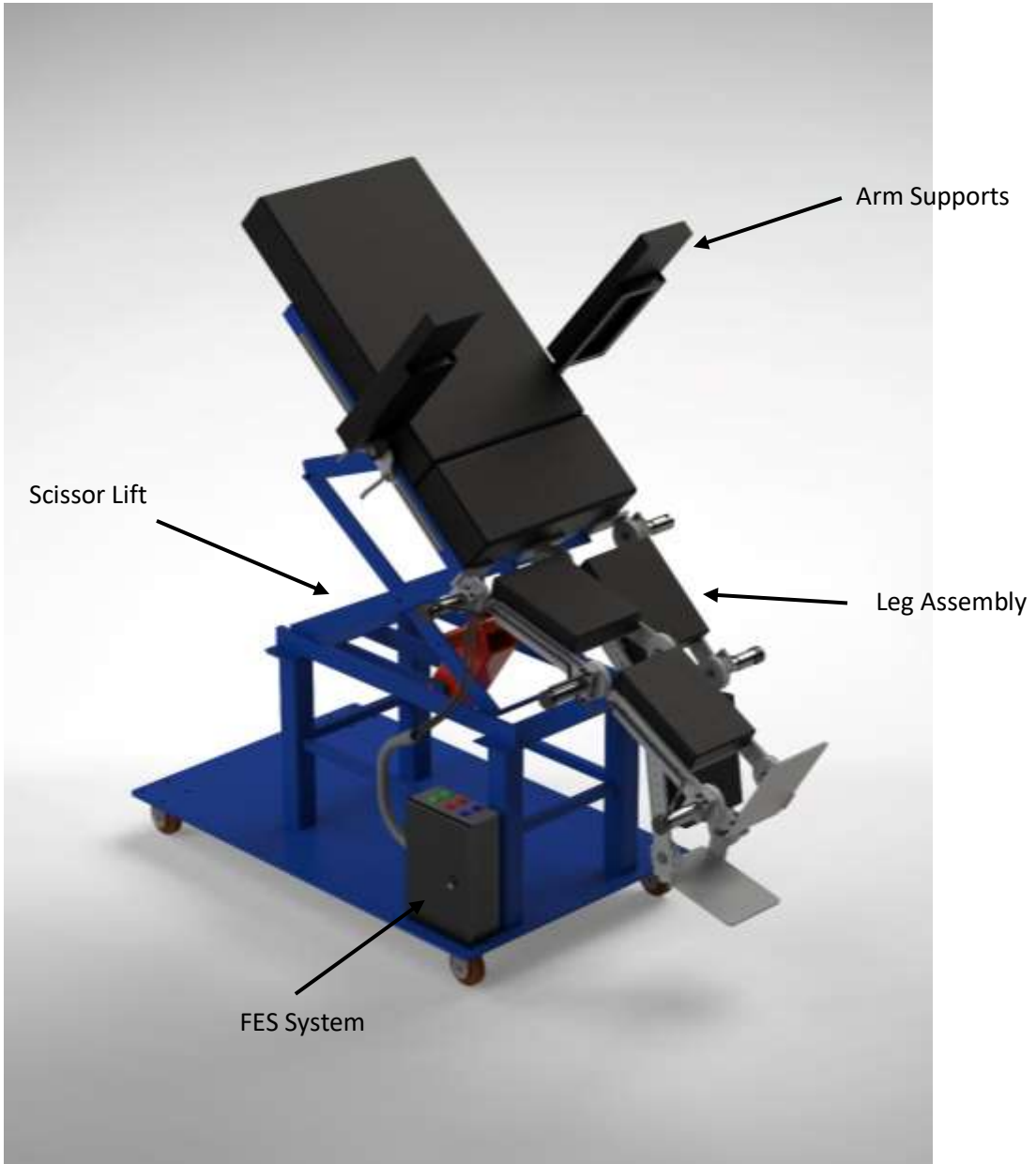


Figure 1. Complete assembly of the RWTD in the upright position.

## Safety

Careful consideration must be taken into account when designing therapeutic or rehabilitative devices; therefore, several aspects of safety were accounted for. Limit switches will be installed to provide an electronic safety, preventing the motor from continuing to drive the assembly beyond a specified degree of rotation. A “kill-switch” will be installed into the main controls which will serve to shut down the entire system instantly to prevent injury. Furthermore, straps along the abdomen and legs provides additional support for the patient and serves as holding straps to prevent the patient from falling out of the device.

The device stability was also analyzed to determine if the device had a possibility of tipping over when in use. To perform this analysis the global center of mass was used. The total mass of the assembly was 341.56 lb. this mass includes a patient weighing 300lb. The center of mass change was insignificant in the X and Y directions, however the Y- direction change was + 6in. when the scissor lift was raised as seen in Figure B.1 and B.2. As the force will be applied in this direction only, the system will remain stable and have a highly improbable chance of titling over during use. The raw data used to calculate the center of masses and the change can be found in Appendix B. Since this device is being used as a therapeutic or a rehabilitative device a decision was made to add extra stability by manufacturing a new base out of steel to move the center of mass closer to the ground as seen in Figure B.3. The new base weighs approximately 200 lb. The new base also allows extra space to storage the FES system and any other required electronic systems.

## Motion Analysis

The gait path in the device is created by the motors at each joint. The ankle motor generates the necessary dorsiflexion and plantarflexion used while taking a step. The knee motor generates the flexion and extension of the lower leg, while the hip motor generates the flexion and extension of the upper leg. The paths shown in Figure 2 and Figure 3 show the gait path of the ankle and knee respectively of a natural human walking. These paths were obtained by RTWD- 2<sup>nd</sup> Generation Team using Vicon Motion Capture Software and tracking nodes on a human subject then analyzed using Excel and the plot generated. The ankle gait path produces a tear-drop shape which can be recreated by motors. The knee gait path produces an infinity shape. However, this shape is impractical to reproduce on the RWTD as a majority of this path is produced due to the human legs contact with the ground while walking. Since the patients using this device will be suspended over the ground an arc path will be used.

To determine if the leg assembly could achieve the teardrop shape produced by the ankle. The data from Figure 4. was extrapolated by RTWD 3<sup>rd</sup> Generation Team and recreated in SolidWorks using Motion Study Analysis. The linkage design was shown to able to recreate the desired path as shown in Figure 4. The motion path data will be further used in the programming portion to time the motor movement correctly so that an accurate path will be generated in the final assembly. After construction of the assembly, an evaluation analysis will be performed to show that the actual path of the RTWD is within 10% of the natural motion path generated.

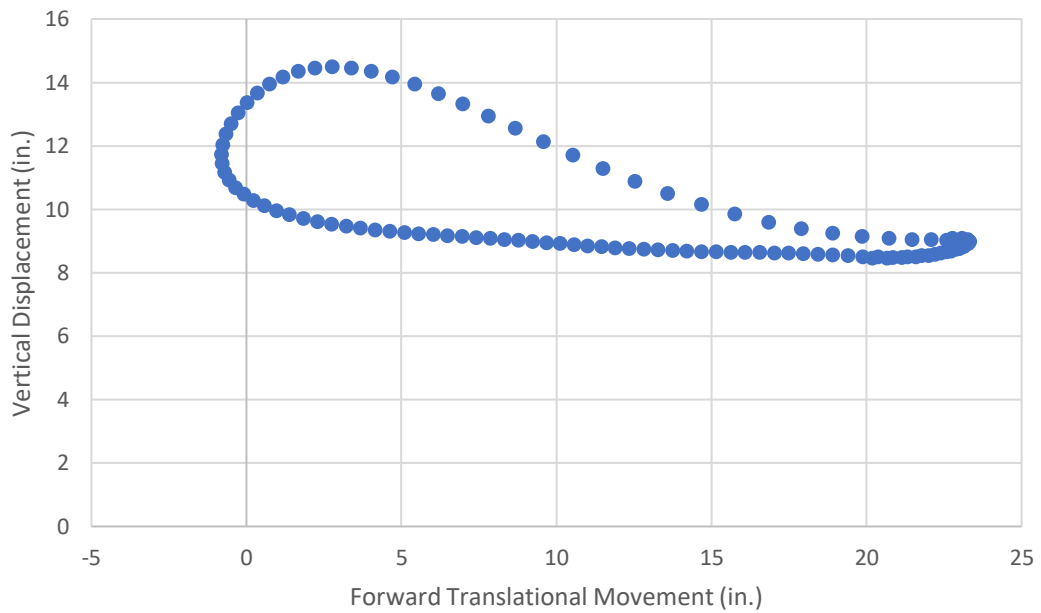


Figure 2. Vicon Motion Capture Analysis-Natural Gait Path of the Ankle.

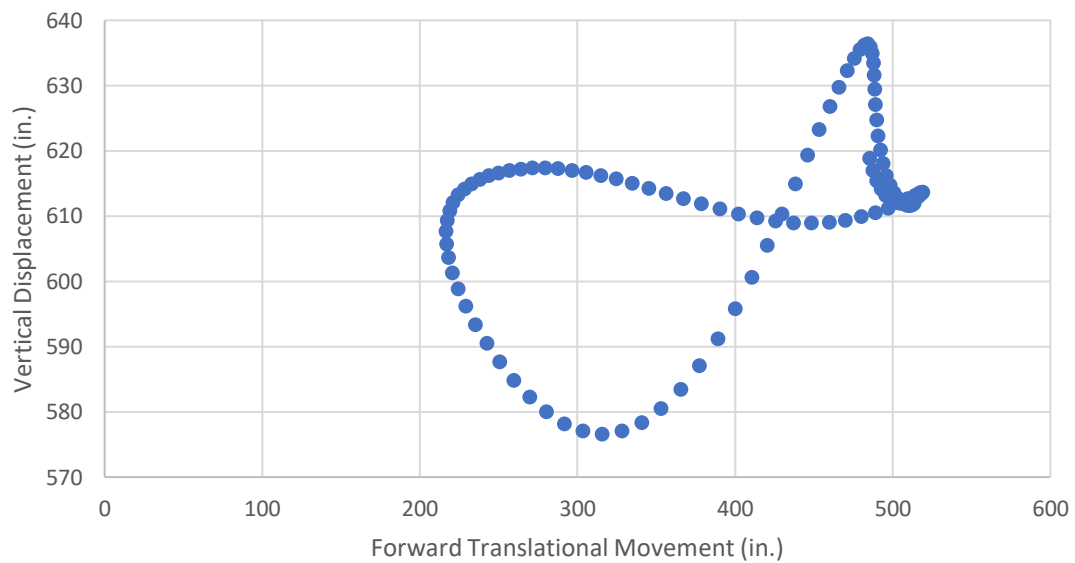


Figure 3. Vicon Motion Capture Analysis-Natural Gait Path of the Knee.





Figure 4. Designed Gait Path from SolidWorks.

## Final System

The RWTD has four main sub systems as seen in Figure 1. It consists of the Scissor Lift, Arm Supports, Leg Assembly and the FES System. A brief overview of the whole project can be seen in Appendix B.

### Scissor Lift

The scissor lift was utilized in the 2<sup>nd</sup> generation RWTD and serves as the frame for the 3<sup>rd</sup> Generation. It has a maximum load capacity of 600 lbs. and a maximum angle of 32°. The scissor lift provided the vertical motion necessary to raise the patient to optimal height and angle. A height of 39 in. allows the leg assembly to fully function without any interference from the floor or the base of the scissor lift. An angle of 31.175 ° is optimal as it allows for some of the patient's body weight to be used in the rehabilitation process. Figure 5 shows the scissor lift frame. Figure 6 and Figure 7 show the black box and functional diagram of the Scissor Lift subsystem respectively.



Figure 5. Scissor Lift-frame of 3rd generation RWTD.

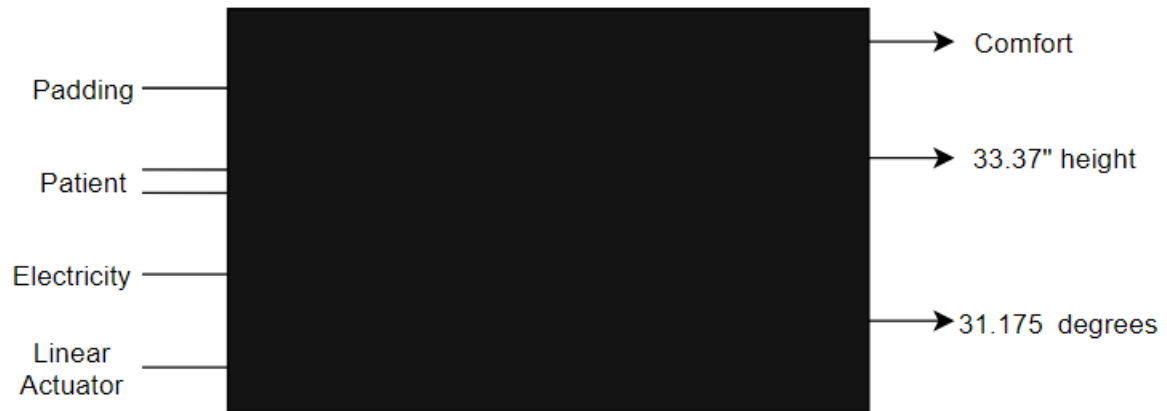


Figure 6. Black Box Diagram of the Scissor Lift.

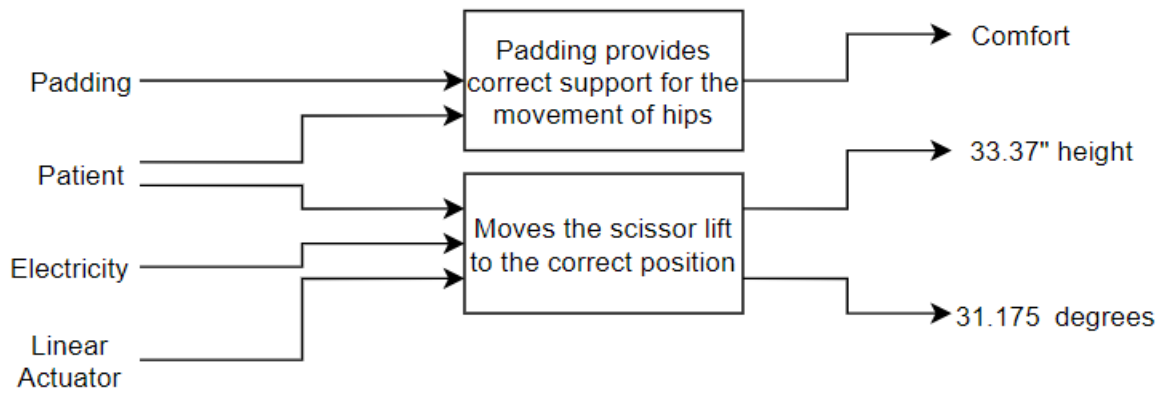


Figure 7. Functional Diagram of the Scissor Lift.

## Arm Support

The arm sub-assembly was utilized in the 2<sup>nd</sup> generation but was altered for its use in the 3<sup>rd</sup> generation. For the 3<sup>rd</sup> generation the arm sub-assembly was altered so the arms to be lifted up to allow the patient to be placed into a device with ease and then lowered down for when the device is in use. It also allows for the arm supports to be moved up and down to accommodate the patient while using the device. Figure 8 shows the arm supports. Figure 9 and Figure 10 show the black box and functional diagrams of the arm support respectively.



Figure 8. Arm Sub-Assembly for RWTD.



Figure 9. Black Diagram of the Arm Support.

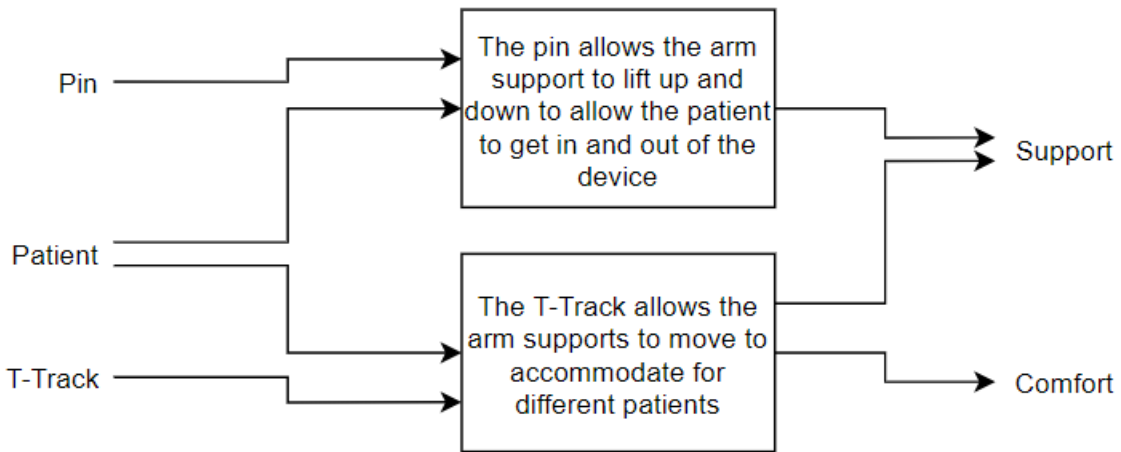


Figure 10. Functional Diagram of the Arm Support.

## Leg Assembly

The leg assembly is machined out of 6061 Aluminum. At each major joint there is a motor attached to allow for the generation of the gait path of the knee and ankle. There is a secondary sub-system of the leg assembly. The electronics of the leg assembly are a key component of the Leg Assembly. Figure 11 shows the Leg Assembly, while, Figure 12 and 13 show the black box and functional diagram for the leg assembly respectively.

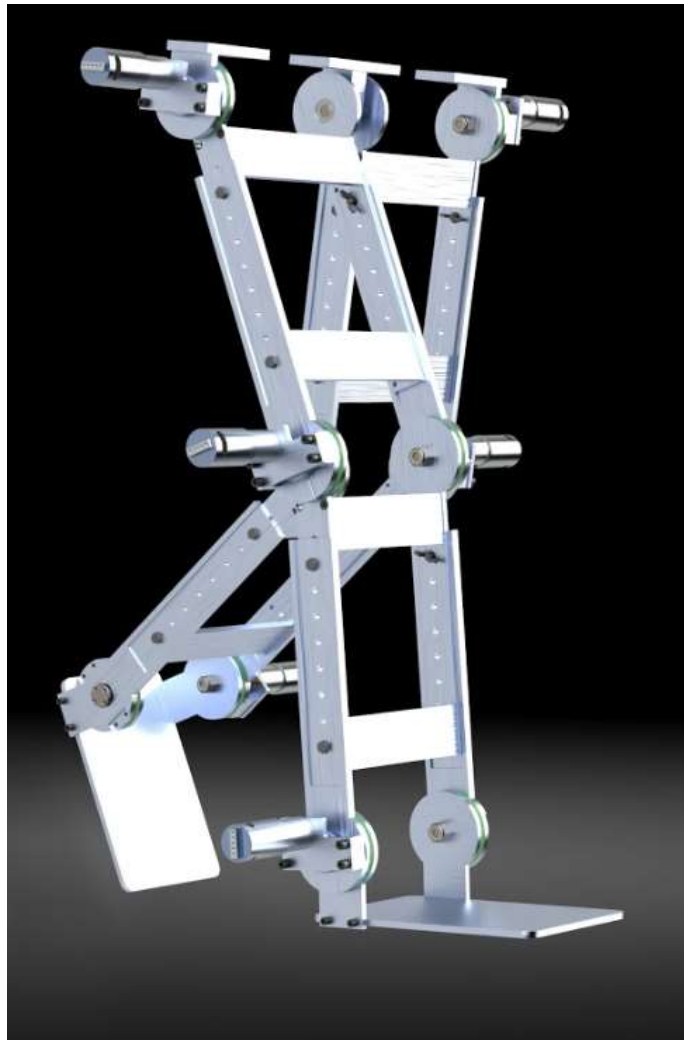


Figure 11. Leg Assembly Constructed of 6061 Aluminum.

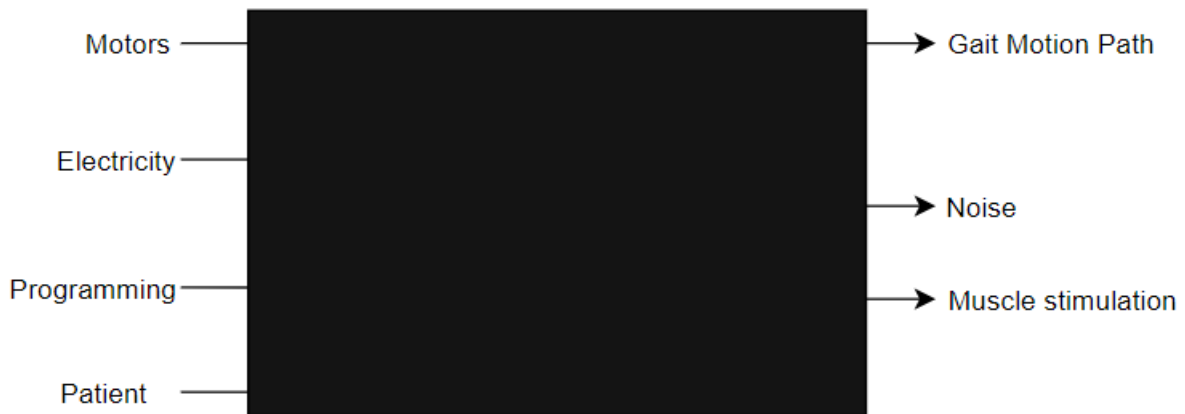


Figure 12. Black Box Diagram of the Leg Assembly.

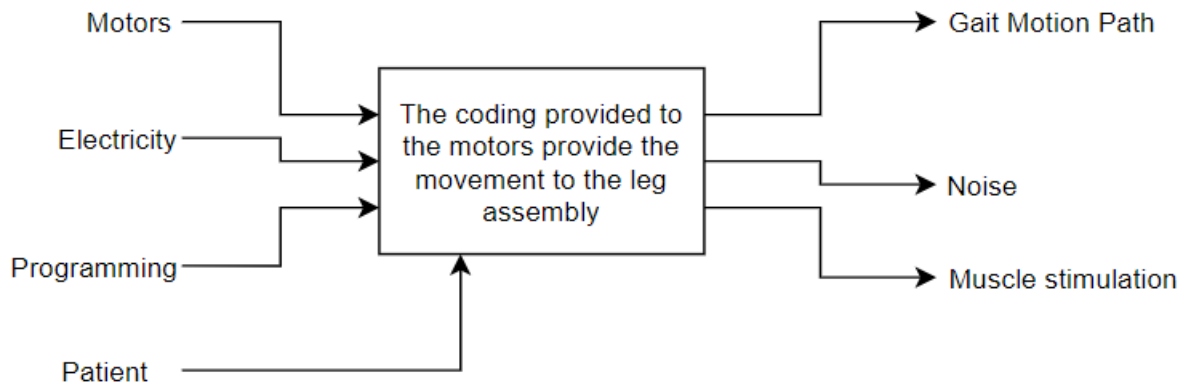


Figure 13. Functional Diagram of the Leg Assembly.

## Electronics for the Leg Assembly

The motors are a key component of the leg assembly. The coding provides the necessary motion needed to reproduce the gait path. Figure 14 shows the motors. Figure 15 and 16 show the black box and functional diagram for the motors respectively.





Figure 14. ServoCity 12 RPM HD Premium Planetary Motor w/Encoder used in RWTD.



Figure 15. Black Box Diagram of the Electronics for the Leg Assembly.

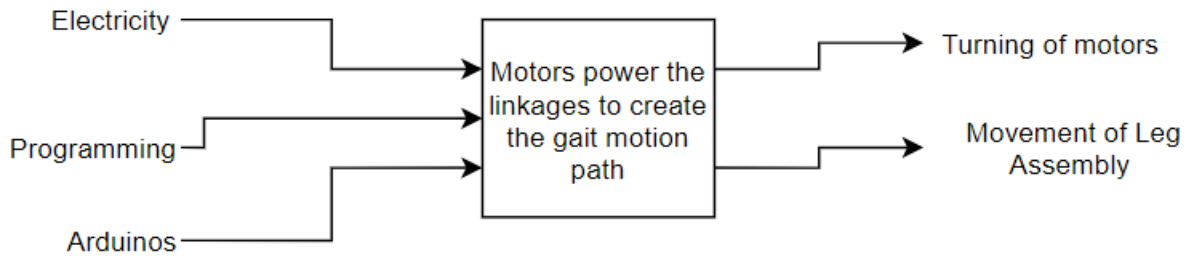


Figure 16. Functional Diagram of the Electronics for the Leg Assembly

## FES System

The FES System provides the muscle stimulation to help rewire synapses that have been damaged during the injuries. Figure 17 shows the FES System. Figure 18 and 19 show the black box and functional diagram for the FES System respectively.



Figure 17. Digitimer Functional Electrical Stimulator used in RWTD.



Figure 18. Black Box Diagram for the FES System.

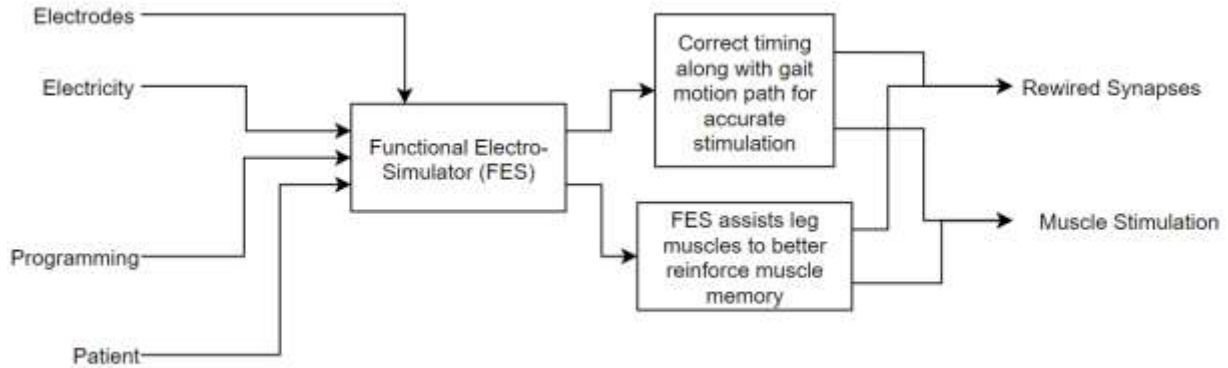


Figure 19. functional Diagram for the FES System

## Electrotherapy Modulation

Neurologic injuries such as stroke and spinal cord injury may cause muscle atrophy due to the lack of use of the muscle. As a rehabilitation approach, Functional Electrical Stimulation (FES) of weak or paralyzed muscles can provide muscle strengthening by directly eliciting contractions in the muscle. The FES does through the application of high frequency electrical pulses to the nerves or direct to the muscle via medical electrodes as seen below in Figure.20. [3-6]



Figure 20. Experimental set up of hybrid FES-exoskeleton rehabilitation system.

However, a downside of solely using FES for muscle rehabilitation is muscle fatigue and poor control of joint trajectories. In contrast, when paired with robotic exoskeletons for gait rehabilitation, such as the RWTD, overall muscle fatigue and joint trajectories can be compensated to deliver increased gait performance and decreased energy expenditure by the FES. Combining these two methods of rehabilitation allows for the offset of disadvantages in both systems while still maintaining the advantages. An example of how the control system for such a setup can be seen in Figure 21. [3-6]

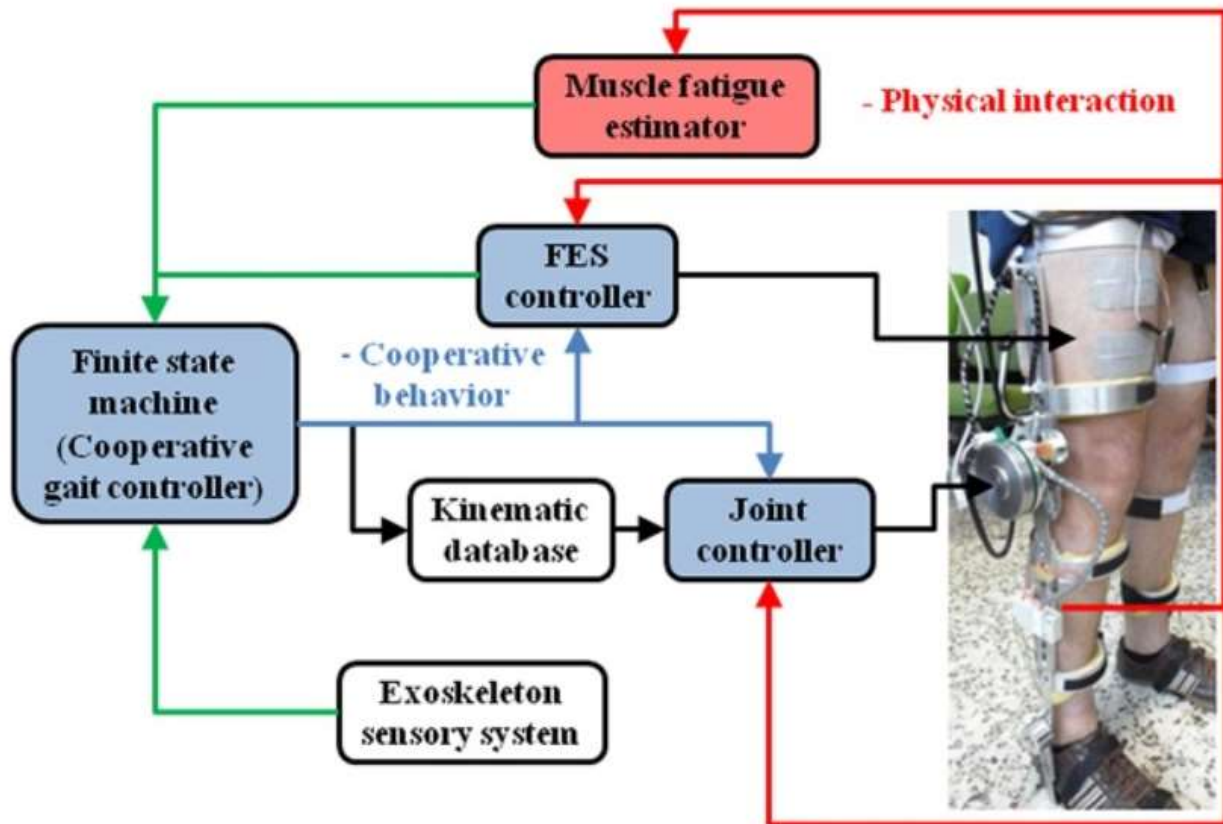


Figure 21. Flow Diagram of FES and GAIT system cooperative controller.

There are many different types of stimulation that can be provided by the FES due to its ability to accept custom made waveforms via software such as LabVIEW and an attached function generator. Because of this customizability, various electrotherapy modulation techniques were researched, and one was chosen based upon the requirements needed to for muscle rehabilitation in stroke and spinal cord injury patients. High-Voltage Pulse Stimulation fits the required criteria. The treatment indications as well as specifications for the pulses and resulting waveforms can be seen in Table 3, Table 4 and Figure 22 respectively. [7]

Table 3. Patient Treatment Indications from FES.

Indications for High-Voltage Pulsed Stimulation Treatment	
Reeducation of peripheral nerves	
Delay of denervation and disuse atrophy by stimulating muscle contractions	
Reduction of post-traumatic edema	
Increase in local blood circulation (unsubstantiated)	
Restoring range of motion	
Reduction of muscle spasm	
Inhibition of spasticity	
Reeducation of partially denervated muscle	
Facilitation of voluntary motor function	

Table 4. Electrotherapy Specifications of High-Voltage Pulsed Stimulation.

High-Voltage Pulsed Stimulation	
Current Type	Monophasic
Current Amplitude	2 – 2.5 A
Amplitude	0 – 500 mA RMS
Voltage	0 – 500 V
Pulse Frequency	13 – 120 PPS
Pulse Duration	13 – 100 $\mu$ s
Phase Duration	13 – 100 $\mu$ s
Treatment Duration	15 – 30 Minutes

Saw Tooth (1 Pulse) M-Wave (2 Pulse) Square Wave (3 Pulse)

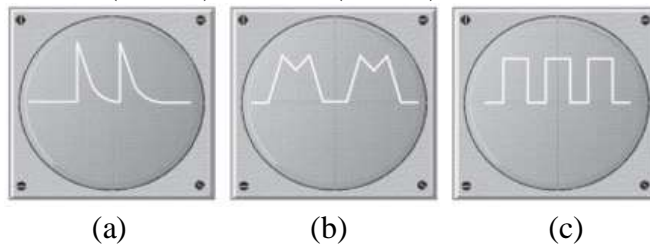


Figure 22. High-Voltage Pulsed Stimulation Waveforms. (a) Saw Tooth, (b) M-Wave, (c) Square Wave.

## Final Design Calculation Results

Below is a table describing the design criteria for the RWTD.

Table 5. Design Criteria for RWTD.

Description	Calculation	Material Chosen
Weight of full leg assembly	<25 lbs.	6061 Aluminum
Torque to move the leg assembly	>278.73 in.-lbs.	12 RPM HD Premium Planetary Gear Motor with Encoder
Lifting the scissor lift with a patient	>371.47 lb.	FA-400-12-2" – P Premium 2" Stroke 400 lb. 12V linear actuator
Pivot Pin needed to withstand stress applied	>1678.08 psi	1020 Cold-Rolled Steel
Screws attaching the leg assembly to the scissor lift	>216.33 in-lb.	FHCS ¼" – 20 x ¾"



## Feasibility Analysis

### Mechanical

For the leg assembly, a lightweight and durable material was needed. To allow for ease of movement of the device, the weight of the full leg assembly was to be kept under 25 lb. Aluminum 6061 was chosen for the leg assembly having a total weight of approximately 22 lb. Having a Rockwell B hardness of 60 means the material is durable. It also has a tensile strength between 18-42 ksi. and a fatigue strength of 14,000 psi. The high tensile strength and fatigue strength mean the device will unlikely fail under tension or from fatigue. However, Aluminum has specific behavior under fatigue. When Aluminum 6061 is under repeated loads, it shows cyclic softening characteristics, with a rapid softening in the beginning stages of repeated loading and then slowing down in the later stages. Also, when the initial stress amplitude of the repeated tensile load is more than 2.5% it has a detrimental effect on the deformability of the aluminum alloy [8]. Therefore, it would be necessary to replace the components of the leg assembly once it reached  $10^7$  cycles or after 1,000,000 therapy sessions lasting 30 minutes is when Aluminum starts experiencing fatigue properties. Calculations to determine the how many cycles are in a therapy session can be seen in Appendix C.

For the motor selection, a minimum torque of 278.73 in.-lb. was required. To determine the highest amount of torque that would be required for the motors to power the linkage system, the hip motor was analyzed as this is where the highest torque would be applied. For this calculation, the weight of a human leg, the leg assembly, and the motors at the knee and ankle were accounted for in the weight. According to *Human Body Dynamics Classical Mechanics and human Movement*, the legs account for 16.5% of body weight for men and 15% for women [9]. For this analysis a male, weighing 300 lb. was chosen and the linkages were taken to be at their fully extended length of 19.5 in. each, equating to 39 in. total from the hip to the ankle, to determine the maximum torque that will be applied to the system. The system was also analyzed when it was in its walking position. Also considered was the speed of the motor. The average human takes approximately one step per second. Since the users of this device will be limited in their lower limb mobility, the time between steps was increased to one step every two seconds which has the added benefit of allowing better use of the FES. This longer time between steps also allows the patient's muscles to rest between the stimulation generated by the FES. As a result of this analysis,

the 12 RPM HD Premium Planetary Gear Motor with Encoder was chosen. The motor and the specification sheet can be found in Appendix D. The torque produced by the motor is 506.875 in.-lb. The final torque was calculated to be 2027.55 *in – lb*. All calculations for this analysis can be seen in Appendix E.1-E.2. The calculations for the speed and torque produced by the motors can be seen in Appendix E.3-E.4

To replace the hydraulic lifting system in the lift with a linear actuator, the maximum force that would be used to lift the whole system needed to be determined. For this analysis, 4 main components were taken into account. The weight of the person on the lift, the leg assembly, the arm assembly and the lifting table. The weight of the person on the lift, the leg assembly, the arm assembly, and the lifting table. The maximum force was calculated to be 371.47 lb. Another factor that was needed to be accounted for when looking for a replacement was the space where the linear actuator would be placed. The space the hydraulic lifting system occupied was measured to determine the size of the actuator. The dimensions of the space when the lift was fully raised was 12 in. x 5in, x 4in. The stroke length necessary to fully raise the device was 2 in. From the calculations, the FA-400-12-2” – P Premium 2” Stroke 400 lb. 12V linear actuator was chosen. The static force capacity of this actuator is 400 lb. The linear actuator was also chosen as it had the appropriate stroke length to raise the device and the was the correct dimensions to fit in the space. All calculations can be seen in Appendix E.5

To determine what material to make the pivot pin out of the shear stress on the pivot pin at the hip was conducted. The hip pivot pin was chosen as this pin would be subjected to the maximum shear stress. For this analysis, a male weighing 300 lb. was considered, as well as the weight of the linkage system and the gear motors. The shear stress on the pivot pin was calculated to be 1678.08 psi. Furthermore, the material chosen needed to be machinable, durable and able to withstand the shear stress applied from the legs. Due to the required criteria, 1020 Steel-Cold Rolled was chosen. The related properties of 1020 Steel-Cold Rolled can be seen in Table 6 below. All calculation can be found in Appendix E.6

Table 6: Properties of 1020 Steel, Cold Rolled.

1020 Steel, Cold rolled	
Mechanical properties	Values (English)
Hardness, Rockwell B	68
Ultimate Tensile Strength	60900 psi
Machinability	65%
Shear Modulus	10400 ksi

A shear stress analysis was performed on the screws connecting the leg assembly to the lift table. The first two screws take the highest amount of shear stress at 216.33 in.-lb. A FHCS ¼” – 20 x ¾” was chosen. The screw has a shear strength of 27,000 psi. All calculations can be found in Appendix E.7

## Electrical

To determine the number and type of Arduinos needed the hall sensor pulse period at full speed was analyzed. The gear ratio is 2163:1, and the counts per revolution of the input motor shaft is 103,824 CPR. The Hall sensor is quadrature using two channels A and B. Only the pulses per revolution of channel A need to be accounted for. The number of pulses coming into the program is 1740 PPS. Each incoming pulse requires an interrupt that halts program execution. Due to the number of incoming pulses a single Arduino would not be able to perform other tasks. It was determined that 6 Arduino Nanos would be used to count the incoming pulses of each motor. While an Arduino Mega 2560 executes the code, which determines motor speed and direction, as well as handles menu display and user interfacing. The calculations to determine the PPS can be found in Appendix F.

To determine what transformer to use a power analysis was performed. The final stall torque of the motor is 2027.55 in.-lb as seen in Appendix E-4. The motor stall current was given as 20A. The amps per lb-in of torque was calculated as  $0.0033 \frac{A}{lb \cdot in}$ . To determine the maximum

current consumption the analysis used the device system limit of a 300 lb. 6'4" person. A total current consumption of 3.96A. All calculations can be seen in Appendix G. The transformer also needed the ability to go from 120V AC to 12 V DC. Due to the requirements of the voltage change and current output needed, the MINZO 120V AC to 12 VDC Transformer was choose. Specifications can be found in Appendix H

## Risk Assessment

The objective of this plan is to implement the process of identifying, analyzing, and responding to potential project risks. A risk is the probability of failure or frequency multiplied by the impact of failure. It is often defined by three main components: the probability of occurrence, the impact of the risk and the consequences that will occur if the risk is not mitigated. Table 7 and 8 show the Risk assessment matrix and the risk levels respectively. These two tables were used to determine the level of risk when constructing the risk assessment and Mitigation Plan seen in Table 9.

Table 7: Risk Assessment Matrix.

Probability of Occurrences			Catastrophic	Critical	Moderate	Minor	Negligible
Definition	Meaning	Value	(A)	(B)	(C)	(D)	(E)
Frequent	Occurs frequently	5	5A	5B	5C	5D	5E
Likely	Occurs less frequently	4	4A	4B	4C	4D	4E
Occasional	Occurs sporadically	3	3A	3B	3C	3D	3E
Seldom	Unlikely to occur	2	2A	2B	2C	2D	2E
Improbable	Highly unlikely to occur	1	1A	1B	1C	1D	1E

Table 8: Risk Levels.

High Risk	
Medium High Risk	
Medium Low Risk	
Low Risk	

Table 9. Risk Assessment and Mitigation Plan.

Risk	Description	Level	Mitigation	Contingency
1	Pivot pin has slippage with the motor shaft	3B	Design a connection between pivot pin and motor shaft	Drill a hole through motor shaft and connect shaft and pivot pin together with a bolt
2	Shipping time for major components is too long causing delays in project build	3D	Check shipping times beforehand to determine the arrival time	Have a secondary component chosen as a backup that has a faster arrival date
3	Manufacturing of components taking too long causing delays in project build	2E	Coordinate to determine when components are needed	Use prototype to start developing the code to decrease the delay time
4	Left and Right Leg Linkages not being in sync with one another	4B	Adjust degrees and speed of rotation for the motors in the code	Use the results from Vicon Motion Capture to adjust the legs
5	Code for leg motion not complete	3A	Get coding help from team members, other Electrical Engineering students, and faculty	Hire a consultant who has extensive experience in coding
6	Unable to use Biomaterials Lab to perform evaluation of code	4C	Work with Dr. Dong to ensure use of Vicon Motion Capture	Talk with Dr. Dong to take Vicon Motion Capture to RBN 1039 for use

## Failure Mode and Effects Analysis

Aluminum linkages will wear down over time as both outer and inner linkages are made of the same material. To provide greater longevity of the entire assembly and to keep maintenance costs low, an Ultra High Molecular Weight plastic wear plate was inserted between the linkages. This allows for not only a lower coefficient of friction, but also providing a buffer between the linkages.

Since this device will be used for rehabilitation, consideration of the device being used by a human subject needs to be taken into account. Potential damage to the device can happen if the patient resists the movement of the linkages. Due to the risk of damaging the device the patient needs to be informed on what to expect when in the device. The padding of the device will also need to be replaced due to wear and tear from the patient. To provide longevity of the padding, it is recommended to clean the padding with disinfectant for patient safety and then also to use a leather protection cleaner to increase the life of the padding covering.

Human operators could cause damage to the device if it is not correctly operated and moved. Due to the motors being on the outside of the leg assembly, they have the potential of being damaged if they are bumped while the device is being moved. The wiring of each motor will be wired on the outside of the leg assembly. If the wiring is damaged it could cause the device to malfunction or to not work. By providing proper training on device use and moving the device. The user manual can be found in Appendix J

## Finite Element Analysis

Through hand calculations during the Feasibility Analysis stage, it was found that the most torque would be applied at the hip joint in the Leg Sub-Assembly. The resultant force for the maximum specified load generated by a 300 lb. patient at the farthest distance of 39 in. from the hip joint was applied. The von mises stress of the leg sub assembly was found to be a maximum of 2912 psi. The yield strength of 6061 Aluminum is approximately 42,000 psi. Since the maximum von mises stress is not greater than the yield strength, the leg sub assembly the part will not fail according to this criteria. The maximum deformation of the thigh sub-assembly under expected loading is 0.007498 in. Due to the minimal deformation it is negligible in comparison to the length of the leg assembly. The safety factor was a minimum of 5.46. The results of this analysis influenced the decision to use 6061 Aluminum for the leg assembly. Having a high yield strength, low deformation and a high safety factor were important as the device will be used for rehabilitation.

The joint pivot pin had a maximum von mises stress of  $8.8808e5$  psi. this point is located at the transition from the cylindrical shaft portion to the threaded portion of the pin. The von mises stress is higher than the yield strength of 1020 cold rolled steel indicating that the Pivot Pin will fail at this location. However, this analysis was performed by directly applying the maximum force on the pin itself. In a real world scenario, the forces would be distributed throughout the hip mount plate and the inner and outer linkages. Since this scenario indicated a worse case it was determined the Pivot Pin would not fail under normal use circumstances. It can also be seen that a majority of the Pivot Pin has a extremely low von mises stress and the maximum location is very small indicating it is negligible in comparison to the rest of the pin. The maximum total deformation on the pin is 0.0026903 in. this deformation is negligible in comparison to the size of the pin. The Pivot Pin was subsequently tested and found to have a safety factor of generally, 1-5, with the key weak point located at the transition from the cylindrical shaft portion to the threaded portion of the pin as seen in the von mises stress analysis. A life cycle analysis was performed on the Pivot Pin and it was found to have a life cycle of, generally between 10,000 and 1,000,000 cycles.

The von mises stress of the arm assembly had a maximum of 29,890 psi. This analysis was performed with the maximum force 300 lb. being applied throughout the sub-assembly as a worse



case scenario. The arm sub-assembly is made out of steel. The yield strength of steel is 50,800 psi. this indicates even under the worse case scenario the arm sub-assembly would not fail. The maximum deformation of the arm sub-assembly is seen at the end farthest away from the pin, with a deformation of  $6.439e-2$ . This deformation can be taken as negligible when it can be accounted for the length and size of the sub-assembly. The safety factor for the arm sub-assembly is generally 3 throughout indicating that assembly is more than equipped to be used for rehabilitation purposes.

All FEA results can be seen in Appendix K

## Final Testing Results

To demonstrate that the RWTD could be manufactured with high reliability that the components will not interfere when in motion. A simulation was performed to show that the leg assembly while attached to the device can produce the required gait motion path. These results can be seen in the video: <https://youtu.be/FY78hqLgfsg>

Through this simulation the RTWD team has proven that when manufacture the device will have the ability to move without any interference of components will occur from the leg assembly when it is in motion.

## Plan to Compare Simulation vs. Actual Testing Results

Due to the inability to complete the manufacturing of the device actual testing results were not able to be completed. However, if the ability to compare the final simulation testing results and final actual testing results was possible the following would list how the testing would be performed.

To prove the device was stable during its use the team was going to place the weights onto the device up to 300 lbs. to prove that the device would be stable during use. To make sure the weights were distributed as a human would be the distribution of the weight was calculated using the Human Body Dynamics: Classical Mechanics and Human Movement percentages to be as close to a patient in the device as possible. The weights would be placed in bags and would be strapped in to guarantee the weight would not move when the device would be in motion affecting the accuracy of the device.

The test to show that the device would be able to accommodate a 6' 4" patient was to ask a 6' 4" person to sit in the device to accurately adjust the leg linkages to the correct position. Then the person would be asked to get off the device to guarantee no injuries would accidentally occur if the device did not meet the requirements. Then the device would be turned on to demonstrate that the leg assembly would not have any interference from the floor or any other components of the device.

To demonstrate the leg assembly produced the gait path within  $\pm 10\%$  of a natural gait path motion. The device in motion was going to be analyzed using the Vicon motion capture. The data gathered from the Vicon motion capture was then going to be compared to the original to prove the path produced was in the 10% range.

To test the accuracy of the FES stimulation timing to that of the necessary moment in the motion path two tests would be performed. First, the FES system would be hooked up to light up a light bulb while the device was in use to analyze that the timing was accurate. The second test would be performed under supervision of Dr. Dong. This test would require a participant to be placed in the device and the FES would be attached. Then the devices would be turned on and the accuracy of the timing would be seen in the participants muscle.

To prove the FEA results that were produced through simulations. Real- life testing would of occurred. The device would have been turned on and left to run. The various components, such as the pins, linkages, and motors, would be analyzed at specified times to determine if there is any noticeable degradation of the components. They would also be looked at under the microscope to determine if there were any microstructural problems occurring.

## Bill of Materials

The table below shows the Bill of Materials for the RWTD. Detailed drawings of all the manufactured parts can be found in Appendix L.1 while Appendix L.2 shows the final manufacturing drawings.

Table 10. Bill of Materials for R.W.T.D.

Part #	Part Name	Qty.	Item Description	Item Number	Category	Material	Weight
1	Handle Nut	4	Zinc-Plated Cast Iron Easy-Grip Handle with 3/8"-16 Thread	McMaster-Carr - #91044A031	Purchased Fasteners	Zinc-Plated Iron	
2	0.5" O.D. Shoulder Screw	4	0.5" O.D. Shoulder Screw - 1.0" Shaft Length	McMaster-Carr - #91259A712	Purchased Fasteners	Alloy Steel - Black Oxide Finish	
3	0.25" x 1.0" Threaded Rod	4	0.25" - 20 x 1.0" High Strength Steel Threaded Rod	McMaster-Carr - #90322A645	Purchased Fasteners	Grade 8 Steel	
4	Arm Plate	2	Arm Plate		Manufactured Component	6061 Aluminum	9.75E-2 <i>lb/in<sup>3</sup></i>
5	10-32, 3/8" Pan Head Machine Screw	16	10-32, 3/8" Pan Head Phillips Screw	McMaster-Carr - #90988A103 - Pkg. Qty. 10	Purchased Fasteners	Black-Oxide 18-8 Stainless Steel	

Part #	Part Name	Qty.	Item Description	Item Number	Category	Material	Weight
6	T-Slot Slider	2	T-Slot Slider		Manufactured Component	6061 Aluminum	9.75E-2 <i>lb/in<sup>3</sup></i>
7	T-Slot Track	2	24" Long Fixturing Track for Hex Head Screws	McMaster-Carr - #1850A14	Purchased Component	Anodized Aluminum	
8	10-32 Lock Nut	16	10-32 Medium-Strength Steel Nylon-Insert Flange Locknut	McMaster-Carr - #93298A109 - Pkg. Qty. 100	Purchased Fasteners	Grade F Zinc-Plated Steel	
9	Arm Pad Assembly	2	2nd Generation Arm Pads				
10	Hip Mount Plate	2	Hip Mount Plate		Manufactured Component	6061 Aluminum	9.75E-2 <i>lb/in<sup>3</sup></i>
11	Hip Motor Mount	2	Hip Motor Mount		Manufactured Component	6061 Aluminum	9.75E-2 <i>lb/in<sup>3</sup></i>
12	Groin Pin Mount	1	Groin Pin Mount		Manufactured Component	6061 Aluminum	9.75E-2 <i>lb/in<sup>3</sup></i>
13	Groin Pin	1	Groin Pin		Manufactured Component	1018 CR Round	0.668 <i>lb/ft</i>
14	Frame Spacer L	4	Upper Frame Spacer		Manufactured Component	6061 Aluminum	9.75E-2 <i>lb/in<sup>3</sup></i>

Part #	Part Name	Qty.	Item Description	Item Number	Category	Material	Weight
15	Frame Spacer Short	4	Lower Frame Spacer		Manufactured Component	6061 Aluminum	9.75E-2 <i>lb/in<sup>3</sup></i>
16	Ankle Swivel	4	Ankle Swivel Mount		Manufactured Component	6061 Aluminum	9.75E-2 <i>lb/in<sup>3</sup></i>
17	Foot Platform	2	Foot Platform		Manufactured Component	6061 Aluminum	9.75E-2 <i>lb/in<sup>3</sup></i>
18	0.25" Lockwasher	16	0.25" Hi-Collar Lockwasher	McMaster-Carr - #93711A500 - Pkg. Qty. 50	Purchased Fasteners	Black Oxide Alloy Steel	
19	0.25" - 20 Wingnut	16	0.25" - 20 Wingnut	McMaster-Carr - #90866A029 - Pkg Qty. 100	Purchased Fasteners	Grade 5 Steel Zinc-Plated	
20	0.25" - 20 x 0.75" Hex Drive Flat Head Screw	4	0.25" - 20 x 0.75" Hex Drive Flat Head Screw	McMaster-Carr - #91253A540 - Pkg. Qty. 50	Purchased Fasteners	Black Oxide Alloy Steel	
21	10-24 x 0.75" SHCS	12	10-24 x 0.75" SHCS	McMaster-Carr - #91251A245 - Pkg. Qty. 100	Purchased Fasteners	Black Oxide Alloy Steel	

Part #	Part Name	Qty.	Item Description	Item Number	Category	Material	Weight
22	12 RPM P.G. Motor	6	12 RPM Motor (12VDC)	ServoCity - SKU#638310	Purchased Transmission Component		
23	10-24 x 0.750" Hex-Drive Flat Head Screw	24	10-24 x 0.750" Hex- Drive Flat Head Screw	McMaster-Carr - #91253A245 - Pkg. Qty. 50	Purchased Fasteners	Black Oxide Alloy Steel	
24	#10 Hi-Collar Lockwasher	24	#10 Hi-Collar Lockwasher	McMaster-Carr - #93711A400 - Pkg. Qty. 50	Purchased Fasteners	Black Oxide Alloy Steel	
25	Gear Motor Mount	6	Gear Motor Mount Plate		Manufactured Component	6061 Aluminum	9.75E-2 <i>lb/in<sup>3</sup></i>
26	8-32 x 0.375" SHCS	24	8-32 x 0.375" SHCS	McMaster-Carr - #91274A052 - Pkg. Qty. 50	Purchased Fasteners	Black Oxide Alloy Steel	
27	Pivot Pin	6	Joint Pivot Pin		Manufactured Component	1018 CR Round	3.38 <i>lb/ft</i>
28	M3 - 0.5mm x 10mm Button Head Hex Screw	24	M3 - 0.5mm x 10mm Button Head Hex Screw	McMaster-Carr - #91239A115 - Pkg. Qty. 100	Purchased Fasteners	Black Oxide Alloy Steel	



Part #	Part Name	Qty.	Item Description	Item Number	Category	Material	Weight
29	Gear Motor Mount Riser	12	Gear Motor Mount Riser		Manufactured Component	6061 Aluminum	9.75E-2 <i>lb/in<sup>3</sup></i>
30	1.125" x 0.500" I.D. Bearing	6	1.125" x 0.500" ID Ball Bearing	McMaster-Carr - #60355K505	Purchased Transmission Component	SAE 52100 Chrome Steel	
31	Outer Link	8	Outer Link		Manufactured Component	6061 Aluminum	9.75E-2 <i>lb/in<sup>3</sup></i>
32	UHMW Wear Plate	10	UHMW Wear Plate	Grainger - Item# 22JL76 (24"x12")	Purchased Transmission Component	Polypropylene Sheet Stock	
33	Inner Link	8	Inner Link		Manufactured Component	6061 Aluminum	9.75E-2 <i>lb/in<sup>3</sup></i>
34	0.5" - 13 Nylock Nut	6	0.5" - 13 Nylock Nut	McMaster-Carr - #95615A210 - Pkg. Qty. 50	Purchased Fasteners	Grade 5 Steel Zinc-Plated	
35	Linear Actuator	1	FA-400-12-2-P	400 lb Capacity Linear Actuator	Purchased Transmission Component		

Part #	Part Name	Qty.	Item Description	Item Number	Category	Material	Weight
36	Motor Controller	6	Cytron MD20A	Motor Controller	Purchased Component		114 g
37	30A 120VAC to 12VDC Transformer	1	Transformer	120VAC to 12V DC Power Supply	Purchased Component		840 g
38	Arduino Nano	6	Arduino Nano	Microprocessor Unit	Purchased Component		7 g
39	Arduino Mega2560	1	Arduino Mega2560	Microprocessor Unit	Provided by Team Member		37 g
40	Eaton Neutral Bar	1	Eaton Neutral Bar	Power & Ground Rails	Provided by Team Member		
41	100' - 18 AWG Wire	4	100' - 18 AWG Wire		Purchased Component		
42	Memory Foam	1	Memory Foam		Purchased Component		

## Budget

The table below shows the budget for the RWTD.

Table 11. Budget for the RWTD Prototype.

Name of Item	Quantity	Price per Unit	Total Price
24" Fixturing Track for Hex Head Screws	2	\$7.10	\$14.20
10-24 x 0.750" Hex-Drive Flat Head Screw (32)	1	\$8.56	\$8.56
1/4 - 20 x 1.25" SHCS (24)	1	\$12.48	\$12.48
8-32 x 0.375" SHCS (24)	1	\$10.89	\$10.89
M3 - 0.5mm x 10mm Button Head Hex Screw (24)	1	\$7.77	\$7.77
1/4 - 20 x 0.750" Grade 5 Hex Bolt (16)	1	\$8.53	\$8.53
1/4 Hi-Collar Lockwasher (16)	1	\$10.38	\$10.38
1/4 - 20 Wingnut (16)	1	\$10.94	\$10.94
1/4 - 20 x 0.750" Hex Drive Flat Head Screw (4)	1	\$8.54	\$8.54
10-24 x 0.750" SHCS (8)	1	\$12.07	\$12.07
#10 Hi-Collar Lockwasher (8)	1	\$8.41	\$8.41
1/2 - 13 Nylock Nut (10)	1	\$10.07	\$10.07
Zinc-Plated Cast Iron Easy-Grip Handle with 3/8"-16 Thread	4	\$3.79	\$15.16
1/2" O.D. Shoulder Screw - 1.0" Shaft Length	4	\$2.61	\$10.44
1/4" - 20 x 1.0" High Strength Steel Threaded Rod	4	\$3.13	\$12.52
10-32, 3/8" Pan Head Phillips Screw (16)	1	\$13.88	\$13.88
10-32 Medium-Strength Steel Nylon-Insert Flange Locknut (16)	1	\$6.85	\$6.85
UHMW Wear Plate (10)	1	\$8.14	\$8.14
12 RPM Motor (12VDC)	6	\$59.99	\$359.94
1.125" x 0.500" ID Ball Bearing	12	\$6.27	\$75.24
FA-400-12-2-P Linear Actuator	1	\$139.00	\$139.00
Cytron MD20A Motor Controller	6	\$19.80	\$118.80
MINZO 120VAC to 12VDC Transformer	1	\$17.99	\$17.99
Arduino Nano	6	\$4.29	\$25.74
Arduino Mega2560	1	\$35.60	\$35.60
Eaton Neutral Bar	1	\$6.55	\$6.55
4x 100' - 18 AWG Wire	1	\$15.95	\$15.95
Universal 5 pin Rocker switch	1	\$8.29	\$8.29
4 pin, 2 position toggle switch	2	\$4.00	\$8.00
Lever limit switches (10)	1	\$7.99	\$7.99
Waterproof 12 pin way connector (10)	1	\$17.31	\$17.31
		<b>Total</b>	<b>\$1,026.23</b>

## Economic feasibility

### Target Market & Competition

The medical community, specifically the physical therapy sector, stands to gain the most from our product. In the United States alone, there are an estimated 38,800 physical therapy clinics [10]. A majority of these clinics work with patients that have issues with their gait that were incurred from either a spinal cord injury or a stroke. Part of the rehabilitation regimens that these patients undergo is gait training. This training currently utilizes multiple rudimentary tools such as body-weight support devices that often require the physical exertion of therapists and assistants in order to assist patients as seen in Figure 23. Our product provides healthcare professionals with a hands-off alternative that does not require any physical exertion and only requires a single operator as opposed to needing two or more individuals assisting a patient in their rehabilitation.



Figure 23. Body-Weight supported device used for Rehabilitation.

Another treatment option that is offered by some rehabilitation regimens is Functional electrical stimulation or neuroprosthesis. This treatment, “stimulates certain muscles in the legs to do the same job as a brace during walking” [11]. Our product integrates a FES device that performs this function.

There are devices that exist that provide a gait rehabilitation via mechanical assembly. One such example is the RoboGait as seen in Figure 24. This device is a large, stationary machine that uses a body-weight support in conjunction with a pair of robotic legs to rehabilitate a patient’s gait.



Figure 24. Example of the RoboGait in use.

The difference between our product and those that currently exist on the market is that our product allows for FES treatment to be performed simultaneously with the gait training provided by the incorporation of mechanical and electrical components into the design while also providing a rehabilitation device that is more compact and mobile. Another difference is that lift table that is incorporated in our design allows for the angle of the patient relative to the ground to be adjustable which allows for incremental allowances of strength to be reclaimed by patients due to gravitational resistance of their own weight working against them. These are factors that make our design unique to those currently available on the market.

## Cost of Prototype

This project was given a budget of \$2,000 for the implementation of a 3<sup>rd</sup> generation RWTD. The costs for the progress made with the prototype barely surpassed 50% of the allocated funds. This is because some of the pre-existing items used by the 2<sup>nd</sup> generation RWTD were able to be reused and incorporated into the newest design. This includes the lift table base, foam padding, several pieces of hardware, and the casters used by the previous base design. Some of the costs that would have been incurred by the prototype were avoided due to donations made by team members in the form of the aluminum, steel plate, and other miscellaneous pieces of metal and items used for upholstering the memory foam pads. Overall, the estimated costs that were recorded for the prototype that were paid for by the sponsor totaled approximately \$1,026.23. The budget can be seen in Table 11.

## Cost of Mass Production

When examining the costs that could be incurred when mass producing this product, several factors were considered. Costs for labor, machining of parts, and fabrication were considered. The cost of having the aluminum parts machined and the included labor were calculated based off information received from a manufacturing website and from individuals that have worked in the industry [12]. These costs come in the amount of \$40 per hour of machine use, in this case a 3-axis CNC milling machine. The labor costs associated with using a machinist is \$35 per hour. The time that was spent by our team machining the parts for our system totaled around 150 hours, this was the estimate used to determine costs associated with use of machines and labor. In addition, some upgrades are recommended for system performance that were not feasible in the prototype phase. One such upgrade that is recommended is using shielded SOOW 18/12 cable over unshielded SOOW 18/12 cable. The reasoning for this recommendation is that the use of unshielded cable opens up the opportunity for the electronic pulses to be interfered with by outside electronic frequencies thus jeopardizing the integrity of the electrical components that are vital to the functioning of our system. The price difference between unshielded and shielded SOOW power cable is \$135.00 versus \$1,851.00. To mitigate that cost it could be recommended to customers that the device be placed in an area that does not permit cell phone or other electronic

use, in which case the unshielded SOOW cable could be used saving \$1,716.00 in production costs. Other costs that appear on the mass production list that do not appear on the prototype list is the purchase of the lift table, the FES system, and other components needed to construct the base that were already available during the prototyping stage in addition to material costs that were covered by team members. With all these things considered, the projected cost of mass-production is estimated to be \$22,727.12. The breakdown of this cost can be seen in Appendix M. This amount does not include discounts that could be available for purchases made in bulk. Other factors that were not considered in this estimate were costs for manual assembly, energy usage, or shipping. A recommended MSRP is not offered due to the absence of the previously mentioned information and desired profit margins.

# Flowcharts of Software

## Electrical Design Flowchart

The Figure below shows the flow of the Electronic design logic.

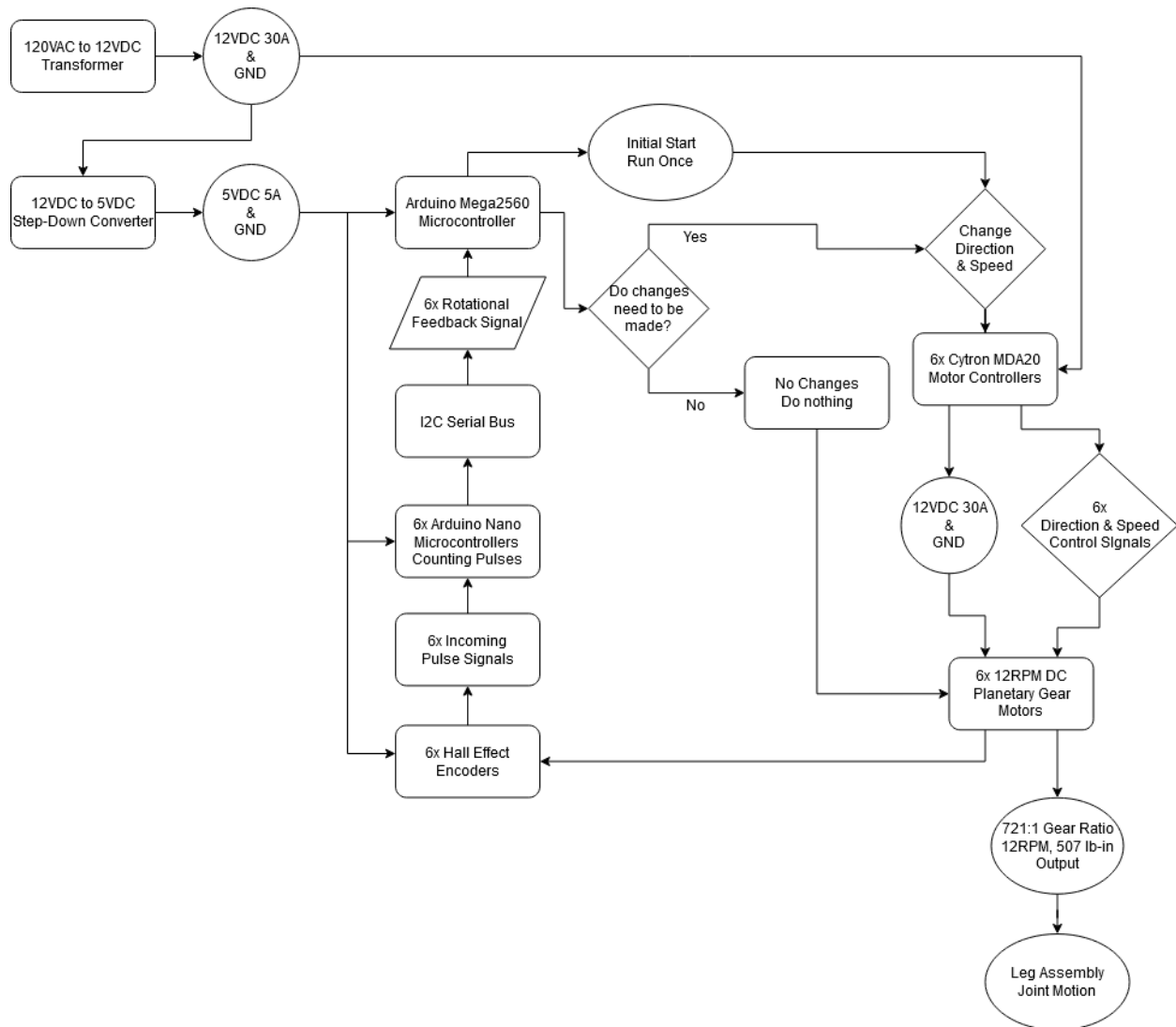


Figure 25. Electrical Design Flowchart.

The entire electrical system is powered by a 120VAC to 12VDC 30A transformer. There are six Cytron MD20A motor controllers that take the 12VDC 30A and use it to power and control the six planetary gear motors for the leg assembly. To control each motor's degree of rotation, each one has a Hall Effect Encoder attached. The six Hall Effect Encoders send signals to six



Arduino Nanos, which calculate the degree of rotation. The six Arduino Nanos send signals via I2C serial bus communication to an Arduino Mega2560 that tells the Cytron MD20A motor controllers to adjust direction and speed on the fly. Since the Hall Effect Encoders, the Arduino Nanos, and the Arduino Mega2560 all require 5VDC for optimal functionality, they are powered through a 12VDC to 5VDC 5A step-down converter.

## Program Flowchart

The Figure below shows the flow of the Program logic.

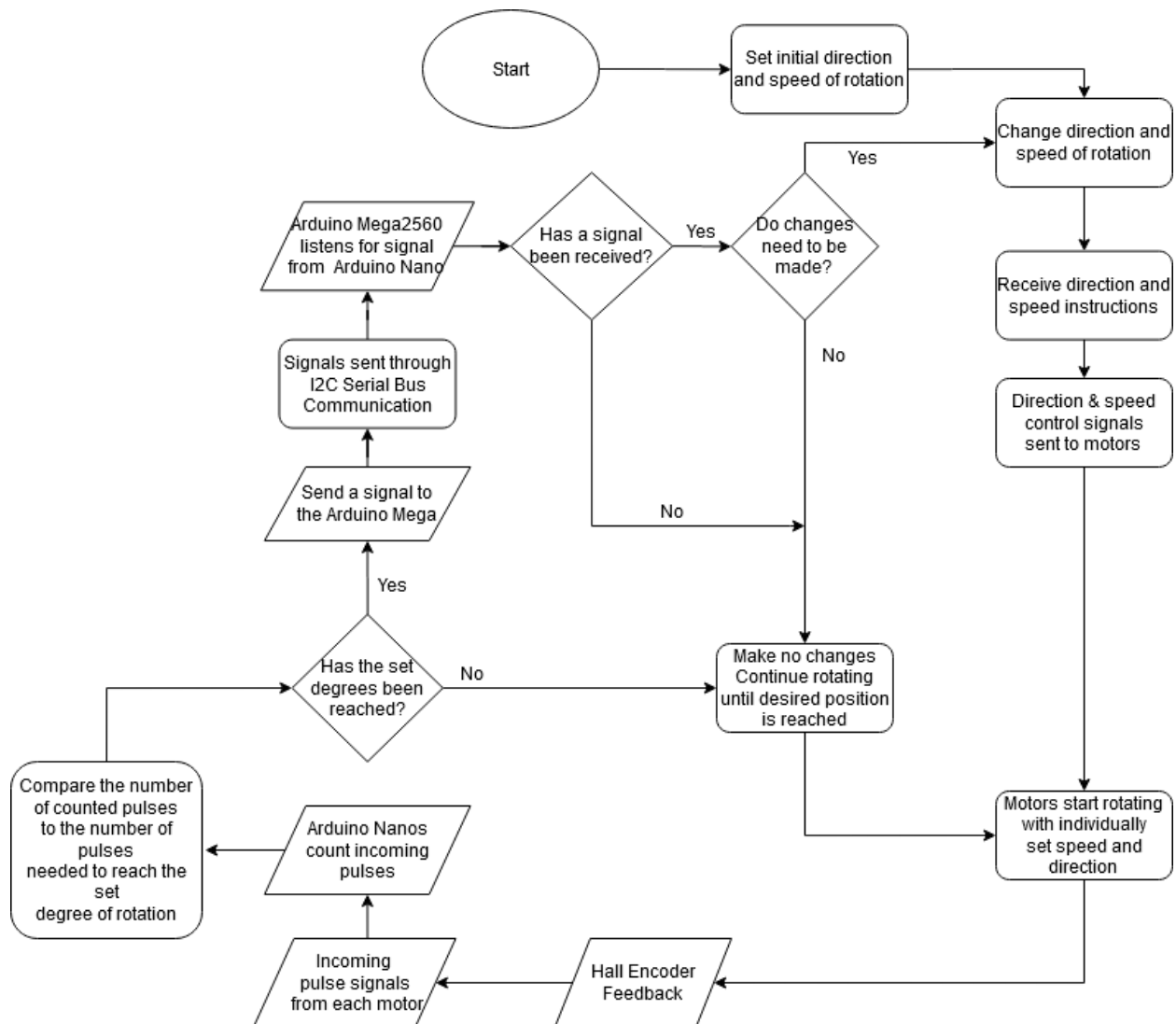


Figure 26. Program Design Flowchart.

At first start after the system is powered, the motor controllers are set to an initial direction and speed for the planetary motors on the leg assembly to begin rotating. The motor controllers receive the initial start instructions from the Arduino Mega2560. As the motors start moving, six Hall Effect Encoders individually attached to each motor will produce pulses that signal a certain amount of degree of rotation for that specific motor. Six Arduino Nanos take in this signal from

each individual Hall Encoder and calculate in real-time the degree of rotation for the motors and compare if the current degree of rotation is equal to the max degree required for the angle of the joint that a motor is moving. Once a specified degree of rotation is reached for accurate gait motion, the Arduino Nanos will send the Arduino Mega2560 a signal to indicate that the direction and/or speed of a motor needs to be changed. At this point, the Arduino Mega2560 will send the new direction and speed instructions to the Cytron MD20A motor controllers and the entire process repeats to produce an accurate walking motion.

Appendix N.1 has the specifications of the electronic components. Appendix N.2 has the wiring diagrams pertinent to the device. Appendix N.3 has additional information concerning the electronics. Lastly, Appendix N.4 has the code for each of the motors.

## Final Acceptance Criteria

The final acceptance criteria for the project were to have simulations of the device. The simulations needed to provide the necessary proof that the device would meet all the specifications that were stated in Table 1. The simulations showed that the device was capable of lifting the maximum weight of 300 lbs. It was also seen that the device was stable when the weight was placed onto the device. The device was also able to take patients of different heights up to 6' 4". This was shown by the legs being extended to the full length for all simulations. The leg length and gait path motion was proved by showing that the leg assembly produces the necessary natural gait path motion within  $\pm 10\%$ . The motion path that was generated was replicated straight from the provided from the excel data gathered through the Vicon Motion capture data. The FES specification was proved by comparing the code generated for the motion path to the code generated for the FES muscle stimulation to ensure that the timing of the FES was verified. The final acceptance criteria was approved by the sponsors as seen in Appendix O.

## Timeline and Milestones

A detailed timeline and ARCI chart can be found in Appendix P.

## Discussion

### Testing of Motors

Before using the motors that were purchased it was decided to test them to confirm the motors performed as expected. They were tested using an oscilloscope and the waveform was analyzed to determine if the motors reached the 12 RPM that was specified in the specifications. They were tested at 25, 50, 75, and 100% . It was shown that the motors performed at 3, 6, 9, and 12 RPM as expected. The oscilloscope waveforms can be seen in Appendix Q. Other components were not able to be tested before the COVID-19 crisis occurred.

### Future Construction

Due to the COVID-19 crisis the team was unable to complete the manufacturing of the device. The next steps to finish the device were as followed. First the adapter plates for the base needed to be welded onto the base. These are positioned with a center hole and the direction was labeled to make sure these are “square”. Then holes needed to be drilled through the plates of the base. After the plates have been welded onto the base the scissor lift is mounted onto the base using bolts and washers (4 per plate). Then the pads needed to be added to the scissor lift using ¼” screws. The small pad would align with the bottom of the lift and the large pad aligns with the top of the small pad. Next, would be to attach the T-tracks for the arms to the sides of the scissor lift. They would need to be centered and pilot holes would need to be drilled into the scissor lift. The T-track needs to be mounted with flat-head machine screws backed by a washer and bolt. Next, the track slider to arm plates using handles. Then the arm assembly needs to be attached to the arm plate using bolt and washers. Then slide the track-slider-arm-assembly into the t-track slot to complete the arm assembly. The next attachment is the leg assembly onto the scissor lift. Now the updated pins need to be inserted into each joint and the motors need to re-mounted. To protect the motors, the rest of the 3D-printed motor enclosures need to be printed. To control the scissor lift switches, need to be installed for the power and linear actuator control. Then the electrical enclosure constructed to protect the electronics would need to be mounted to the base. Lastly, to

guarantee the safety of the patient limit switches will be installed to prevent the hyper-extension of the joints should the programming fail-safe fail.

## Challenges

A major challenge that the team occurred during the construction of the project was the slippage of the pins when the motors shaft turned to move the leg linkages. Due to the pins being the key component that provide the movement to the linkages it was essential to resolve this issue. To overcome this issue, it was decided to drill a small hole through the motor shaft and the pivot pin to insert a pin to negate the slippage between the motor shaft and the pivot pin.

## Recommendations

When manufacturing the project potential improvements for the project were determined. Many of the potential improvements were electrical based. To protect the electronics and the wiring it an electrical enclosure box should be constructed. Install purchased electrical connectors between motors and wiring to electrical enclosures. To purchase 18/12 Shielded SOOW cable of approximately 75 ft and use for connections to each motor for a clean look and minimal wiring. Create a control box for all control switches. Change motors to stepper motors with gearbox reduction for better control. This would require a redesign of pins and attachment blocks. This should boost the performance of the system.

## Conclusion

As explained in detail in this report, the RWTD team was to build and optimizing a training device for the Department of Nursing and Health Sciences and Department of Health and kinesiology at UT Tyler. The goal of this device was to accurately recreate the motion of the ankle and knee in a gait cycle, and to electrically stimulate the appropriate muscle groups that function for the goal of rehabilitation for individuals who have had a minor spinal cord injury or a stroke. This device is significant as current rehabilitation devices require heavy manual labor for the physical therapist which can result in injury to the therapist.

The RWTD team have developed a linkage system that use 6 motors in conjunction with each other to produce the necessary gait path of the ankle and knee. While the FES system will be used to generate electrical simulations to rewire the synapses that have been damaged due to the injury. Multiple simulations were performed to test the viability of the design. The device was shown to be stable under the maximum applied load. The leg assembly was also proved to be capable of holding the maximum weight during the use of the rehabilitation. Multiple FEA showed that the key components of the device had the ability to withstand the rehabilitation sessions. A final simulation was performed to demonstrate that the leg assembly while attached to the scissor lift to show that the linkages would not have interference with any of the components.

The device was partial manufactured. The leg assembly was fully constructed, and all major components were ready for the complete assembly of the device before the occurrence of the COVID-19 pandemic. During the construction of the leg assembly, there was a challenge encountered with the pivot pins. Multiple options were devised. However, the decision to drill a small hole through the motor shaft and pivot pin to insert a small pin to negate slippage.

The code for the motors was constructed to generate the motion gait path. Individual codes were generated for each of the 6 motors. The FES system allows for the stimulation of the muscles in use during the rehabilitation leading to the optimization of the rehabilitation.

A brief overview of the project can be found in Appendix R.



## References

- [1] Luu, T. P., Low, K. H., Qu, X., Lim, H. B., & Hoon, K. H. (2014). Hardware Development and Locomotion Control Strategy for an Over-Ground Gait Trainer: NaTUre-Gaits. *Rehabilitation Devices and Systems*, 9.
- [2] Kim, J.-H., Chung, Y., Kim, Y., & Sujin, H. (2012) Functional electrical stimulation applied to gluteus medius and tibialis anterior corresponding gait cycle for stroke. *Gait & Posture*, 3.
- [3] Stewart, A., Pretty, C., & Chen, X. (2019). A Portable assist-as-need upper-extremity hybrid exoskeleton for FES-induced muscle fatigue reduction in stroke rehabilitation. *BMC Bio Medical Engineering*, 17.
- [4] Zhang, D., Ren, Y., Gui, K., Jia, J., & Xu, W. (2017). Cooperative Control for A HYbrdi Rehabilitation System Combining Functional Electrical Stimulation and Robotic Exoskeleton. *frontiers in Neuroscience*, 5.
- [5] J del-Ama, A., Gil-Agudo, A., Pons, J. L., & Juan, M. C. (2014). Hybrid FES-robot cooperative control of ambulatory gait rehabilitation exoskeleton. *Journal of Neuroengineering and Rehabilitation*, 15.
- [6] Anaya, F., Thangavel , P., & Yu, H. (2018). Hybrid FES–robotic gait rehabilitation technologies: a review on mechanical design, actuation, and control strategies. *International Journal of Intelligent Robotics and Applications*, 28.
- [7] Starkey, C. (2013). *Therapeutic Modalities*. Philadelphia: F.A. Davis Company.
- [8] Zhao, X., Li, H., Chen, T., Cao, B., & Li, X. (2019). Mechanical Properties of Aluminum Alloys under Low-Cycle Fatigue Loading. *materials*, 18.
- [9] Tözeren, A. (2000). *Human Body Dynamics: Classical Mechanics and Human Movement*. York: Springer-Verlag.
- [10] LaRosa, J. (2019, July 1). *U.s Physical Therapy Clinics Constitute a Growing \$34 Billion Industry*. Retrieved from Market Research Blog: <https://blog.marketresearch.com/u.s.-physical-therapy-clinics-constitute-a-growing-34-billion-industry>
- [11] VanHiel, L. (n.d.). *Spinal Cord Injury and Gait Training*. Retrieved from Model Systems Knowledge Translation Center: <https://msktc.org/sci/factsheets/Gait-Training-and-SCI>
- [12] Varotsis, A. B. (2018, September 5). *CNC Machining Is More Accessible Than You May Think*. Retrieved from Manufacturing.net: <https://www.manufacturing.net/industry40/article/13245730/cnc-machining-is-more-accessible-than-you-may-think>

## Appendix A

## Appendix B

### Analysis of the Center of Mass: Lowered vs. Raised System

The mass of the RWTD Assembly is as follows:

- Mass = 341.56 *lb*

The lowered system, as seen in Figure A.1, has a center of mass of:

- X = 8.03 *in.*
- Y = 11.77 *in.*
- Z = 19.65 *in.*

The raised system, as seen in Figure A.2, has a center of the mass of:

- X = 8.03 *in.*
- Y = 17.43 *in.*
- Z = 19.49 *in.*

#### Lowered

- Principal axes of inertia and principal moments of inertia: (*lb \* in.<sup>2</sup>*)
- Taken at the center of mass.
  - $I_x = (-0.01, 0.17, 0.98)$        $P_x = 37638.72$
  - $I_y = (0.28, -0.94, 0.17)$        $P_y = 86272.22$
  - $I_z = (0.96, 0.28, -0.04)$        $P_z = 90809.10$
- Moments of inertia: (*lb \* in.<sup>2</sup>*)
- Taken at the center of mass and aligned with the output coordinate system.
  - $L_{xx} = 90435.36$      $L_{xy} = -1322.39$      $L_{xz} = -381.70$
  - $L_{yx} = -1322.39$      $L_{yy} = 85185.92$      $L_{yz} = 8311.57$
  - $L_{zx} = -381.70$      $L_{zy} = 8311.57$      $L_{zz} = 39098.76$
- Moments of inertia: (*lb \* in.<sup>2</sup>*)
- Taken at the output coordinate system.
  - $I_{xx} = 269668.07$      $I_{xy} = 30949.42$      $I_{xz} = 53501.00$

- $I_{yx} = 30949.42$      $I_{yy} = 239108.90$      $I_{yz} = 87318.15$
- $I_{zx} = 53501.00$      $I_{zy} = 87318.15$      $I_{zz} = 108427.41$

Raised

- Principal axes of inertia and principal moments of inertia: ( $lb * in.^2$ )
- Taken at the center of mass.
  - $I_x = (-0.02, 0.99, -0.15)$      $P_x = 73766.07$
  - $I_y = (-0.03, 0.15, 0.99)$      $P_y = 86649.43$
  - $I_z = (1.00, 0.02, 0.02)$      $P_z = 126668.07$
- Moments of inertia: ( $lb * in.^2$ )
- Taken at the center of mass and aligned with the output coordinate system.
  - $L_{xx} = 12661.12$      $L_{xy} = -1186.40$      $L_{xz} = -942.58$
  - $L_{yx} = -1186.4$      $L_{yy} = 74080.67$      $L_{yz} = -1296.20$
  - $L_{zx} = -942.58$      $L_{zy} = -1926.20$      $L_{zz} = 86385.78$
- Moments of inertia: ( $lb * in.^2$ )
- Taken at the output coordinate system.
  - $I_{xx} = 36002.16$      $I_{xy} = 46596.45$      $I_{xz} = 52489.8$
  - $I_{yx} = 46596.45$      $I_{yy} = 225807.97$      $I_{yz} = 114076.24$
  - $I_{zx} = 52489.80$      $I_{zy} = 114076.24$      $I_{zz} = 212132.44$

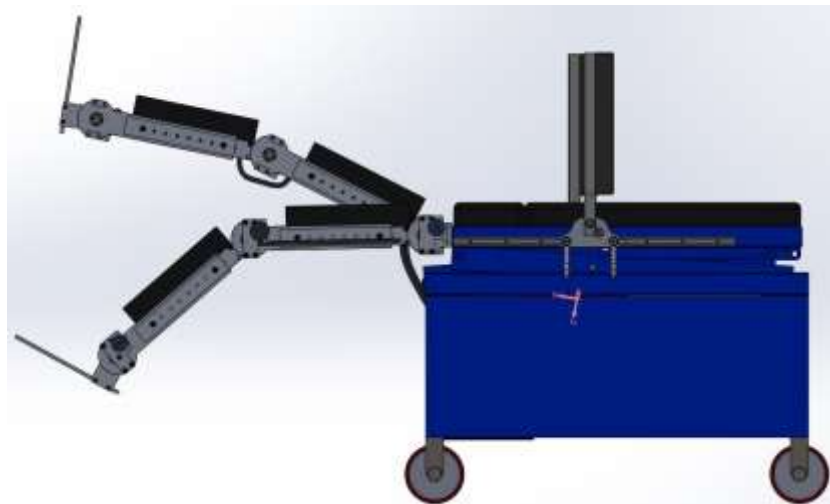


Figure B 1. Assembly Center of Mass- Lift Lowered.



Figure B 2. Assembly Center of Mass- Lift Raised.



Figure B 3. New Steel Base for RWTD.

## Appendix C

It was determined that approximately  $100 \text{ steps} = 1 \text{ cycle}$ . Assuming a therapy session lasts 30 minutes. During this time 900 steps will be taken as seen in Equation (1).

$$30 \frac{\text{min}}{\text{session}} = 1800 \text{ secs} * \frac{1 \text{ step}}{2 \text{ secs}} = 900 \frac{\text{steps}}{\text{session}} \quad (1)$$

Thus, in one session there is 9 cycles.

Finally, as the Aluminum will fatigue at  $10^7$  cycles, Equation (2) shows how many sessions the Aluminum can be used before replacement is needed.

$$\frac{10^7 \text{ cycles}}{9 \frac{\text{cycles}}{\text{session}}} \cong 1,111,111 \text{ sessions} \quad (2)$$

The number of sessions used was rounded down to 1,000,000 to allow for the material to be changed before any fatigue behavior would start to occur in the Aluminum.

## Appendix D

The table below displays the motor specifications.

Table D 1. Motor Specifications of the ServoCity Motor.

Model	ServoCity 12 RPM HD Premium Planetary Gear Motor w/ Encoder
Part Number	638310
Input Voltage Nominal	12 V
Input Voltage (recommended)	6 V – 12 V
Speed (No Load)	12 RPM
Current (No Load)	0.54 A
Current (Stall)	20 A
Torque (Stall)	8,110.2 oz-in (584 kgf-cm)
Gear Ratio	720.989:1
Gear Material	Brass primary, nylon secondary, steel tertiary
Gearbox Style	Planetary
Motor Type	DC
Motor Brush Type	Graphite
Output Shaft Diameter	6 mm
Output Shaft Style	D-shaft
Output Shaft Support	Dual Ball Bearings
Electrical Connection	PH Series JST 6-pin Connector (2 mm Pitch)
Operating Temperature	–10° C ~ + 60° C
Mounting Screw Size	M3 x 0.5 mm
Weight	380 g
Encoder: Cycles Per Revolution (Motor Shaft)	12
Encoder: Cycles Per Revolution (Output Shaft)	8,651.868
Encoder: Countable Events Per Revolution (Motor Shaft)	48
Encoder: Countable Events Per Revolution (Output Shaft)	34,607.427
Encoder Type	Relative, Quadrature
Encoder Sensor Type	Magnetic (Hall Effect)
Encoder Sensor Input Voltage Range	2.4 V – 26 V
Encoder Sensor Output Pulse Amplitude	≅ Sensor Input Voltage

## Appendix E

### Appendix E1

#### Defined Variables for Calculations

Table E 1. Percent of Weight for Body Parts.

Body Part	Male	Female
Thigh	10.5 %	8.3 %
Lower Leg	4.5 %	5.5 %
Foot	1.5 %	1.2 %

Since the leg assembly will be at an angle of  $\theta = 31.175^\circ$  when in use. The distributed mass of each leg section was evaluated at an that angle. The forces were applied in the middle of each subassembly as the loads were assumed to be evenly distributed. The linkages extend out to be 19.5 *in* each equating to a total of 39 *in*.

Weight of a Thigh Subassembly at  $\theta = 31.175^\circ$  as seen in Equation (1):

$$W_{ta} = 4.36 \text{ lb} * \sin 31.175 = 2.26 \text{ lb} \quad (1)$$

Weight of a Lower Leg Subassembly at  $\theta = 31.175^\circ$  as seen in Equation (2):

$$W_{la} = 3.81 \text{ lb} * \sin 31.175 = 1.97 \text{ lb} \quad (2)$$

Weight of a Foot Sub Assembly at  $\theta = 31.175^\circ$  as seen in Equation (3):

$$W_{fa} = 2.25 \text{ lb} * \sin 31.175 = 1.16 \text{ lb} \quad (3)$$

Weight of the Motor at  $\theta = 31.175^\circ$  as seen in Equation (4):

$$W_m = 0.21 \text{ lb} * \sin 31.175 = .108 \text{ lb} \quad (4)$$

Weight of the Thigh:

$$W_t = 31.5 \text{ lb}$$

Weight of the Lower Leg:

$$W_l = 13.5 \text{ lb}$$

Weight of the Foot:

$$W_f = 4.5 \text{ lb}$$



Weight of the total leg assembly and a human leg

$$W_{total} = 55.11 \text{ lb}$$

Distances for analysis:

$$d_1 = 9.75 \text{ in}$$

$$d_2 = 19.5 \text{ in}$$

$$d_3 = 29.25 \text{ in}$$

$$d_4 = 39 \text{ in}$$

$$d_5 = 40 \text{ in}$$

## Appendix E.2

### Torque Needed

The torque is defined in Equation (5)

$$T = F * d \quad (5)$$

Where

$F$  = force

$d$  = distance from the point of the torque to the force

Therefore, the amount of torque needed to power the leg assembly is  $278.73 \text{ in} - \text{lb}$ .

## Appendix E.3

### Speed Motors Output

The maximum amount the gears have to turn at any of the gears is  $38^\circ$ . The speed of the gear motor is  $12 \text{ RPM}$  which is reduced to  $4 \text{ RPM}$  due to the 3:1 gear ratio between the driver and the driven gear. The gear turns  $24^\circ$  per second as seen in Equation (6).

$$4 \frac{\text{rev}}{\text{min}} * \frac{360^\circ}{1 \text{ rev}} * \frac{1 \text{ min}}{60 \text{ sec}} = 24 \frac{^\circ}{\text{sec}} \quad (6)$$

Equation (7) shows that the gear takes  $1.583 \text{ seconds}$  to go  $38^\circ$ .

$$\frac{38^\circ}{24^\circ/\text{sec}} = 1.583 \text{ sec} \quad (7)$$

## Appendix E.4

### Torque of the Motor

The original torque output from the gear motor is  $506.8875 \text{ in} - \text{lb}$ .

This torque was increased as the output shaft is being used at  $\frac{1}{4} \text{ in}$  instead of  $1 \text{ in}$  allowing the torque to be quadrupled to  $2027.55 \text{ in} - \text{lb}$ .

## Appendix E.5

### Static Load of Device

The weight of the components that the linear actuator needs to be able to move are as following:

- Weight of the person,  $W_p = 300 \text{ lb}$
- Weight of the whole leg assembly,  $W_{la} = 11.05 \text{ lb}$
- Weight of the arm assembly,  $W_{aa} = 10.42 \text{ lb}$
- Weight of the table lift,  $W_l = 50 \text{ lb}$

The total weight,  $W_t$ , defined in Equation (8).

$$W_p + W_{la} + W_{aa} + W_l = W_t \quad (8)$$

The total weight needs to be less than the static force of the linear actuator, defined in Equation (9).

$$W_t < F_s \quad (9)$$

Where  $F_s = 400 \text{ lb}$  is the static force of the linear actuator.

## Appendix E.6

### Shear Stress on Pivot Pin

The shear stress is defined in Equation (10)

$$\tau = \frac{Tr}{J} \quad (10)$$

Where

$T$  =torque

$r$  = distance from center to stressed surface

$J$  = polar moment of inertia

The pivot pin at the hip joint will be analyzed, as this is the point that will have the highest amount of shear stress when compared to the other joints.

For the analysis of the pivot pin, four polar moments of inertia have to be defined in Equation (11), (12), (13) and (14) respectively.

$$J_{cl} = \frac{1}{2}\pi r^4 = 10.953 \text{ in}^4 \quad (11)$$

Where  $r = 1.625 \text{ in}$

Where  $J_{cl}$  is defined as the polar moment of inertia of the circular part of the linkages.

$$J_s = \frac{1}{12}bh_s(b^2 + h_s^2) = 0.169 \text{ in}^4 \quad (12)$$

Where  $h_s = 2 \text{ in}$  and  $b = 0.25 \text{ in}$

Where  $J_s$  is defined as the polar moment of inertia of spacers between the two outside linkages.

$$J_l = \frac{1}{12}bh_l(b^2 + h_l^2) = 0.074 \text{ in}^4 \quad (13)$$

Where  $h_l = 1.51 \text{ in}$  and  $b = 0.25 \text{ in}$

Where  $J_l$  is defined as the as the polar moment of inertia of rectangular part of the linkage.

$$J_a = \frac{1}{12}bh_a(b^2 + h_a^2) = 6.973 \text{ in}^4 \quad (14)$$

Where  $h_a = 6.94 \text{ in}$  and  $b = 0.25 \text{ in}$

Where  $J_a$  is defined as the as the polar moment of inertia of the ankle sub assembly.

The shear stress was divided into 5 areas to simplify the final calculation as seen in Equation (15), (16), (17), (18), and (19) respectively.

$$\tau_1 = \frac{(W_t + W_{ta}) * (d_1)^2}{4J_{cl} + 2J_s + 4J_l} = 72.21 \text{ psi} \quad (15)$$

$$\tau_2 = \frac{(W_m) * (d_2)^2}{2J_{cl}} = 1.87 \text{ psi} \quad (16)$$

$$\tau_3 = \frac{(W_l + W_{la}) * (d_3)^2}{4J_{cl} + 2J_s + 4J_l} = 297.79 \text{ psi} \quad (17)$$

$$\tau_4 = \frac{(W_m) * (d_4)^2}{2J_{cl}} = 7.49 \text{ psi} \quad (18)$$

$$\tau_5 = \frac{(W_f + W_{fa}) * (d_5)^2}{J_a} = 1298.72 \text{ psi} \quad (19)$$

Thus, the total shear stress,  $\tau_t$ , defined in Equation (20)

$$\tau_t = \tau_1 + \tau_2 + \tau_3 + \tau_4 + \tau_5 \quad (20)$$

$$\tau_t = 1678.08 \text{ psi}$$

## Appendix E.7

### Shear Stress On the 4 Bolts at the Hip Mount Joint Connection to the Lift

The centroid of the bolt plane had to be determined to analyze the Moment. The coordinates of each screw can be seen in Table E.2.

Table E.2. Coordinates of Each Screw.

Point	X-Coordinate (inch)	Y-Coordinate (inch)	Z-Coordinate (inch)
1	0	0	0
2	1.5	0	0
3	0	0	1.25
4	1.5	0	1.25

The centroid is then determined using Equations (21), (22), and (23).

$$x_c = \frac{x_1 + x_2 + x_3 + x_4}{4} = 1.5 \text{ in} \quad (21)$$

$$y_c = \frac{y_1 + y_2 + y_3 + y_4}{4} = 0 \text{ in} \quad (22)$$

$$z_c = \frac{z_1 + z_2 + z_3 + z_4}{4} = 0.625 \text{ in} \quad (23)$$

Next, the moment about the centroid is determined. The z-coordinate is not necessary in this calculation as there is no forces acting in the z-direction.

The coordinates for the forces were defined as the following

Table E.3. Coordinates for the Forces acting on the Leg Subassembly.

Force (lb.)	X-Coordinate (inch)	Y-Coordinate (inch)
$W_t$	0	9.75
$W_{ta}$	0	9.75
$W_{m1}$	0	19.5
$W_{la}$	0	29.75
$W_l$	0	29.25
$W_{m2}$	0	39
$W_{fa}$	0	40
$W_f$	0	40



The moment of the Centroid was found using Equation (25)

$$M_c = (F_y * dx) - (F_x * dy) \quad (24)$$

The Moment was found to be 1288.997 *lb – in* in the counter-clockwise direction.

The reaction of each fastener can be determined as a function from the centroid of the pattern and the load at the centroid. There are two parts of the reactions to determine the shear. The first part has X and Y components which is based on the moment that is applied, while the second part is the same for all fasteners.

The first part is determined by Equation (25) and (26).

$$P_{x-direction\ from\ Moment,i} = \frac{M_c * (y_i - y_c)}{\sum dist_{all\ fastners}^2} \quad (25)$$

$$P_{y-direction\ from\ Moment,i} = \frac{M_c * (x_i - x_c)}{\sum dist_{all\ fastners}^2} \quad (26)$$

Where  $x_i$  and  $y_i$  are the X and Y coordinates from the original position

The second part is determined by Equation (27) and (28).

$$P_{from\ shear\ x} = \frac{applied\ shear\ in\ x - direction}{number\ of\ fastners} \quad (27)$$

$$P_{from\ shear\ y} = \frac{applied\ shear\ in\ y - direction}{number\ of\ fastners} \quad (28)$$

Finally, the total load acting on the fastener,  $P_i$  is calculated by Equation (29).

$$P_i = \sqrt{(P_{x-direction\ from\ Moment,i} - P_{from\ shear,x})^2 + (P_{y-direction\ from\ Moment,i} - P_{from\ shear,y})^2} \quad (29)$$

To calculate the distance from the fastener to the centroid is determined by Equation 30.

$$dist_i = \sqrt{(x_i - x_c)^2 + (y_i - y_c)^2} \quad (30)$$

Where  $x_i$  and  $y_i$  are the X and Y coordinates from the original position.

The distances are as shown:

$$dist_1 = 1.5\ in$$

$$dist_2 = 0 \text{ in}$$

$$dist_3 = 1.5 \text{ in}$$

$$dist_4 = 0 \text{ in}$$

The load at each fastener/screw needs to be determined to locate where the highest load is being applied.

The load at each fastener can be seen:

$$P_1 = 432.71 \text{ in} - lb$$

$$P_2 = 17.03 \text{ in} - lb$$

$$P_3 = 432.71 \text{ in} - lb$$

$$P_4 = 17.03 \text{ in} - lb$$

## Appendix F

The gear ratio is 2163:1 and counts per revolution (CPR) of the input motor shaft is 103,824 CPR. The Hall sensor is quadrature using two channels A and B. Only the pulses per revolution of channel A need to be accounted for as seen in Equation (1).

$$\frac{103824 \text{ CPR}}{4} = 25956 \text{ PPR} \quad (1)$$

The speed of the motor is 4 RPM. Next, the rotations per second can be calculate, as seen in Equation (2).

$$\frac{4 \text{ Rotations}}{60 \text{ sec}} = 0.067 \text{ RPS} \quad (2)$$

Now, in Equation (3) the number of pulses per second can be calculated.

$$(0.067 \text{ RPS})(25956 \text{ PPR}) = 1740 \text{ PPS} \quad (3)$$

Finally, the period between each rising edge of the square wave pulse can be determined as seen in Equation (4).

$$\frac{1}{1740 \text{ PPS}} = 575 \mu\text{s} \quad (4)$$

## Appendix G

### Electrical Calculations-Power Analysis

The final stall torque of the motor is  $2027.55 \text{ in} - \text{lb}$ , calculations for this can be seen in Appendix E.4.

Given the motor stall current is 20A, we can calculate the amps per  $\text{lb} \cdot \text{in}$  of torque as seen in Equation 6.

$$\frac{20 \text{ A}}{6082.8 \text{ lb} \cdot \text{in}} = 0.0033 \frac{\text{A}}{\text{lb} \cdot \text{in}} \quad (6)$$

Now, the hip, knee and ankle motor current consumption for the gait system's maximum limit of a 300lb. with a 6'4" tall person can be determined using Equation 7, 8, and 9 respectively. The torque on the motors for such a person is  $1377.0 \text{ in} - \text{lb}$  at the hip,  $392.7$  at the knee, and  $8.8 \text{ lb} \cdot \text{in}$  at the ankle.

$$\text{Hip motor current usage} = \left(0.0033 \frac{\text{A}}{\text{lb} \cdot \text{in}}\right) (278.73 \text{ lb} \cdot \text{in}) = 0.9 \text{ A} \quad (7)$$

$$\text{Knee motor current usage} = \left(0.0033 \frac{\text{A}}{\text{lb} \cdot \text{in}}\right) (94.1 \text{ lb} \cdot \text{in}) = 0.3 \text{ A} \quad (8)$$

$$\text{Ankle motor current usage} = \left(0.0033 \frac{\text{A}}{\text{lb} \cdot \text{in}}\right) (6.8 \text{ lb} \cdot \text{in}) = 0.002 \text{ A} \quad (9)$$

Since the calculated ankle and knee motor current usage is so small, it is assumed it has negligible load applied to it. In addition, the no load current of a motor is 0.54A. Therefore, the calculations assume the ankle and knee motor current usage is 0.54A. Now, the total current consumption can be determined using Equation 10.

$$\text{Total current consumption} = (2)(4.5 + 0.54 + 0.54) \text{ A} = 3.96 \text{ A} \quad (10)$$

In conclusion, the chosen transformer used to power the system that has an output current of 30A is sufficient to drive all six of the motors under load.

## Appendix H



Figure H 1. MINZO 120V AC to 12VDC Transformer.

Table H 1. MINZO 120VAC to 12VDC Transformer Specifications.

Model	MINZO S-120-12
AC Input Voltage	100 V – 240 V
Input Voltage Frequency	50 Hz – 60 Hz
DC Output Voltage	12 V
Output Current	0 A – 30 A
Output Voltage Adjustable Range	±10%
Output Voltage Tolerance	±1%
Nominal Power	360 W
Fan Temperature Control	45° C
Dimensions	215 mm x 115 mm x 50 mm

## Appendix J

### **User Manual**

This manual describes the step by step instructions of how to operate the Robotic Walking Training Device (R.W.T.D).

1. Move the device into position and lock the wheels.
2. Lift the arm rests into the upward position.
3. Carefully move the patient into the R.W.T.D and strap the patient in using the abdominal and leg straps. Attach the FES on the quadricep. Then lower the arm rests.
4. Slowly raise the R.W.T.D past the necessary position. Lower the lock bars on the scissor lift and the lower the scissor lift till the lock bars are securely in place.
5. Before starting the R.W.T.D ensure that all the wires are secure and will not interfere with the leg assembly when it is in motion.
6. Start the R.W.T.D and then once the patient is comfortable with the device turn on the F.E.S
7. Sessions last for 30 minutes to ensure the patient muscles are not over worked or over-stimulated.
8. Once the session is over, turn off the R.W.T.D and the F.E.S. Raise the scissor lift and raise the lock bars then lower the scissor lift back to a horizontal position.
9. Raise the arm supports and unstrap the patient and remove the F.E.S.
10. Remove the patient from the device

## **Safety**

To ensure the safety of the patient when the device is in use these steps should be taken before every patient is placed into the device.

1. Inspect all the wires for any breaks or tears that might lead to a short circuit or cause potential harm to the patient.
2. Inspect the leg assembly to make sure that there is no damage.
3. Examine the U.H.M.W spacer that is located between each of the linkages. If there is visible wear, replace the spacer.
4. Check the straps for any tears or defects that might lead to the patient become injured.
5. Clean the device with disinfectant after each patient to ensure the health and safety of the next patient.

## Appendix K

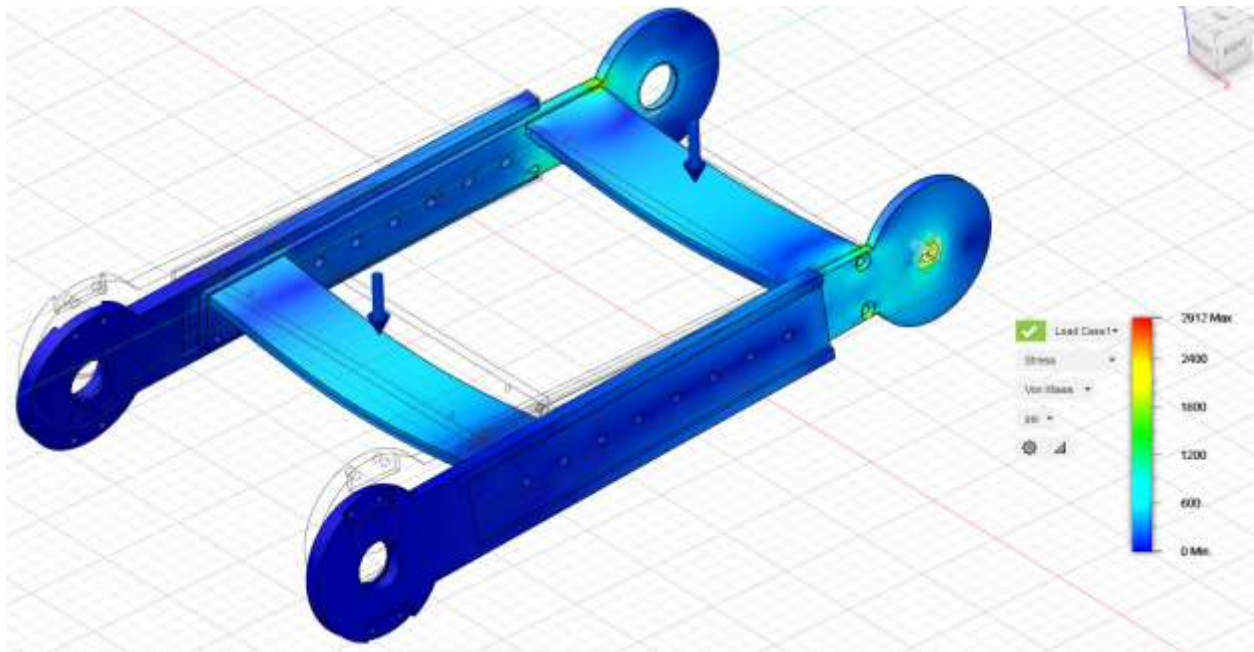


Figure K 1. Von Mises Stress of Thigh Sub-Assembly Under Expected Loading.

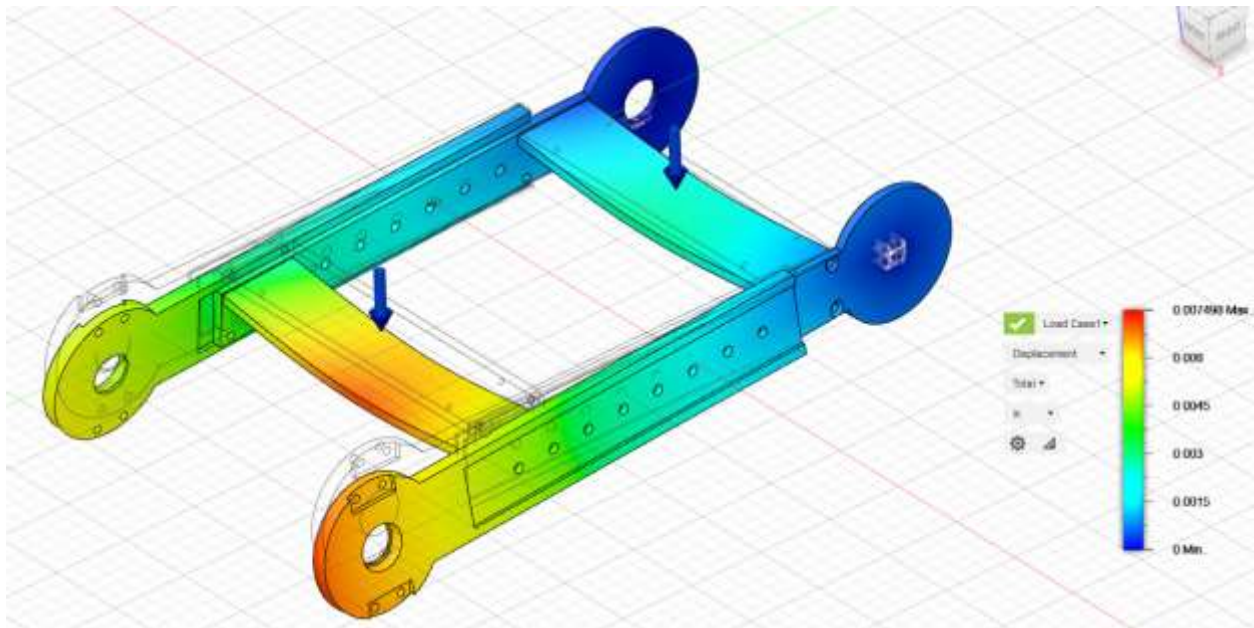


Figure K 2. Total Deformation of Thigh Sub-Assembly Under Expected Loading.



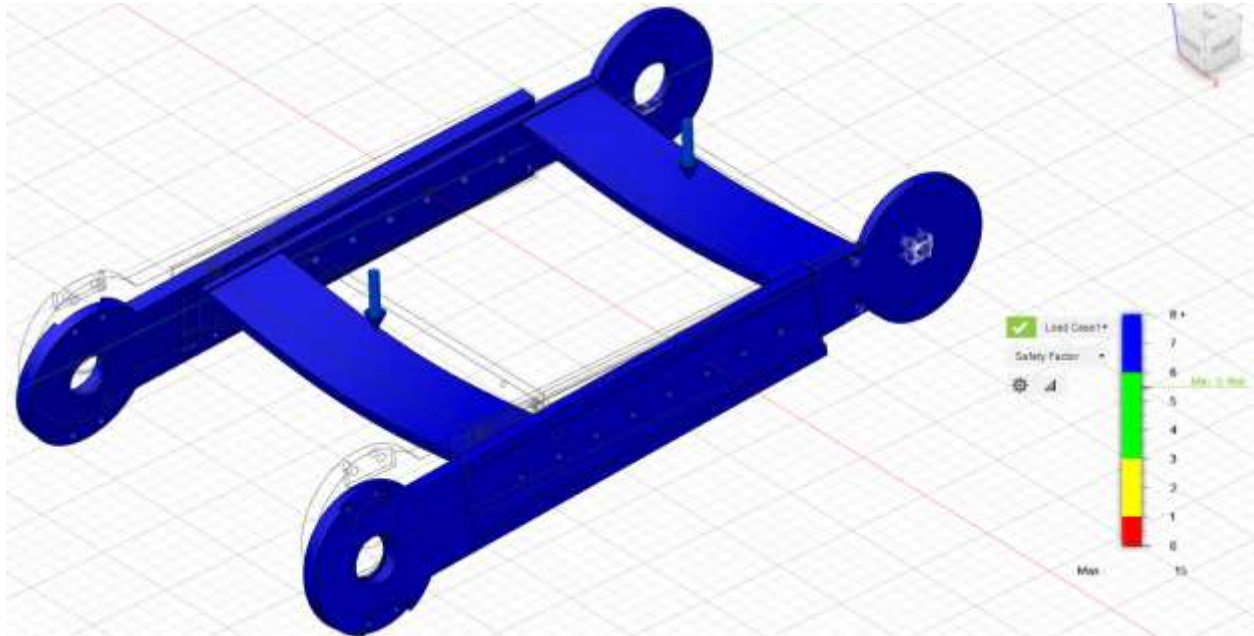


Figure K 3. Safety Factor of Thigh Sub-Assembly Under Expected Loading.

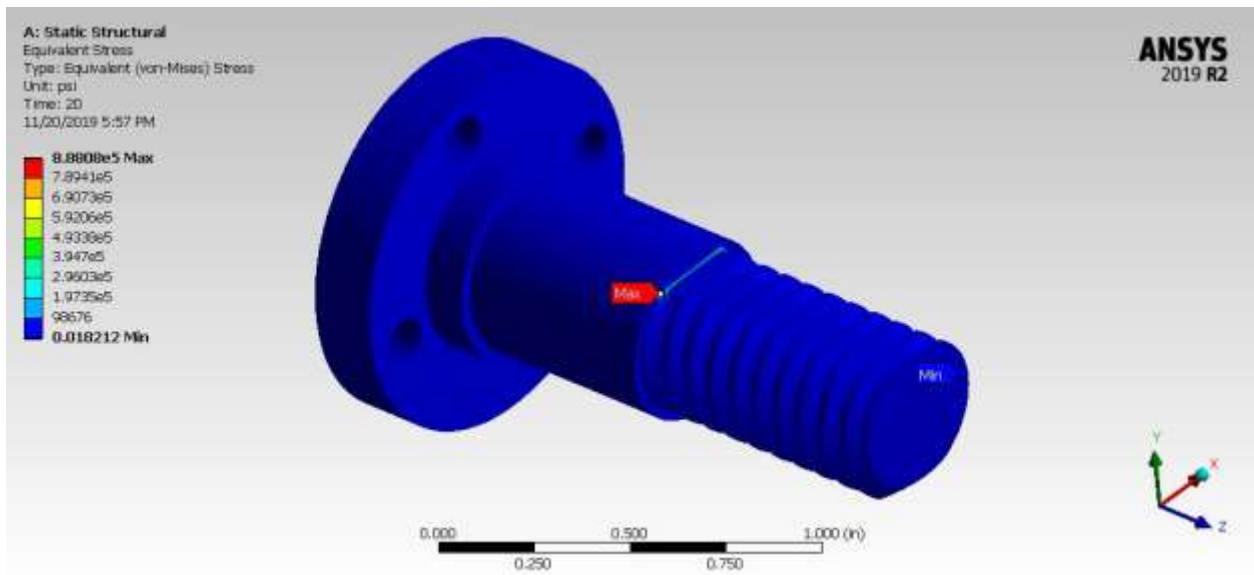


Figure K 4. Von-Mises Stress on Pivot Pin.

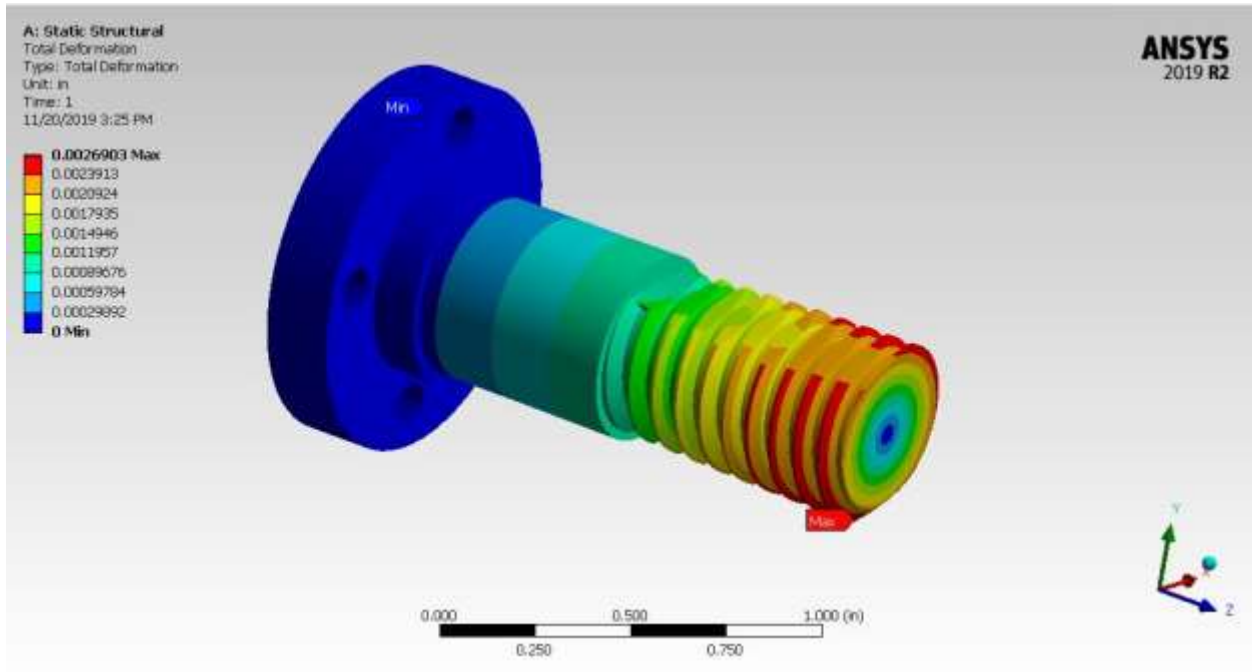


Figure K 5. Total Deformation of the Pivot Pin.

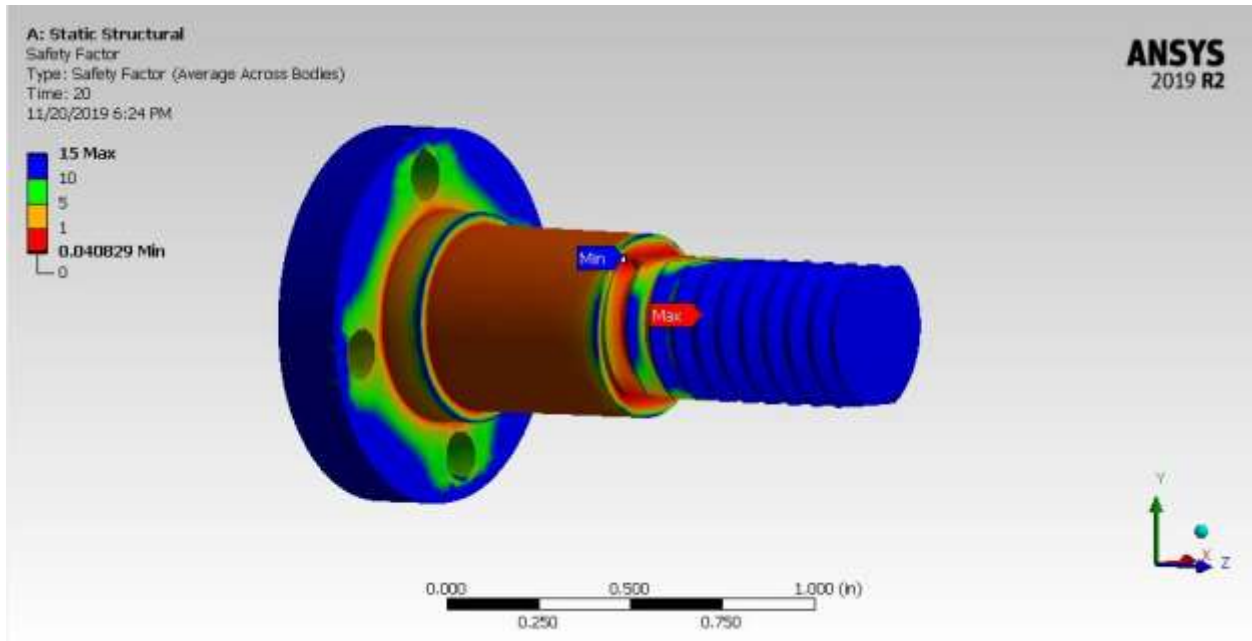


Figure K 6. Safety Factor of the Pivot Pin.

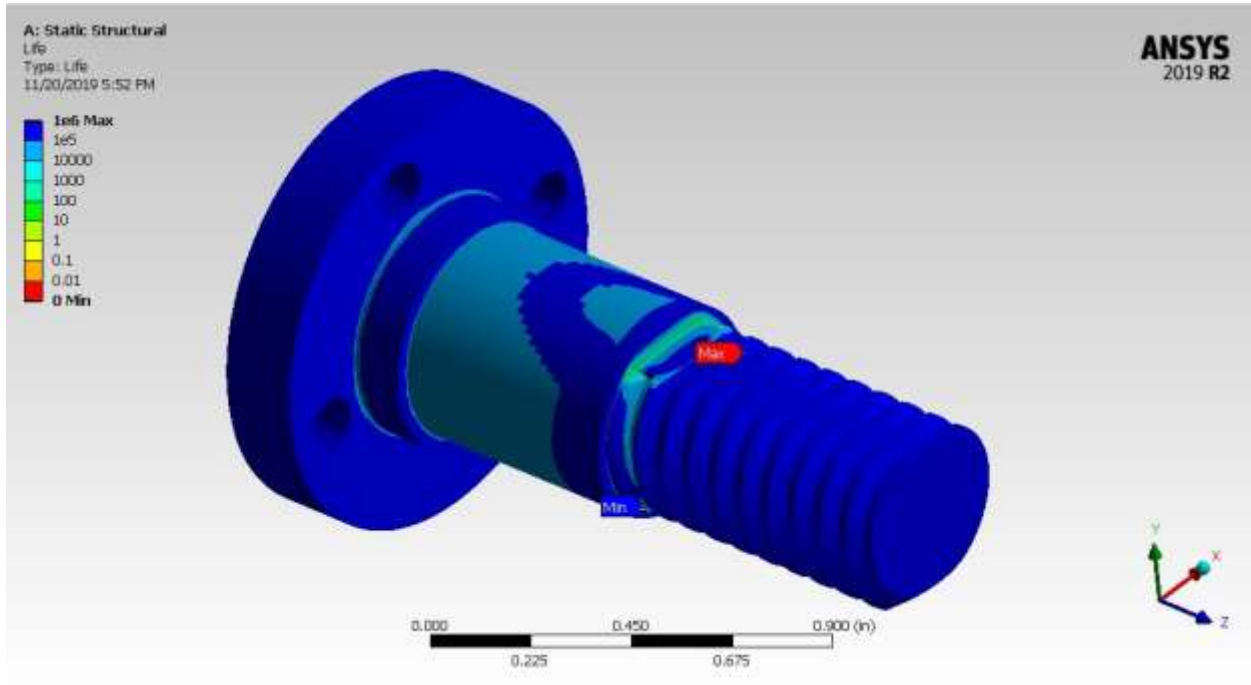


Figure K 7. Life Cycle of the Pivot Pin.

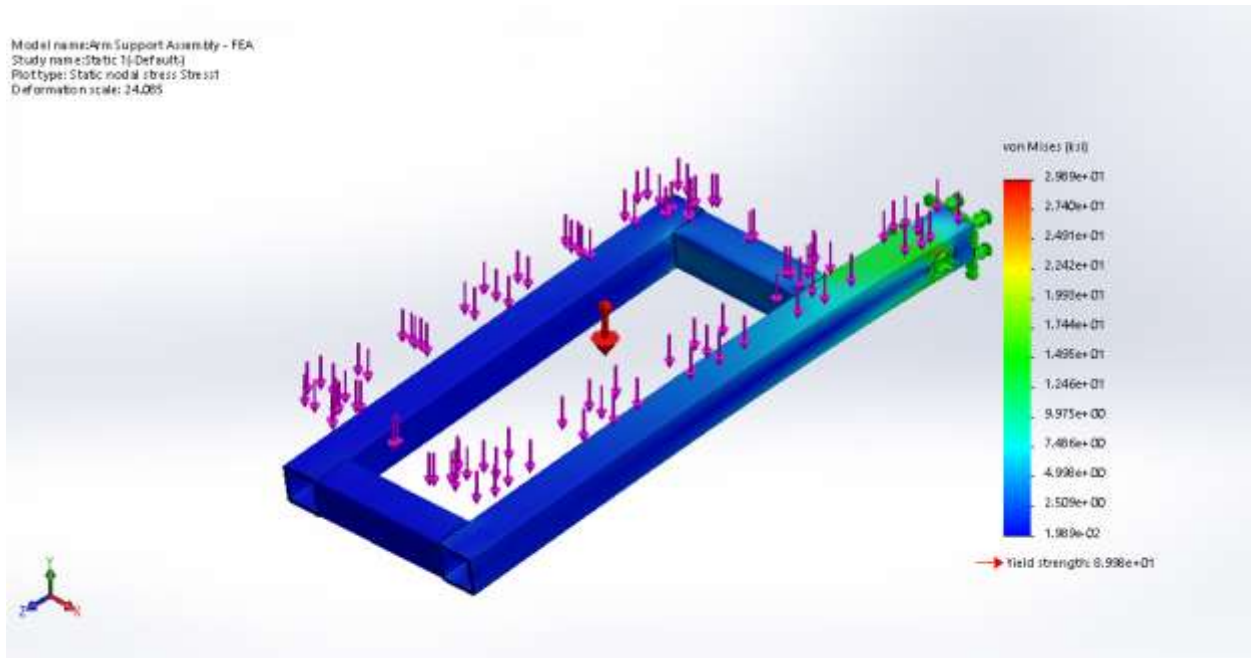


Figure K 8. Von Mises Stress of Arm Support Under Expected Maximum Loading.

Model name: Arm Support Assembly - FEA  
Study name: Static 1 (Default)  
Plot type: Static displacement, Displacement1  
Deformation scale: 24.065

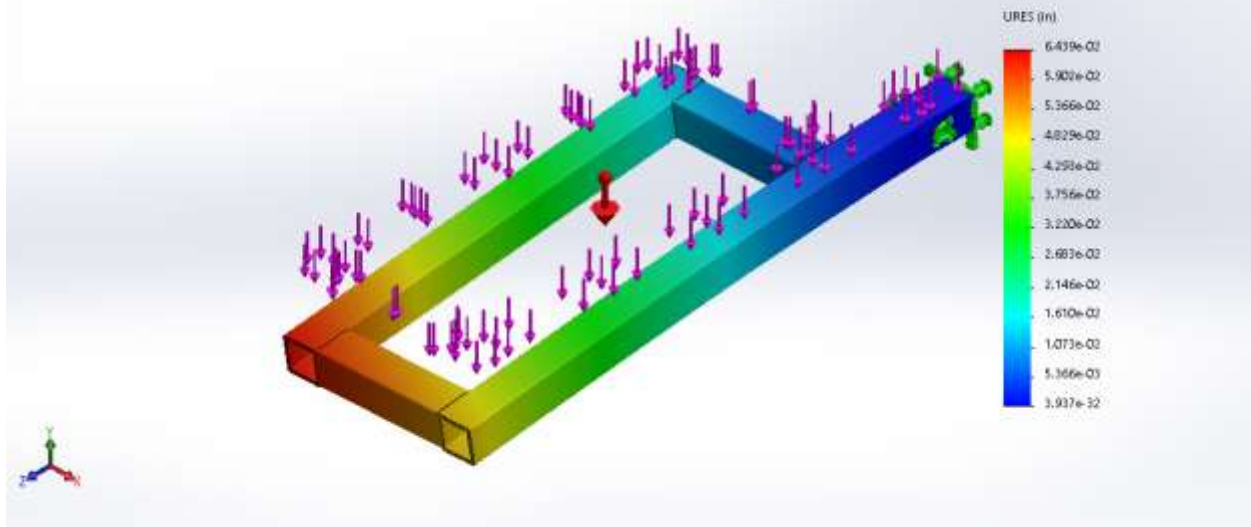


Figure K 9. Total Deformation of Arm Support Under Expected Maximum Loading.

Model name: Arm Support Assembly - FEA  
Study name: Static 1 (Default)  
Plot type: Static stress, Sstress1  
Deformation scale: 24.065

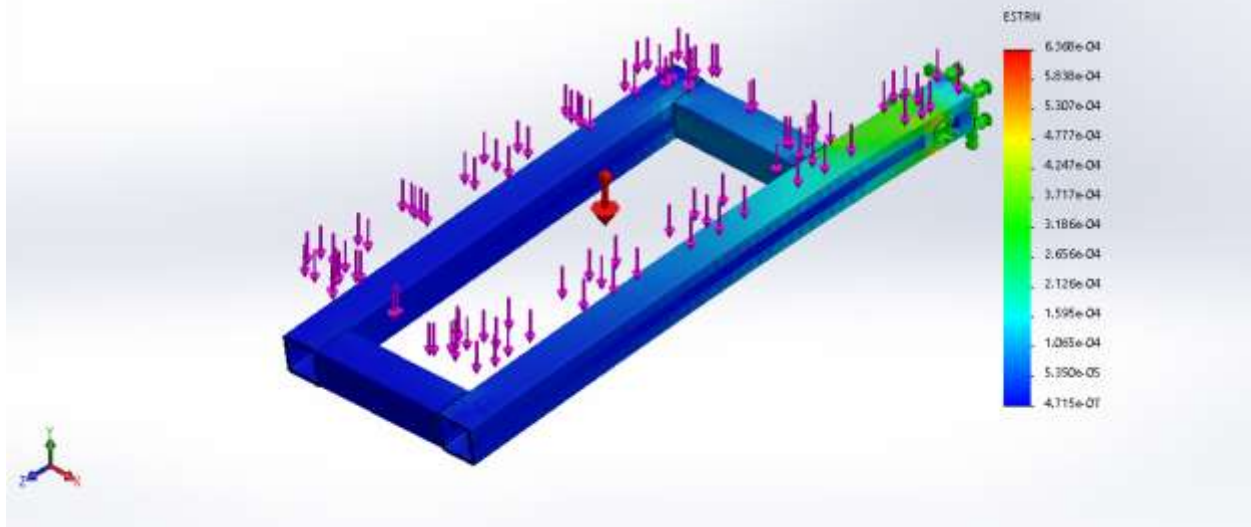


Figure K 10. Equivalent Stress of Arm Support Under Expected Maximum Loading.

Model name: Arm Support Assembly - FEA  
Study name: Static 1 (Default)  
Plot type: Factor of Safety Factor of Safety1  
Criteria: Max von Mises Stress  
Factor of safety distribution: Min FOS = 3

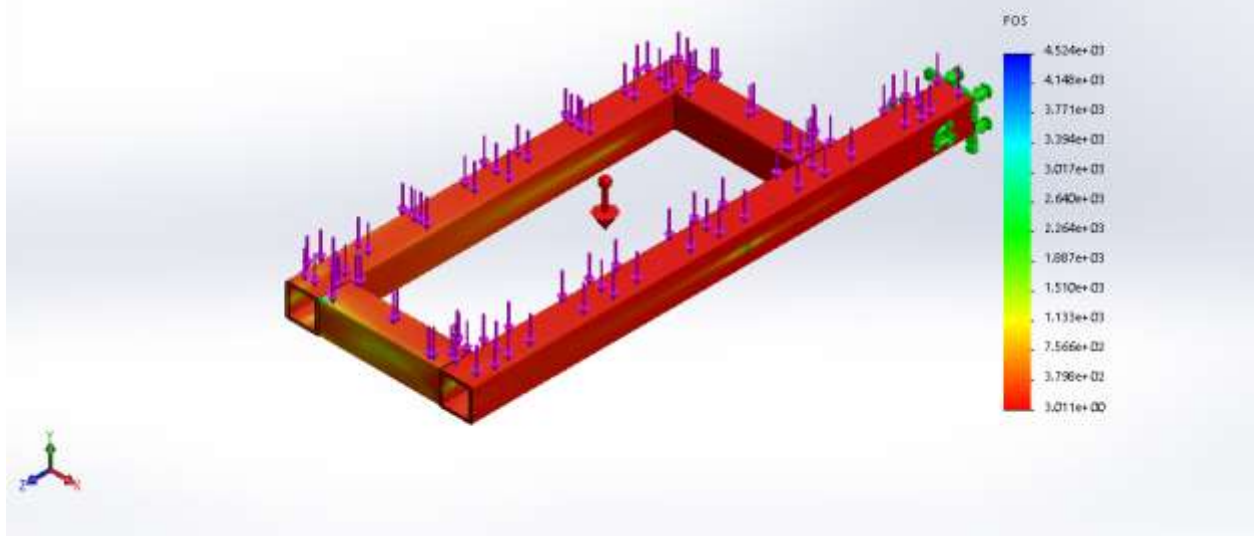


Figure K 11. Safety Factor of Arm Support Under Expected Maximum Loading.

## Appendix L

This Appendix shows all Mechanical Drawings and Final Manufacturing drawings

## Appendix L.1

Contained within this Sub Appendix is the Mechanical Drawings of the RWTD

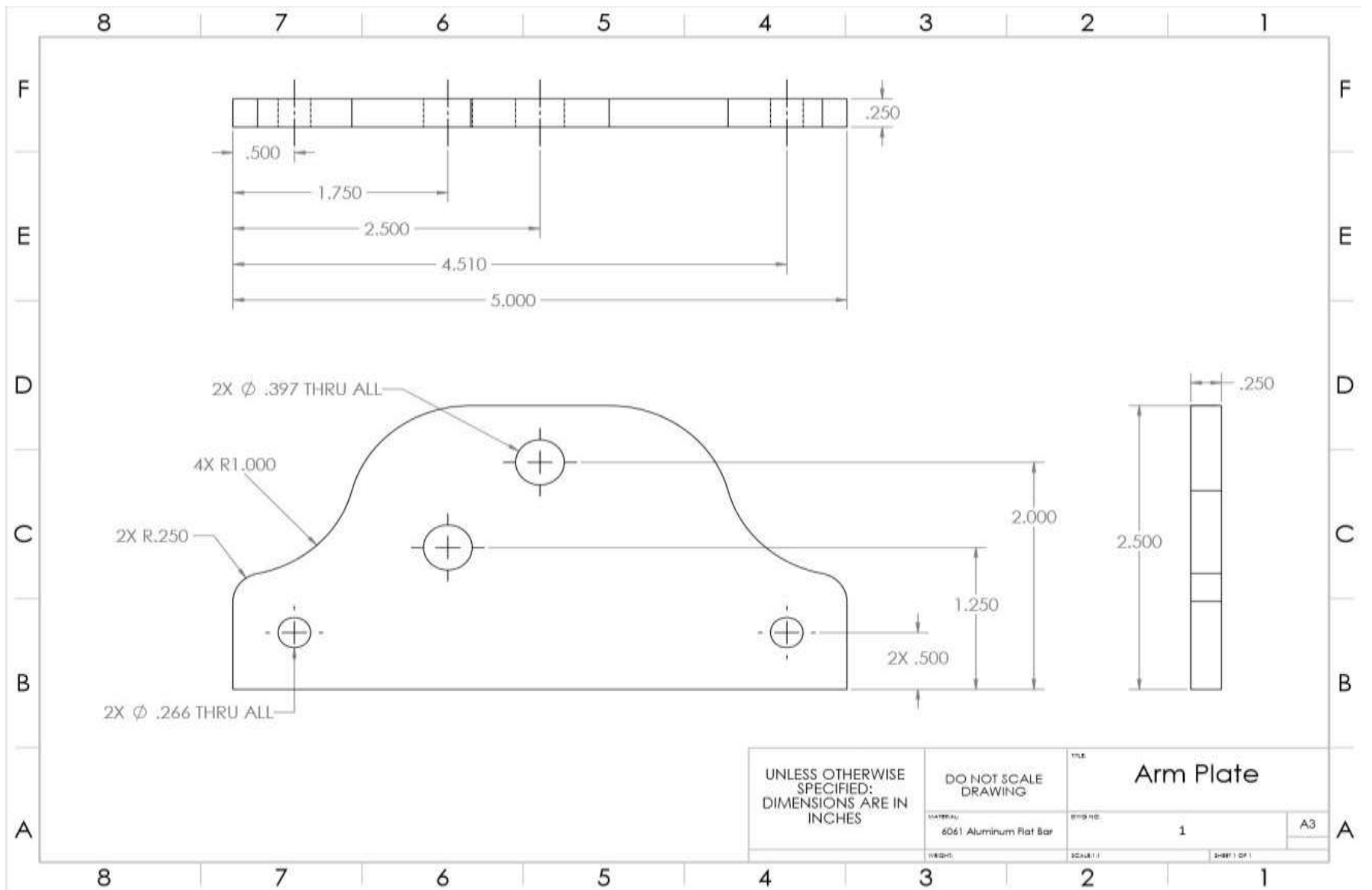


Figure L.1. 1. Mechanical Drawing of Arm Plate.



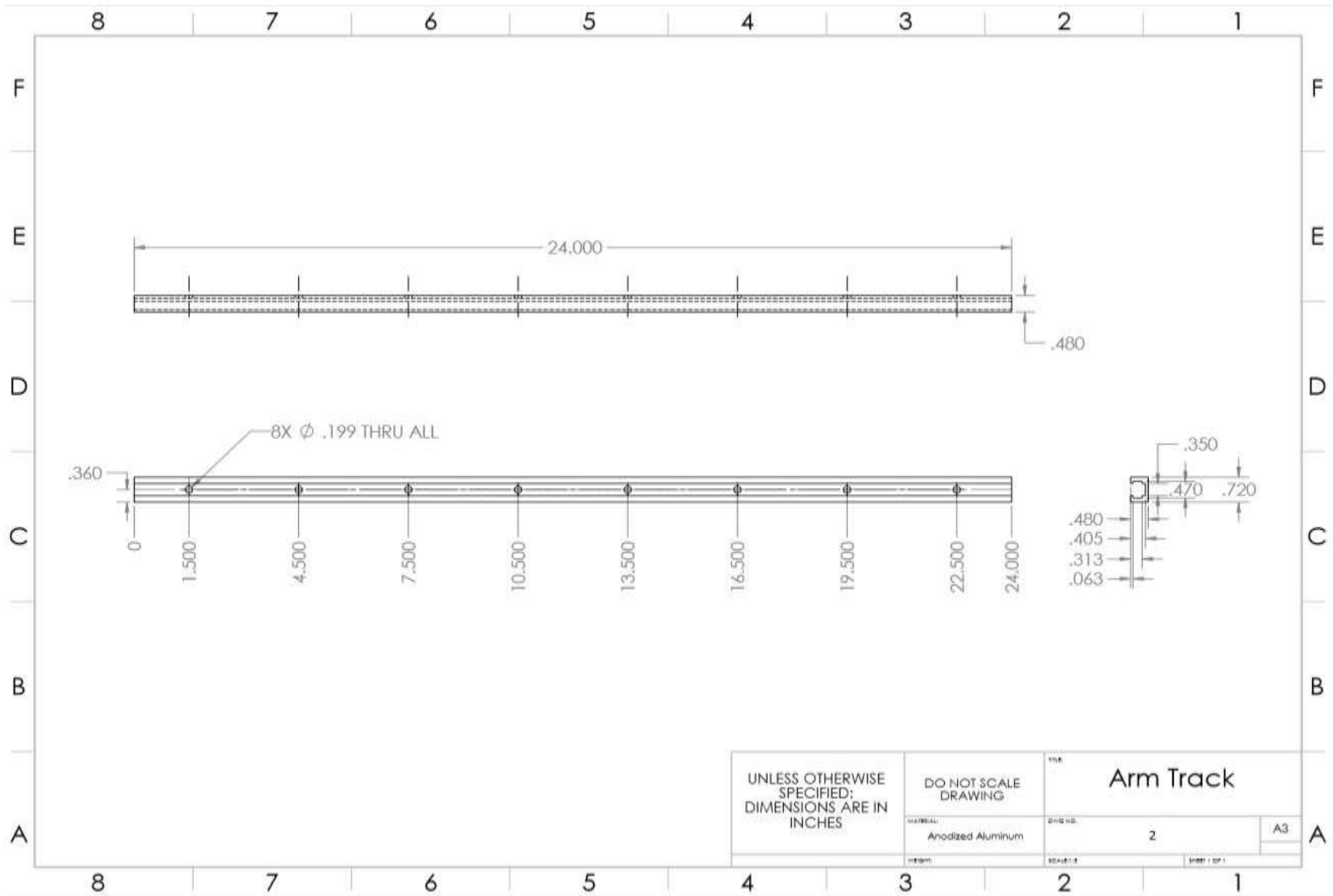


Figure L.1. 2. Mechanical Drawing of Arm Track.

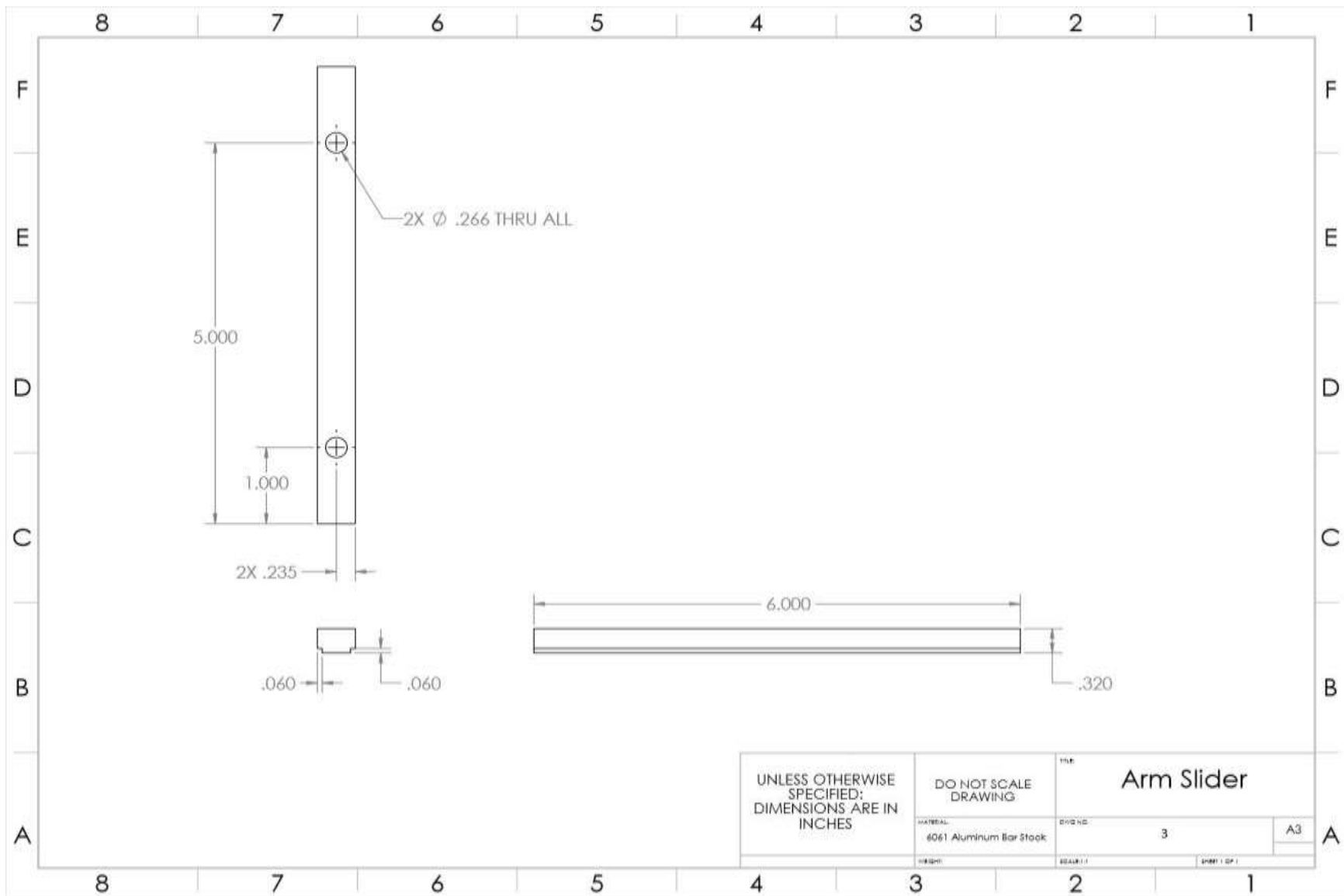


Figure L.1. 3. Mechanical Drawing of Arm Slider.

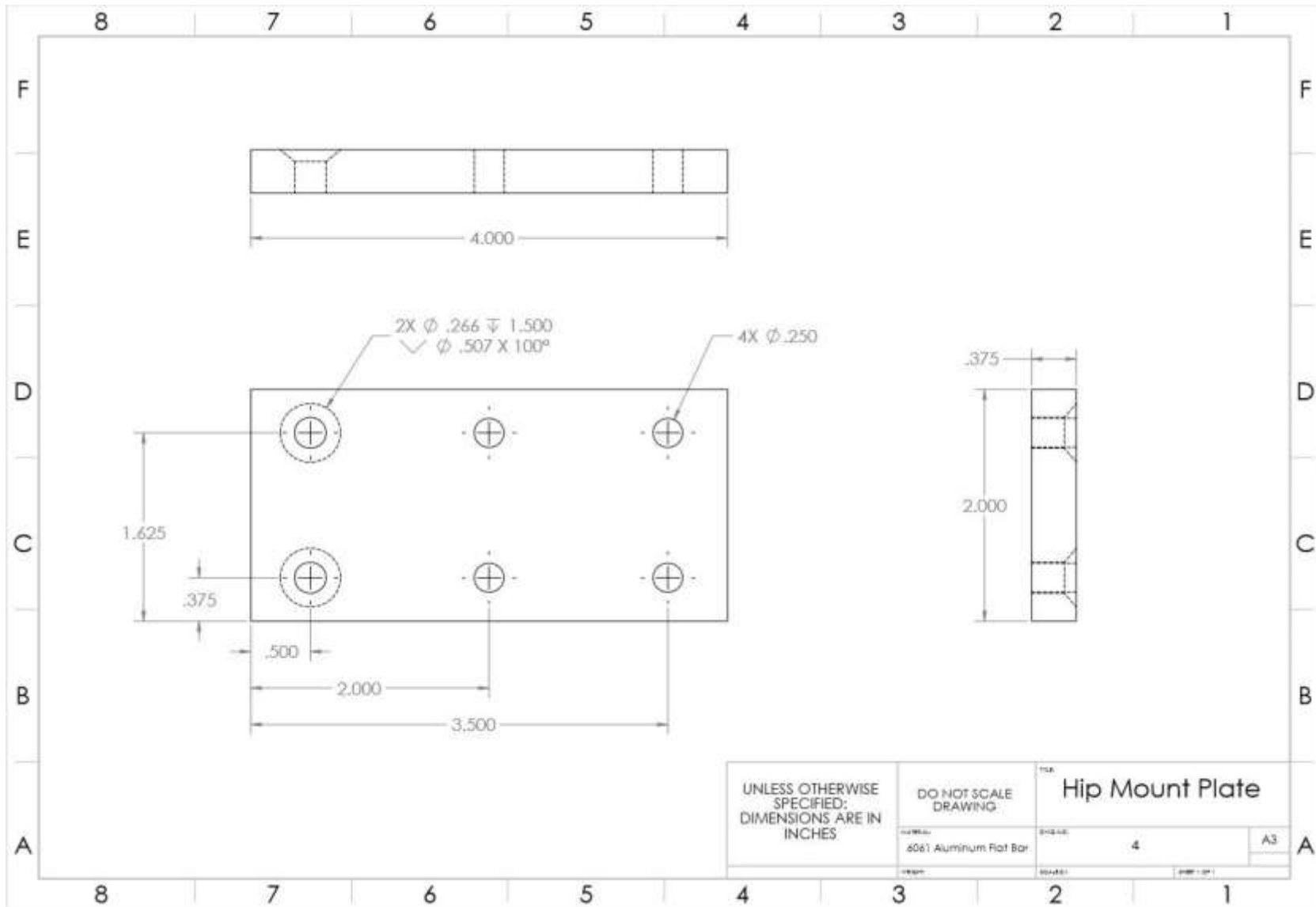


Figure L.1. 4. Mechanical Drawing of Hip Mount plate.



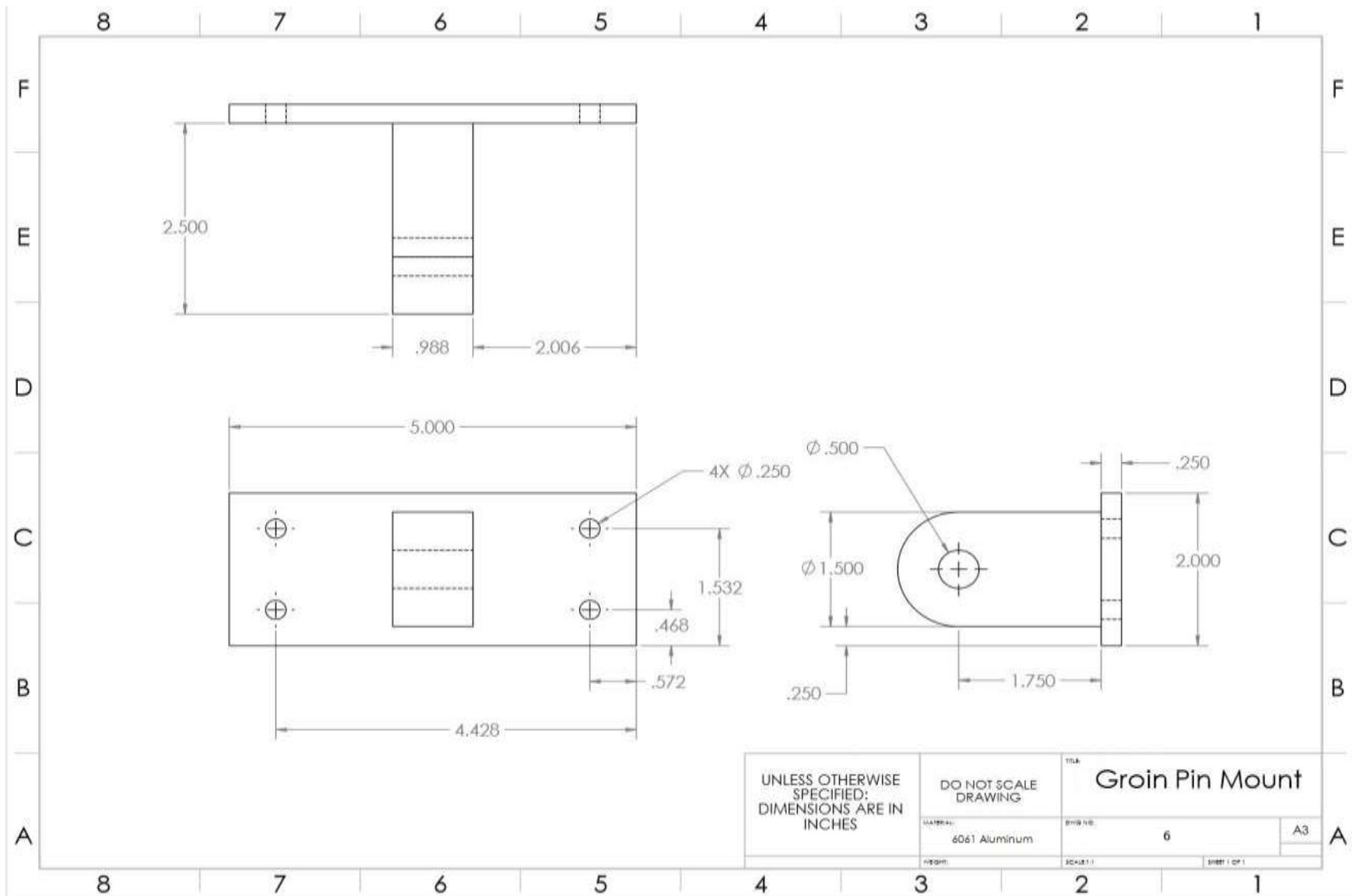


Figure L.1. 6. Mechanical Drawing of Groin Pin Mount.

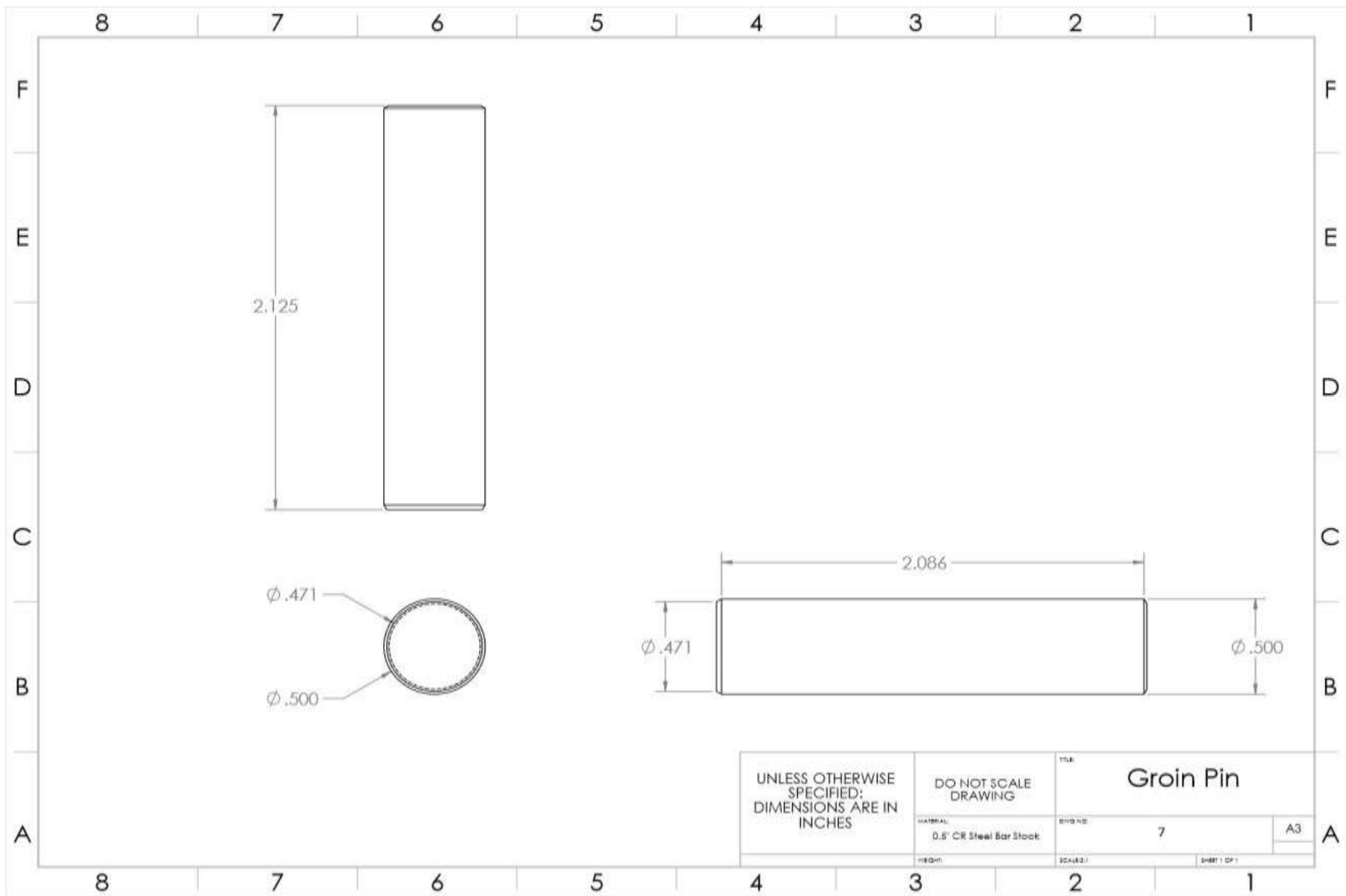


Figure L.1. 7. Mechanical Drawing of Groin Pin.

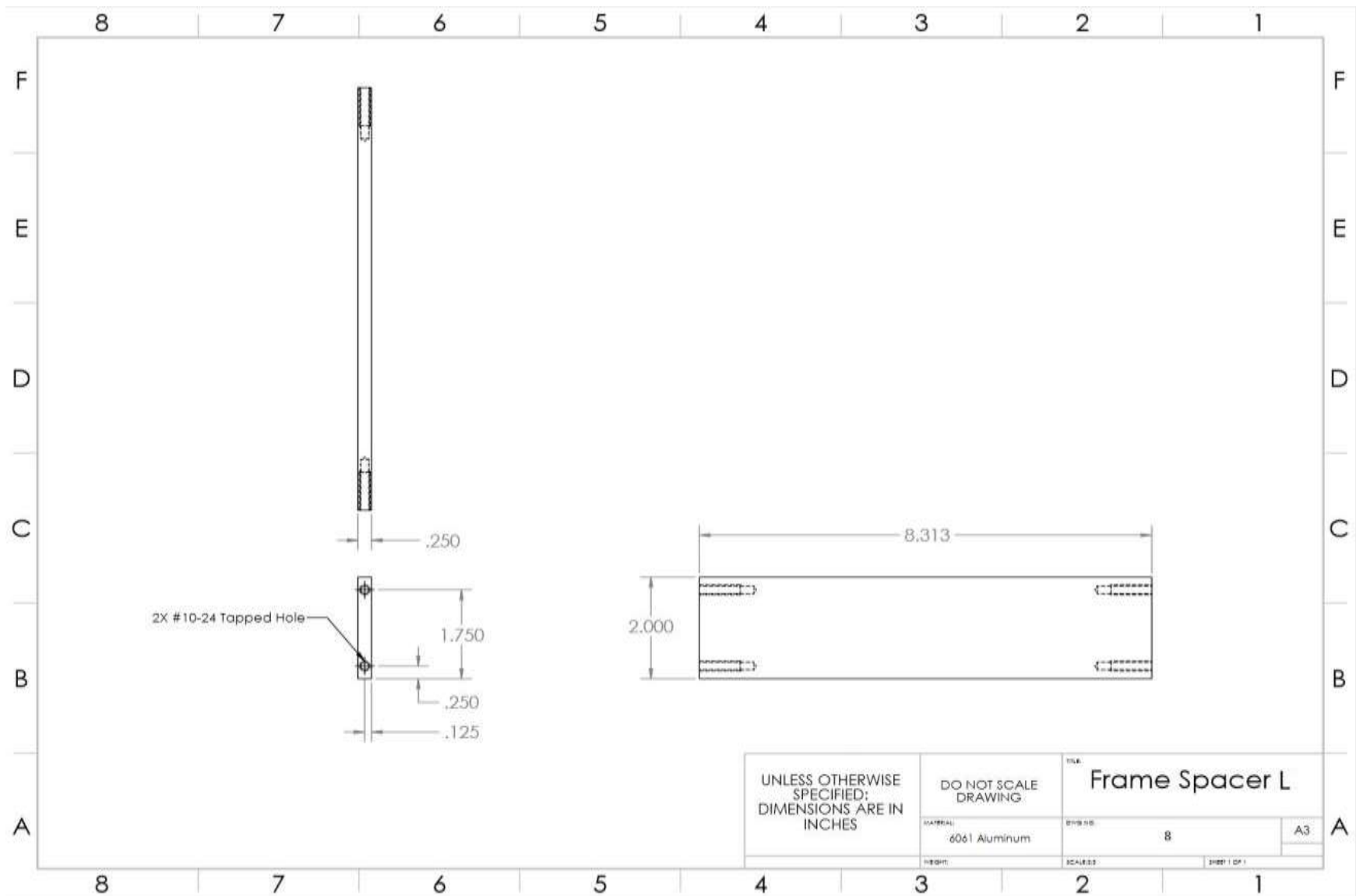


Figure L.1. 8. Mechanical Drawing of Frame Spacer Long.

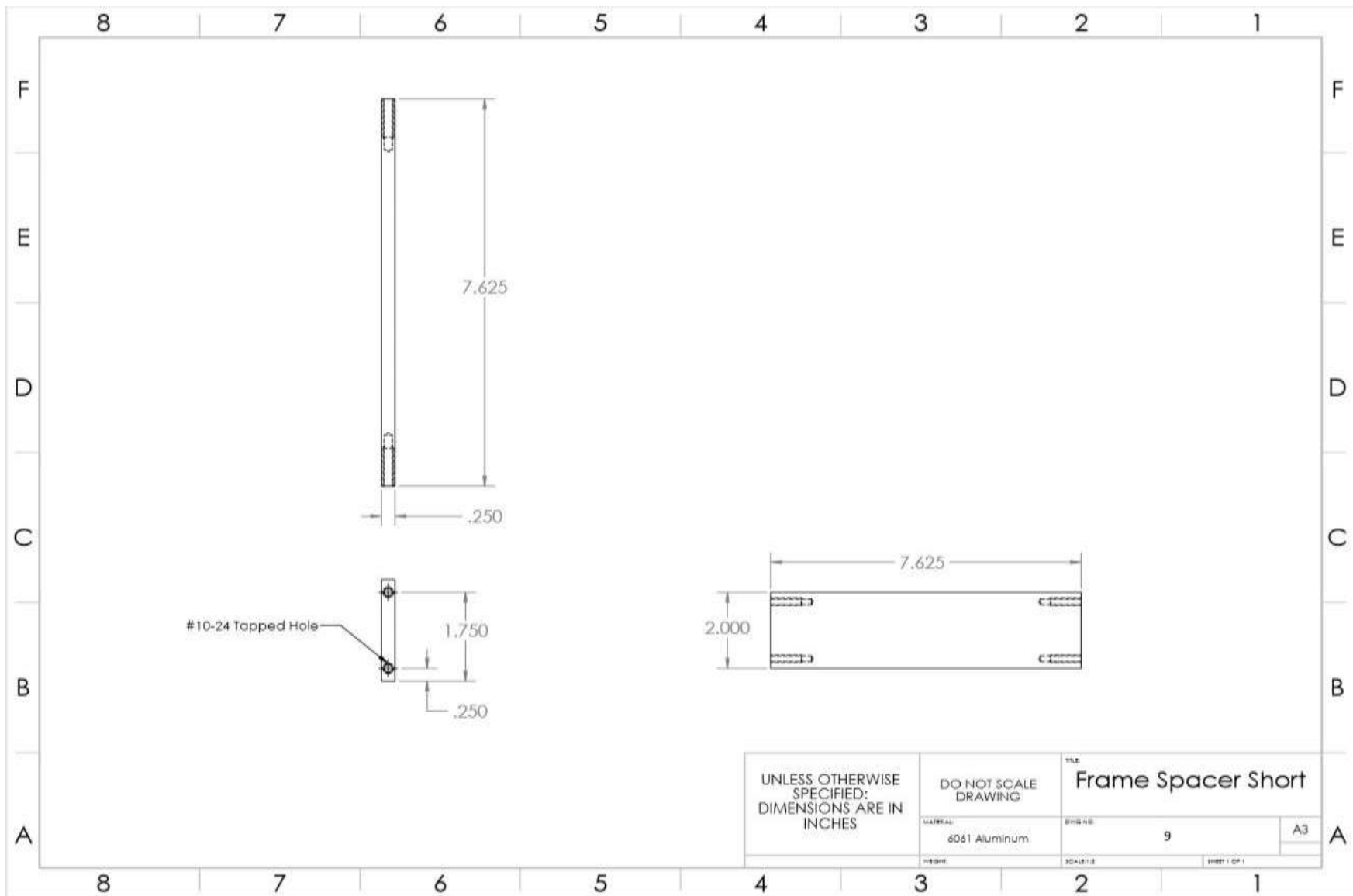


Figure L.1. 9. Mechanical Drawing of Frame Spacer Short.



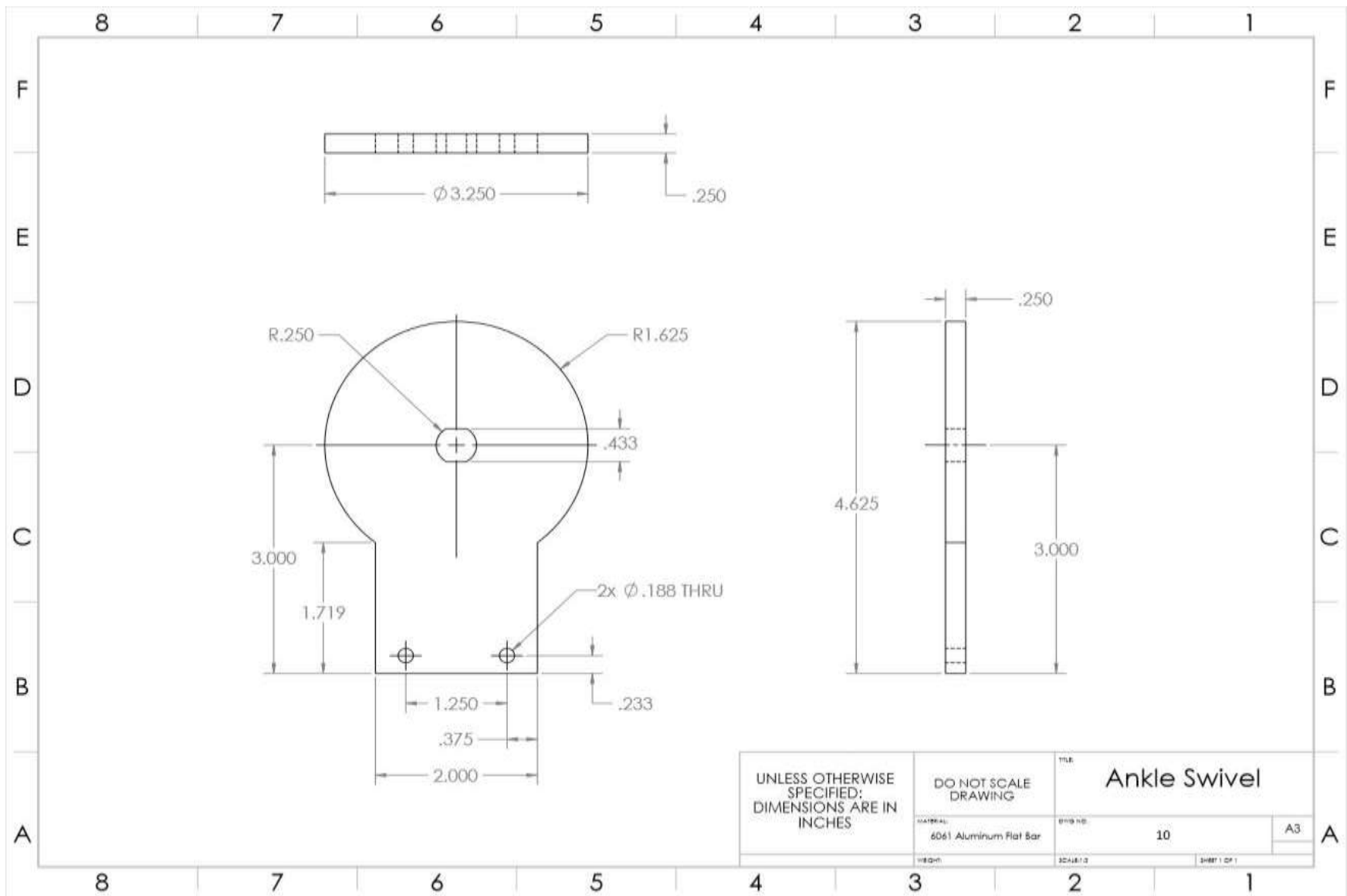


Figure L.1. 10. Mechanical Drawing of Ankle Swivel.

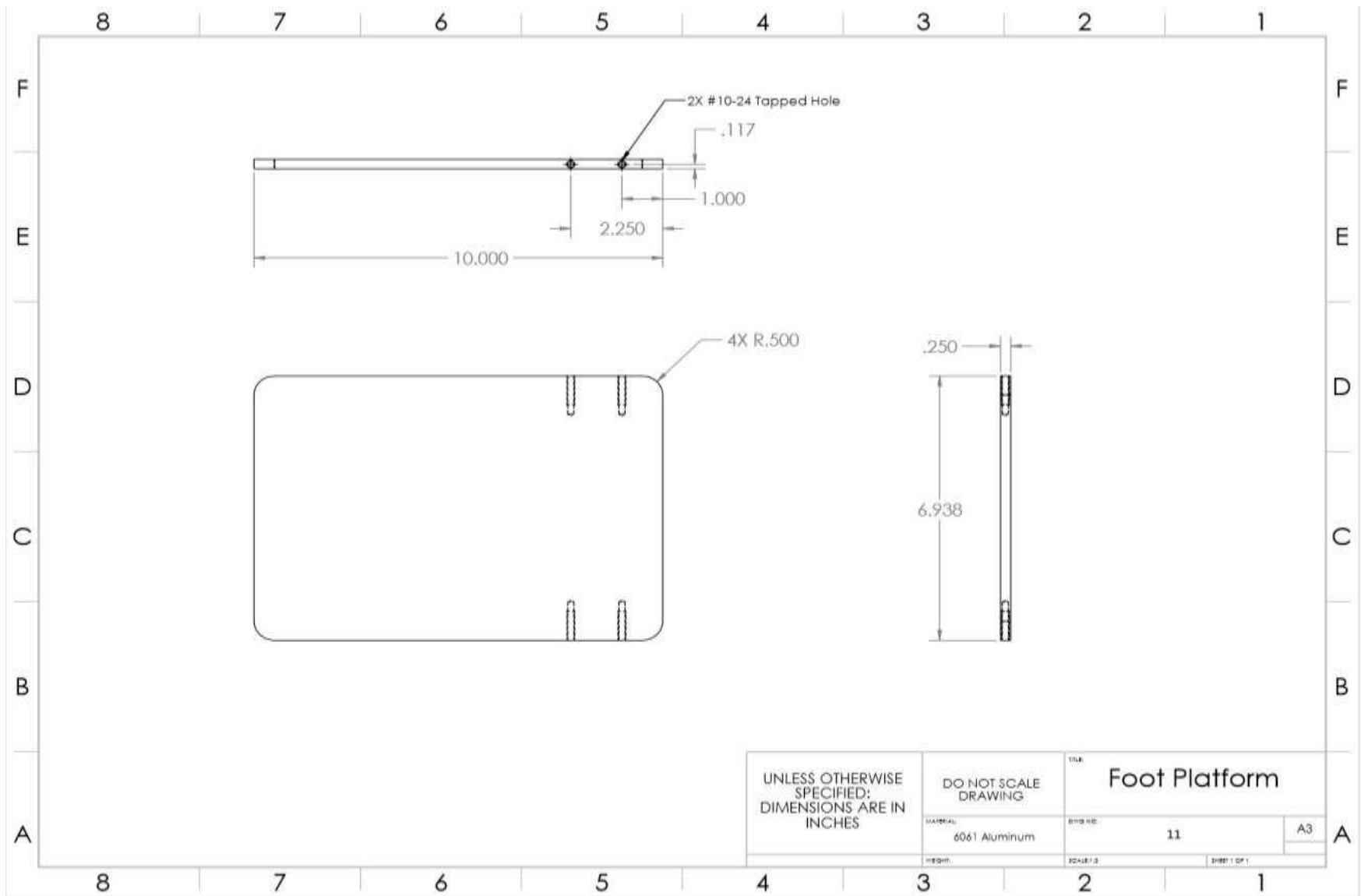


Figure L.1. 11. Mechanical Drawing of Foot Platform.

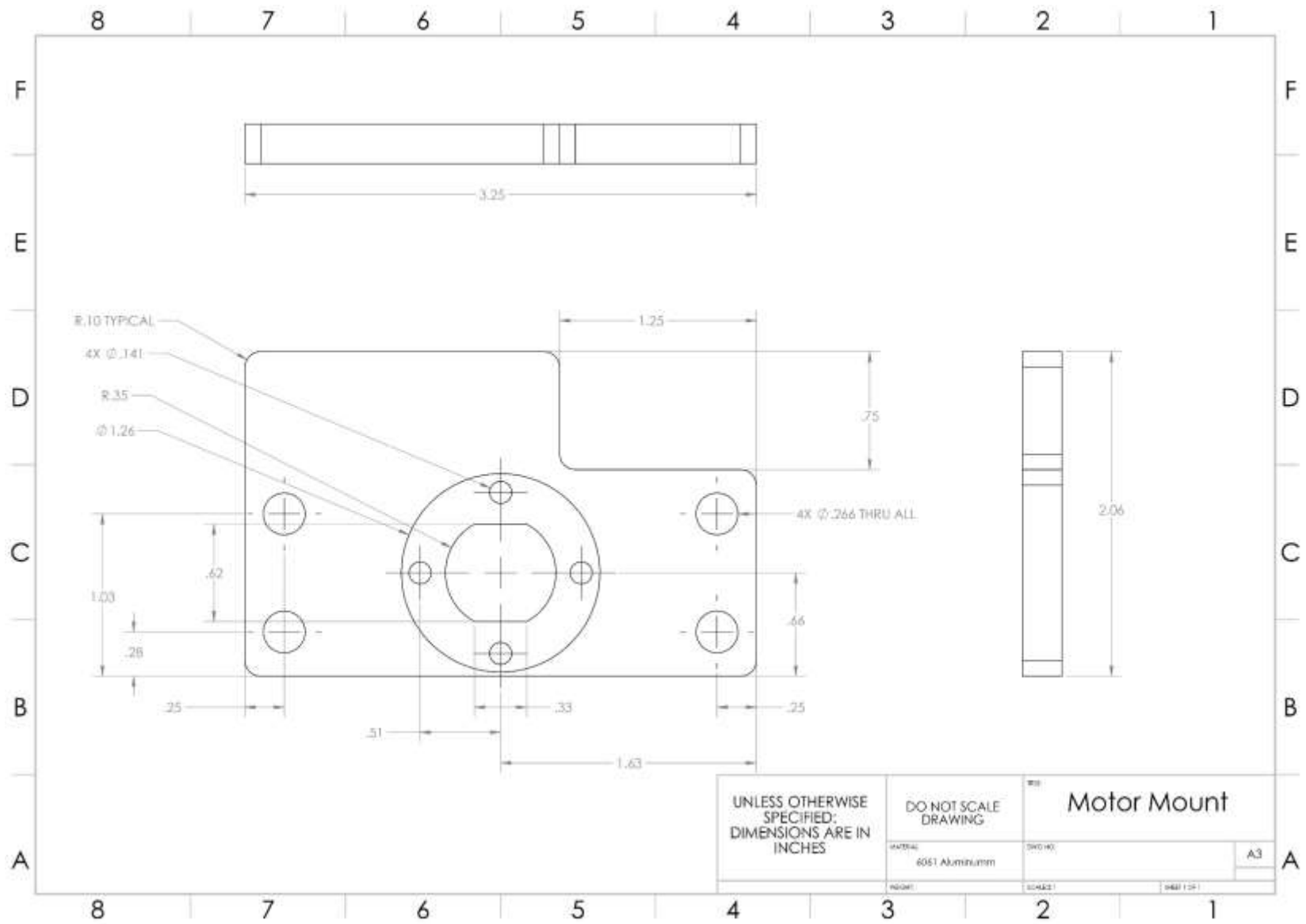


Figure L.1. 12. Mechanical Drawing of Motor Mount.

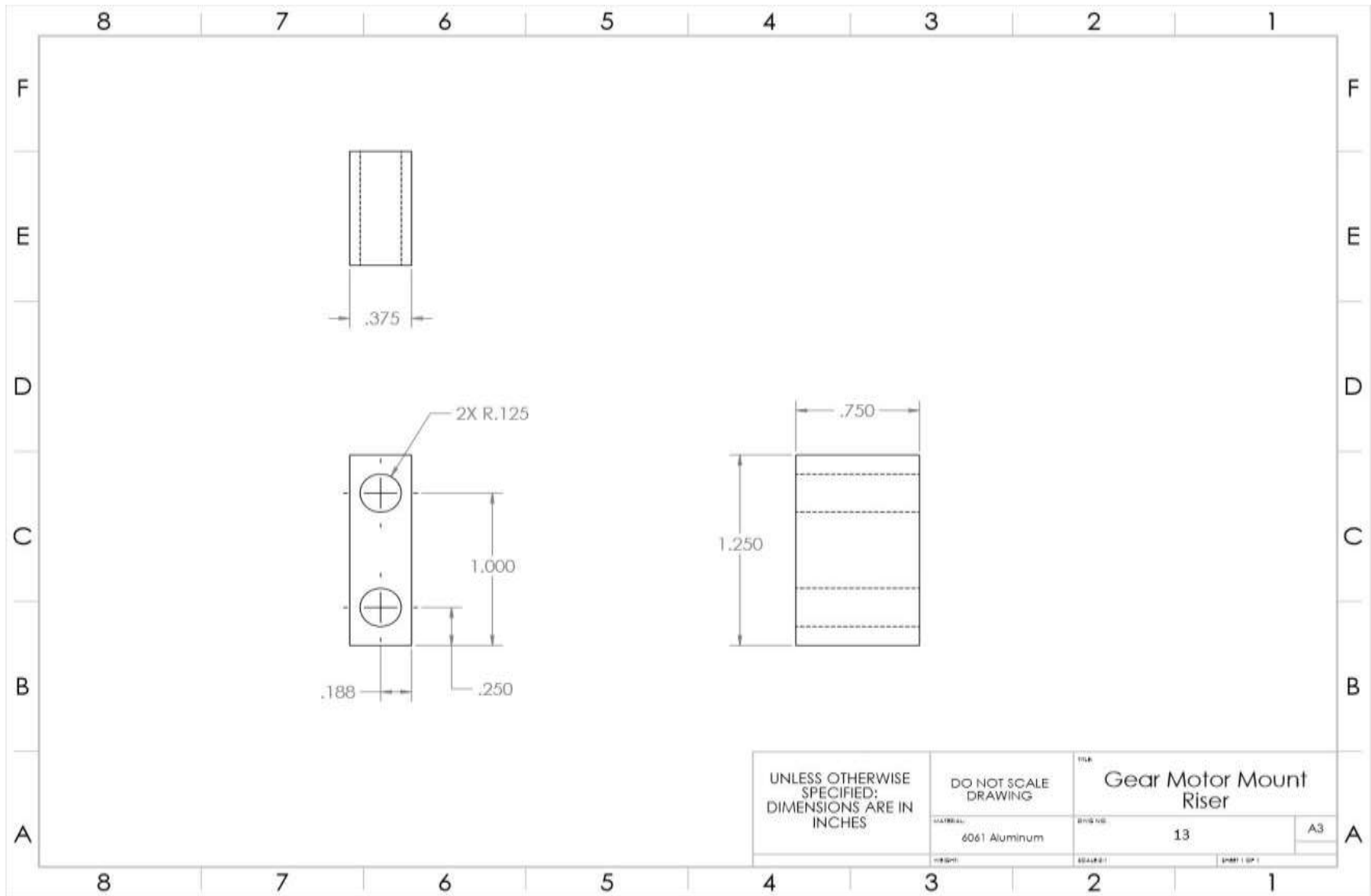


Figure L.1. 13. Mechanical Drawing of Gear Motor Mount Riser.

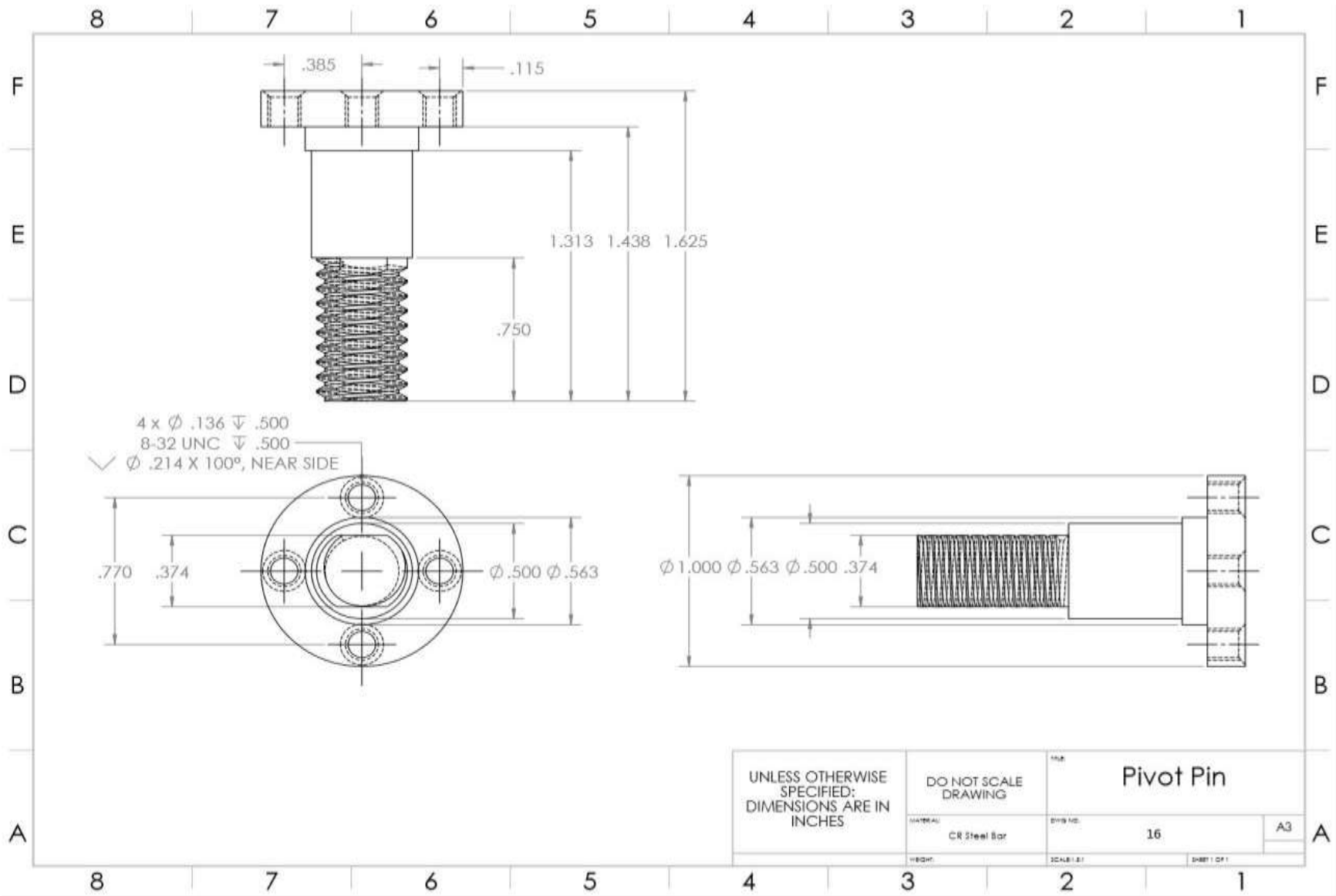


Figure L.1. 14. Mechanical Drawing of Pivot Pin.

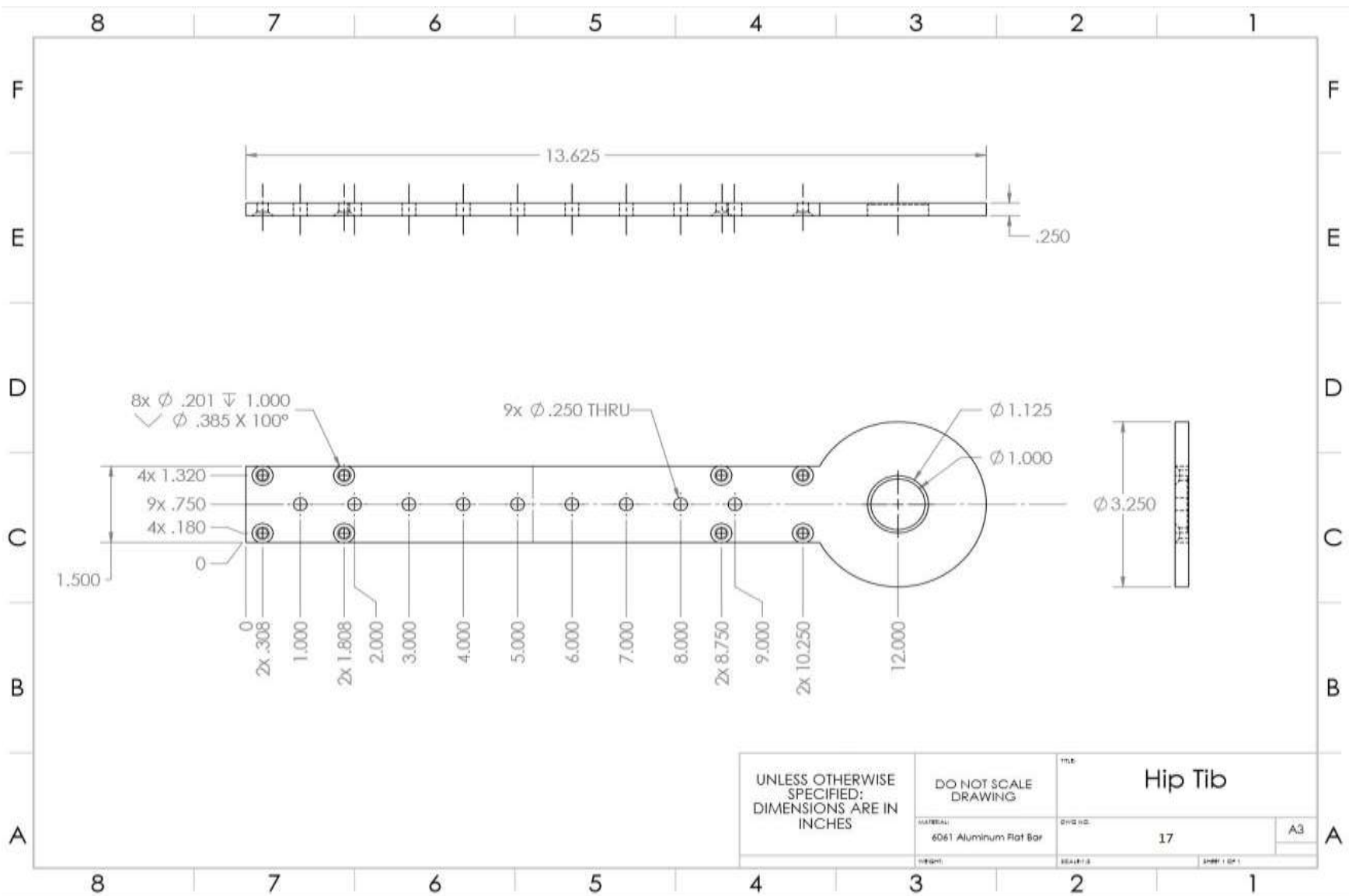


Figure L.1. 15. Mechanical Drawing of Linkages.

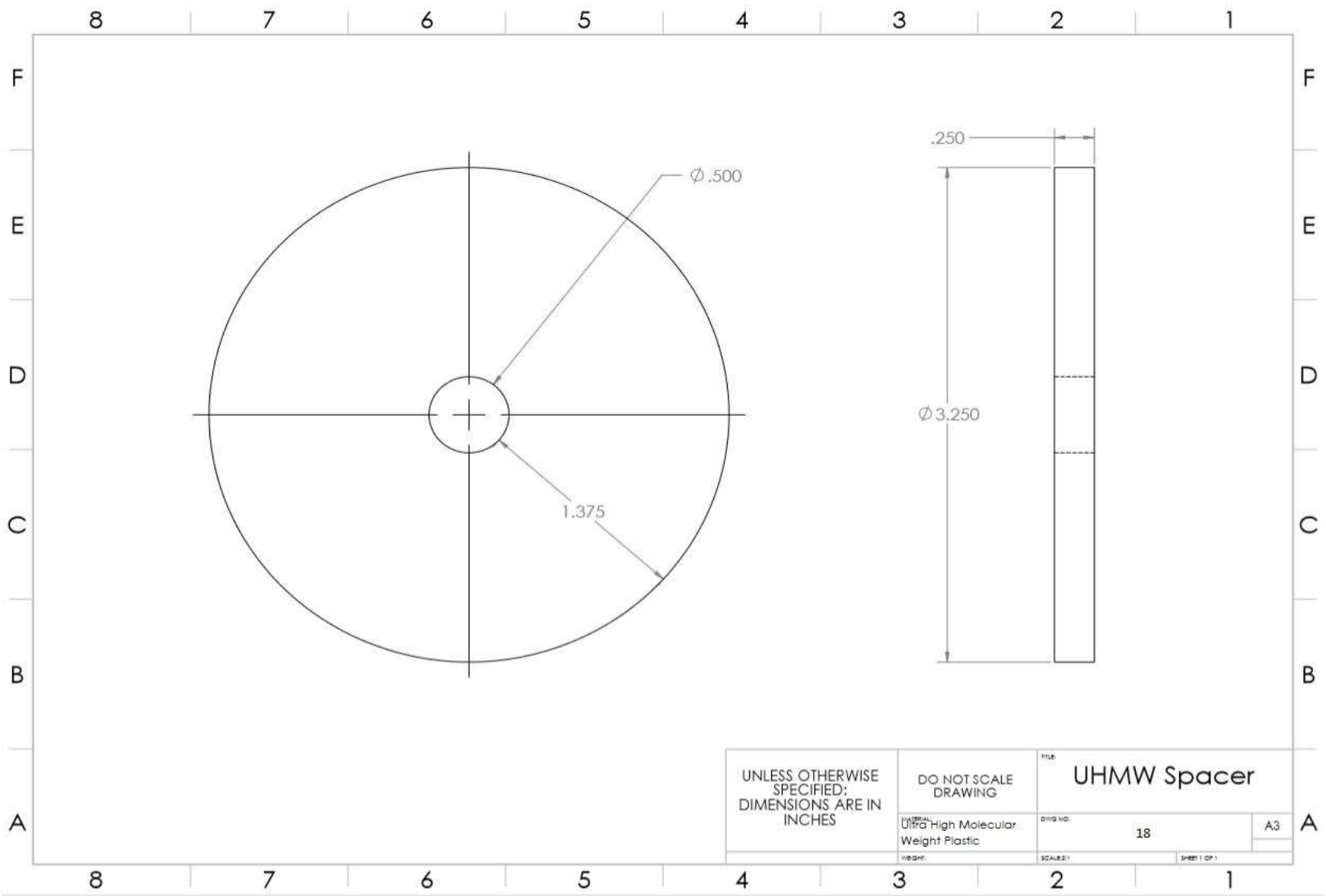


Figure L.1. 16. Mechanical Drawing of UHMW Spacer.

## Appendix L.2

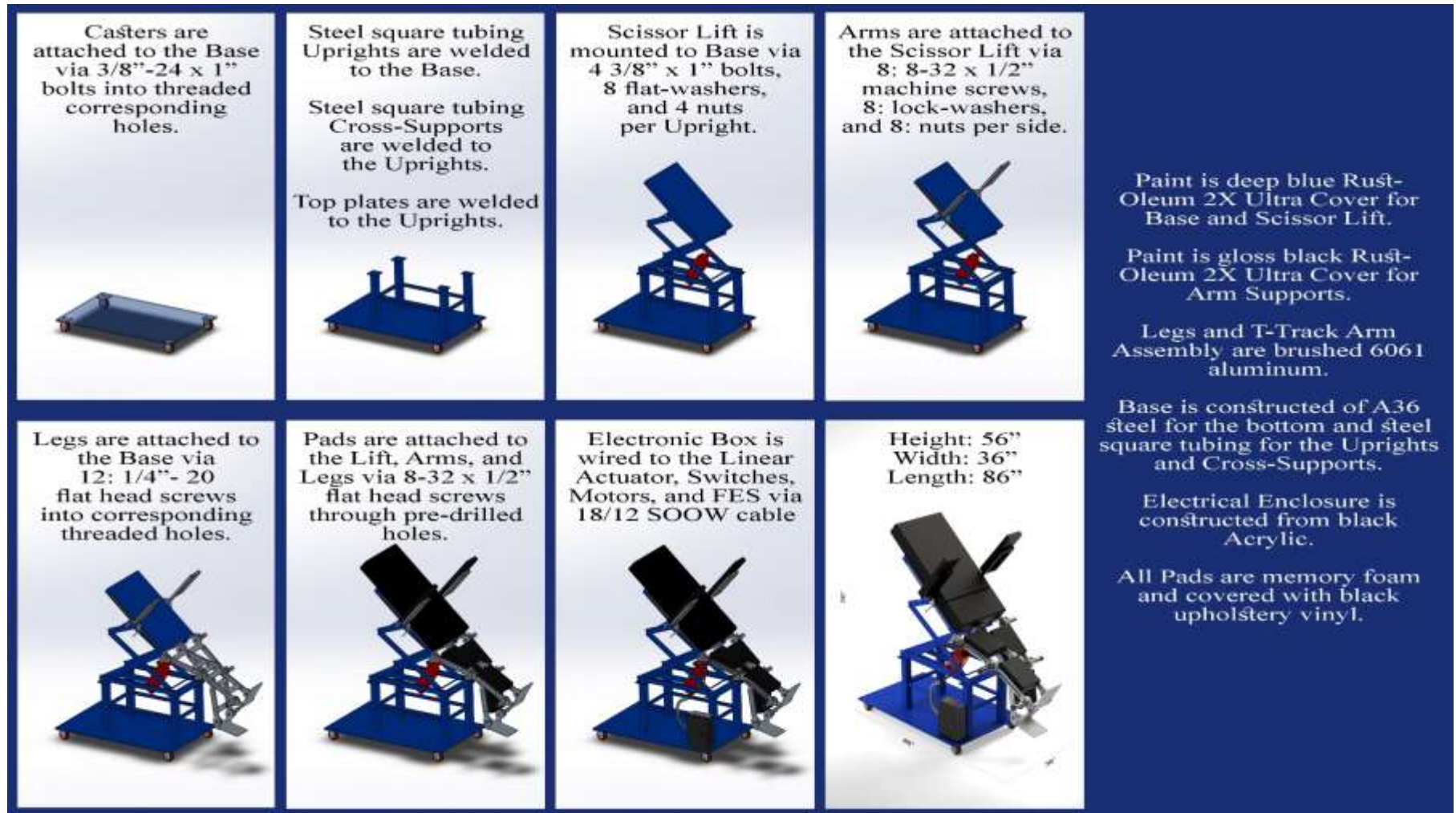


Figure L.2 1. Manufacturing Drawing of the RWTD.



## Appendix M

Table M 1. Estimated Costs of Mass Production.

Name of Item	Quantity	Price per Unit	Total Price
24" Fixturing Track for Hex Head Screws	2	\$7.10	\$14.20
10-24 x 0.750" Hex-Drive Flat Head Screw (32)	1	\$8.56	\$8.56
1/4 - 20 x 1.25" SHCS (24)	1	\$12.48	\$12.48
8-32 x 0.375" SHCS (24)	1	\$10.89	\$10.89
M3 - 0.5mm x 10mm Button Head Hex Screw (24)	1	\$7.77	\$7.77
1/4 - 20 x 0.750" Grade 5 Hex Bolt (16)	1	\$8.53	\$8.53
1/4 Hi-Collar Lockwasher (16)	1	\$10.38	\$10.38
1/4 - 20 Wingnut (16)	1	\$10.94	\$10.94
1/4 - 20 x 0.750" Hex Drive Flat Head Screw (4)	1	\$8.54	\$8.54
10-24 x 0.750" SHCS (8)	1	\$12.07	\$12.07
#10 Hi-Collar Lockwasher (8)	1	\$8.41	\$8.41
1/2 - 13 Nylock Nut (10)	1	\$10.07	\$10.07
Zinc-Plated Cast Iron Easy-Grip Handle with 3/8"-16 Thread	4	\$3.79	\$15.16
1/2" O.D. Shoulder Screw - 1.0" Shaft Length	4	\$2.61	\$10.44
1/4" - 20 x 1.0" High Strength Steel Threaded Rod	4	\$3.13	\$12.52
10-32, 3/8" Pan Head Phillips Screw (16)	1	\$13.88	\$13.88
10-32 Medium-Strength Steel Nylon-Insert Flange Locknut (16)	1	\$6.85	\$6.85
UHMW Wear Plate (10)	1	\$8.14	\$8.14
12 RPM Motor (12VDC)	6	\$59.99	\$359.94
1.125" x 0.500" ID Ball Bearing	12	\$6.27	\$75.24
FA-400-12-2-P Linear Actuator	1	\$139.00	\$139.00
Cytron MD20A Motor Controller	6	\$19.80	\$118.80
MINZO 120VAC to 12VDC Transformer	1	\$17.99	\$17.99
Arduino Nano	6	\$4.29	\$25.74
Arduino Mega2560	1	\$35.60	\$35.60
Eaton Neutral Bar	1	\$6.55	\$6.55
4x 100' - 18 AWG Wire	1	\$15.95	\$15.95
Upholstery Foam 2" x 24" x 72" High Density Cushion	1	\$38.00	\$38.00
Universal 5 pin Rocker switch	1	\$8.29	\$8.29
4 pin, 2 position toggle switch	2	\$4.00	\$8.00
Lever limit switches (10)	1	\$7.99	\$7.99
Waterproof 12 pin way connector (10)	1	\$17.31	\$17.31
Vinyl Fabric	4	\$12.00	\$48.00
Hi-Strength 90 Spray Adhesive	1	\$12.98	\$12.98
Rustoleum Spray Paint (Blue)	2	\$3.98	\$7.96

Name of Item	Quantity	Price per Unit	Total Price
Rustoleum Spray Paint (Black)	1	\$3.98	\$3.98
Strap Buckle	4	\$2.00	\$8.00
Nylon strap	2	\$2.00	\$4.00
24"x48" 1/4" Project panel board	1	\$15.97	\$15.97
24" x 48" x 1/2" A36 Steel Plate	1	\$322.40	\$322.40
(100 FT.) SOOW 18/12 Power Cable (Shielded)	1	\$1,851.00	\$1,851.00
(4 pk.) 4" Nonmarking Polyurethane Casters	1	\$49.99	\$49.99
2-1/2" x 2-1/2" x 1/4 wall A500 Square Steel Tube (72")	1	\$69.66	\$69.66
1-1/2" x 1-1/2" x 3/16" wall A500 Square Steel Tube (96")	1	\$56.28	\$56.28
Everbilt 3/8"-16 x 3/4" Chrome Hex Bolt (2 pk.)	16	\$3.37	\$53.92
Everbilt 3/8" Zinc Flat washers (100 pk.)	1	\$15.30	\$15.30
Crown Bolt 3/8" Zinc-Plated Split Lock Washer	32	\$0.25	\$8.00
Everbilt 3/8" -16 Zinc Plated Hex Nut (25 pk.)	1	\$3.56	\$3.56
4' x 8' x 1/4" - 6061 Aluminum	1	\$527.04	\$527.04
1-1/4" x 36" 1045 Carbon Steel	1	\$110.85	\$110.85
Global Industrial Mobile Lift & Tilt Scissor Lift Table (29x19 Platform)	1	\$659.00	\$659.00
Digitimer DS7A Constant Current High Voltage Stimulator	1	\$6,585.00	\$6,585.00
Cost of Machine Use (hrs.)	150	\$40.00	\$6,000.00
Cost of Labor (hrs.)	150	\$35.00	\$5,250.00
		<b>Total</b>	<b>\$22,727.12</b>

## Appendix N

### Appendix N.1



Figure N 1. Arduino Mega 2560.

Table N 2. Arduino Mega 2560 Specifications.

Model	ATmega2560
Operating Voltage	5V
Input Voltage (recommended)	7-12V
Input Voltage (limit)	6-20V
Digital I/O Pins	54 (15 of which are PWM)
Analog Input Pins	16
DC Current per I/O Pin	20 mA
DC Current for 3.3V Pin	50 mA
Flash Memory	256 KB (8 KB used by bootloader)
SRAM	8 KB
EEPROM	4 KB
Clock Speed	16 MHz
Operating Temperature	-25° C ~ 50° C
Dimensions	101.52 mm x 53.3mm

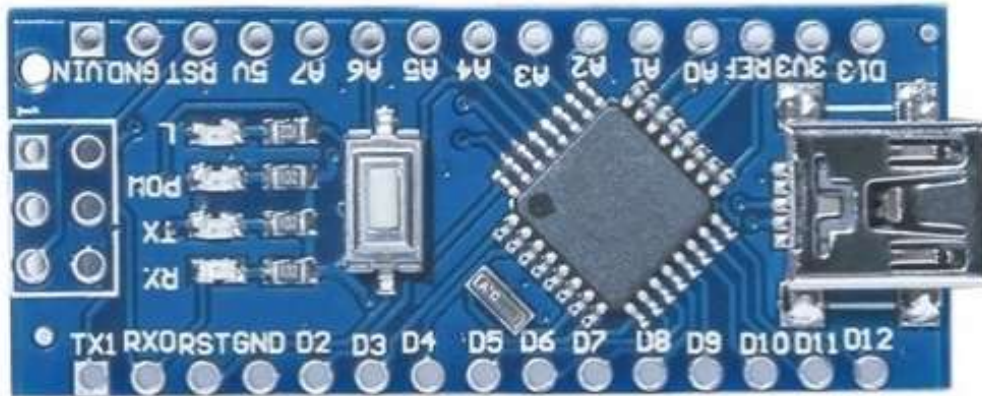


Figure N 2. Arduino Nano.

Table N 3. Arduino Nano Specifications.

Microcontroller	ATmega328
Operating Voltage	5V
Input Voltage	7-12V
Input Voltage (limit)	6-20V
Digital I/O Pins	14 (6 are PWM)
Analog Input Pins	8
DC Current per I/O Pin	40 mA
Flash Memory	32 KB
SRAM	1 KB
EEPROM	1 KB
Clock Speed	16 MHz
Operating Temperature	-25° C ~ 50° C
Dimensions	43.18 mm x 18.54 mm

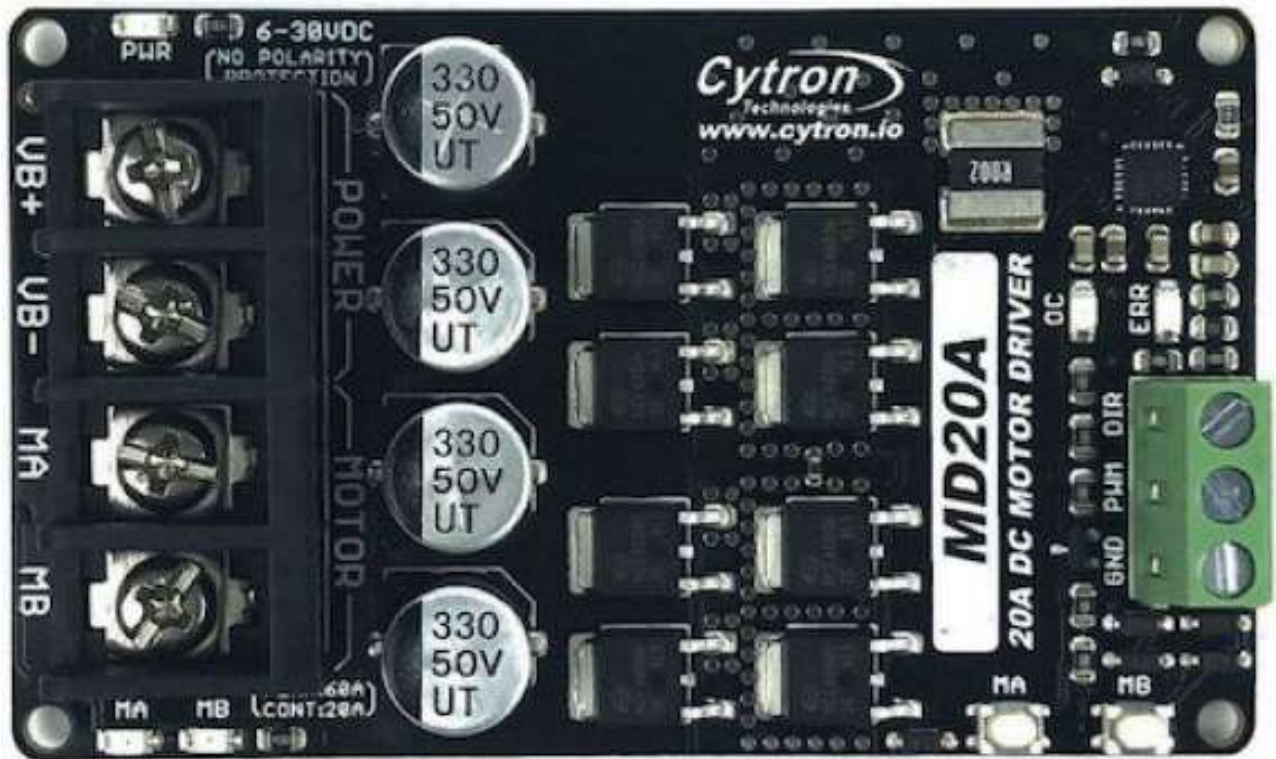


Figure N 3. Cytron MD20 Motor Driver.

Table N 4. Cytron MD20 Motor Driver Specifications.

Model	Cytron MD20A
Logic Operating Voltage	0 V - 1.5 V
Motor Input Voltage	6 V - 30 V
Max Continuous Motor Current	20 A
Peak Motor Current	60 A
Digital Input Pins	3
DC PWM Frequency	20 kHz
Continuous Current Operating Temperature	25° ~ °30 C
Dimensions	86 mm x 52 mm

## Appendix N.2

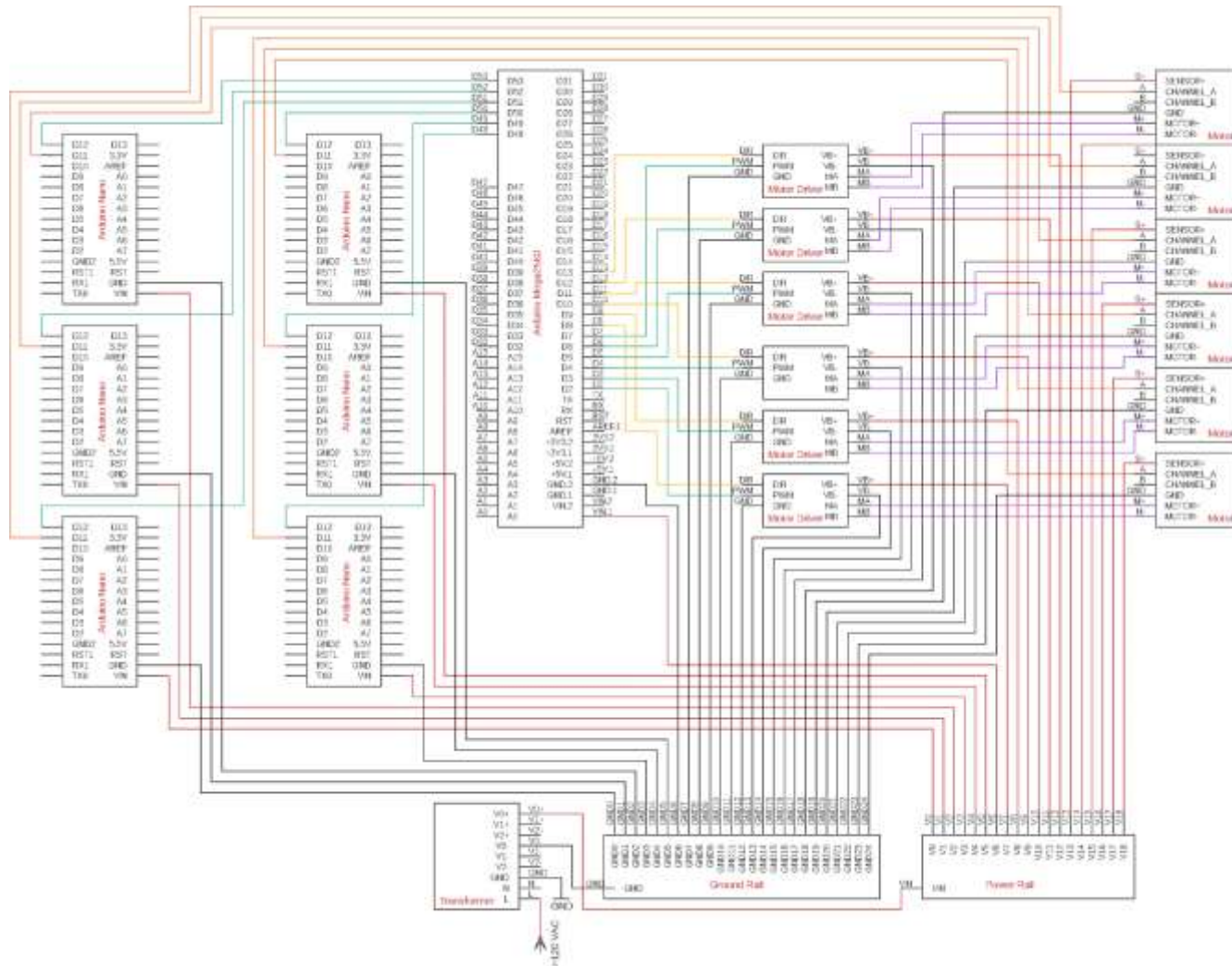


Figure N 4. Schematic Depicting all Connections.

## Arduino Mega2560 Power

The Arduino Mega2560 will be powered via VIN and GND.1 from a power rail and ground rail which are connected to the 110-120VAC to 12V DC transformer. Since the Arduino Mega2560 is the control unit, it will share a common ground with everything through the ground rail.

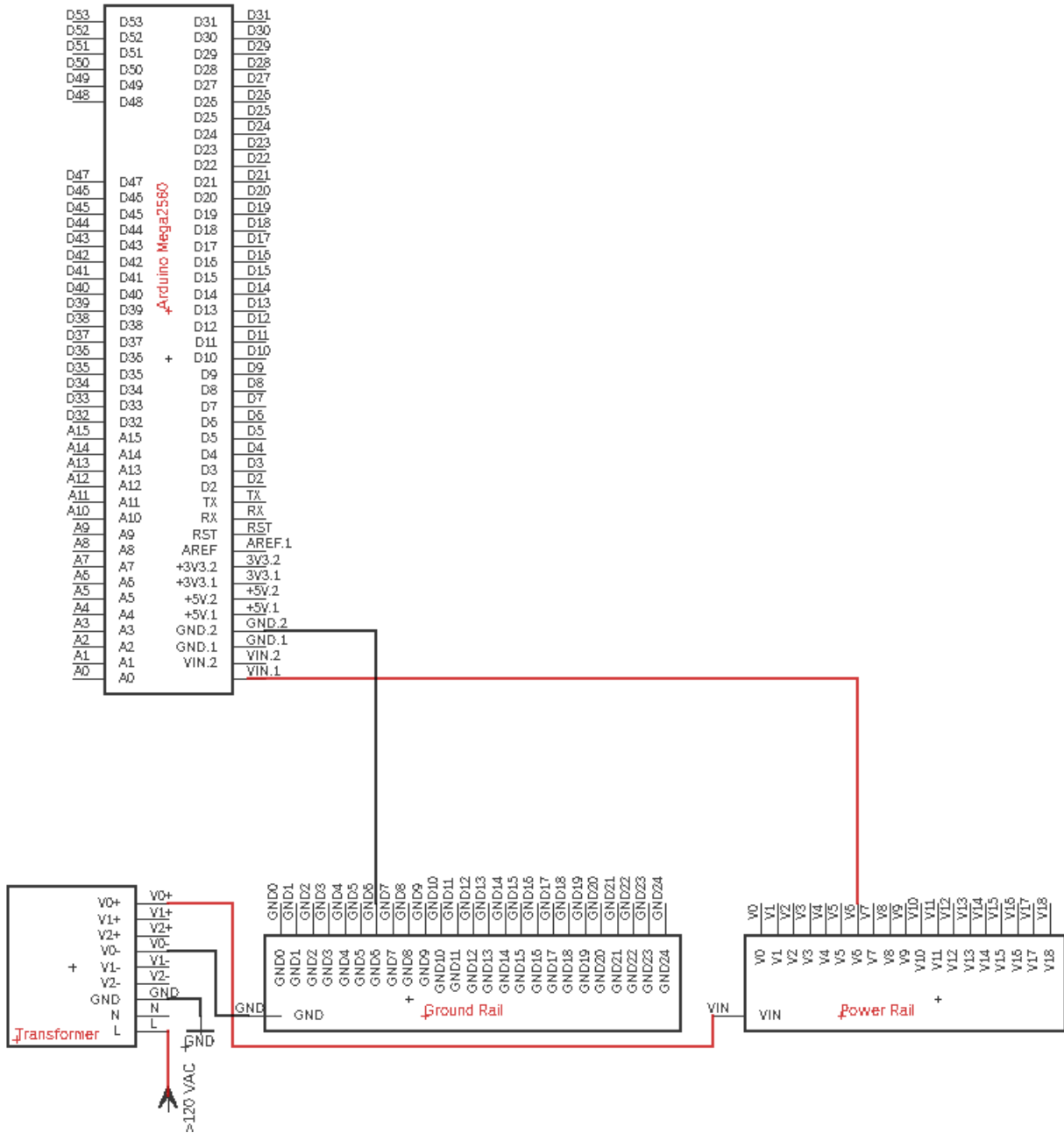


Figure N 5.Arduino Mega2560 Power Connections.

## Arduino Nano Power

The six Arduino Nano's will be powered via the VIN and GND pins from a power rail and ground rail that is connected to the AC to DC transformer.

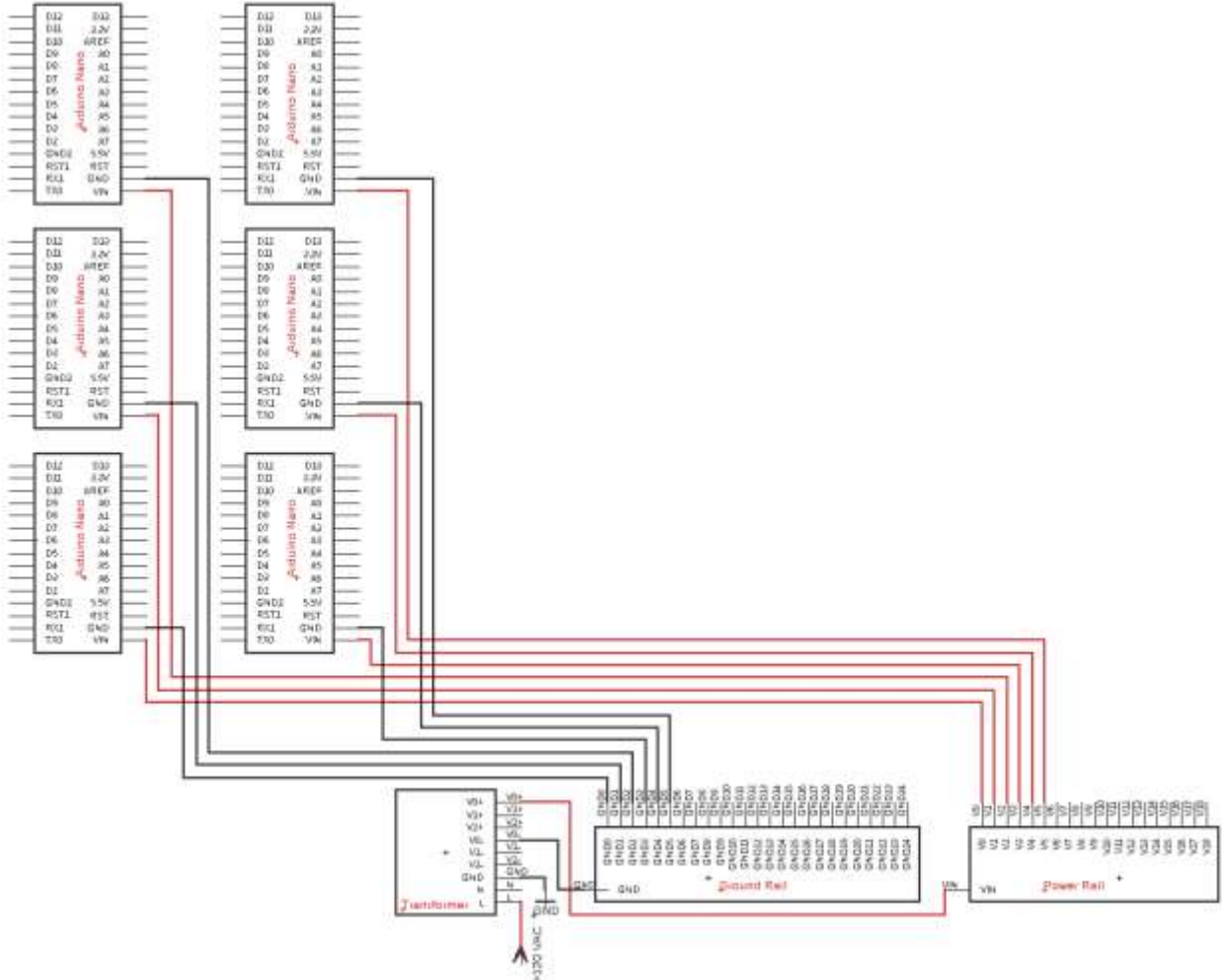


Figure N 6.Arduino Nano Power Connections



## Motor Driver Power

The motor drivers will be powered via the  $VB^+$  and  $VB^-$  pins from a power rail and ground rail that is connected to the AC to DC transformer.

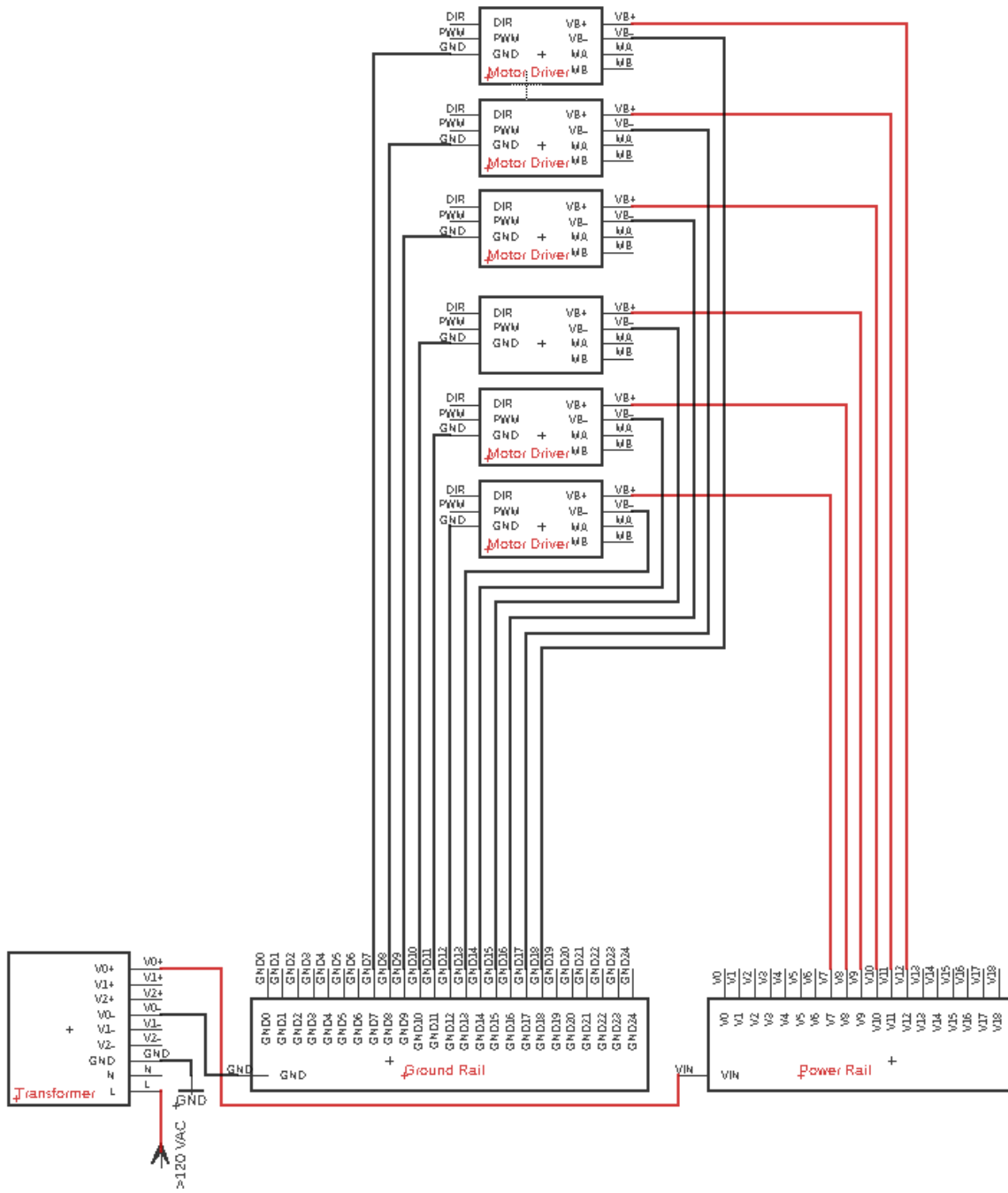


Figure N 7.Motor Driver Power Connections.

## Hall Encoder Power

The motor Hall encoders will be powered via the  $S^+$  and GND pins from a power rail and ground rail that is connected to the AC to DC transformer.

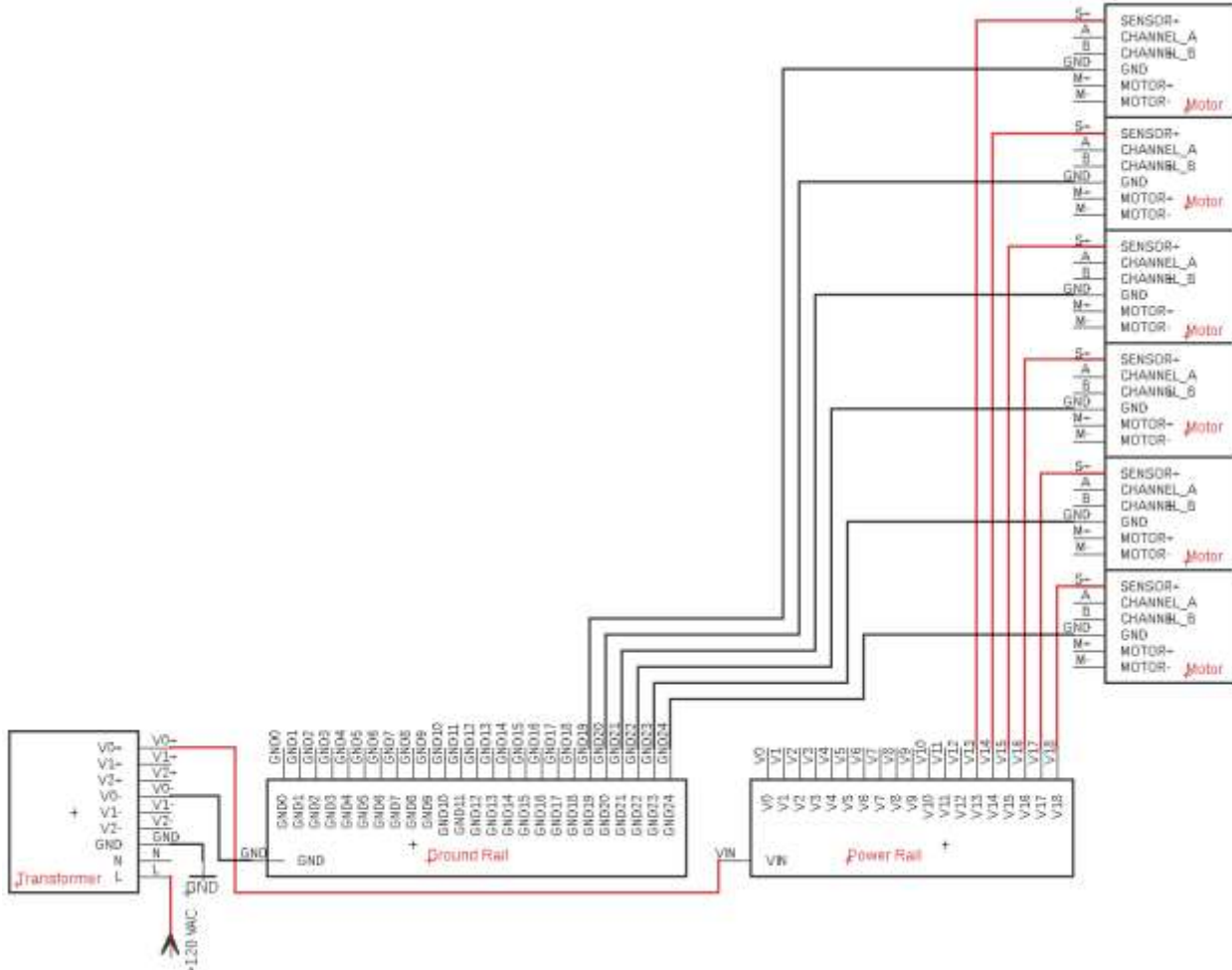


Figure N 8.Motor Power Connection.

## Motor Direction Control and Power

Each motor driver MB and MA output is connected to each motor M<sup>+</sup> and M<sup>-</sup> input. This powers the motors and controls the direction the motors rotate. Below is a figure with the wiring connections and a table with the HIGH and LOW combinations that determine motor direction.

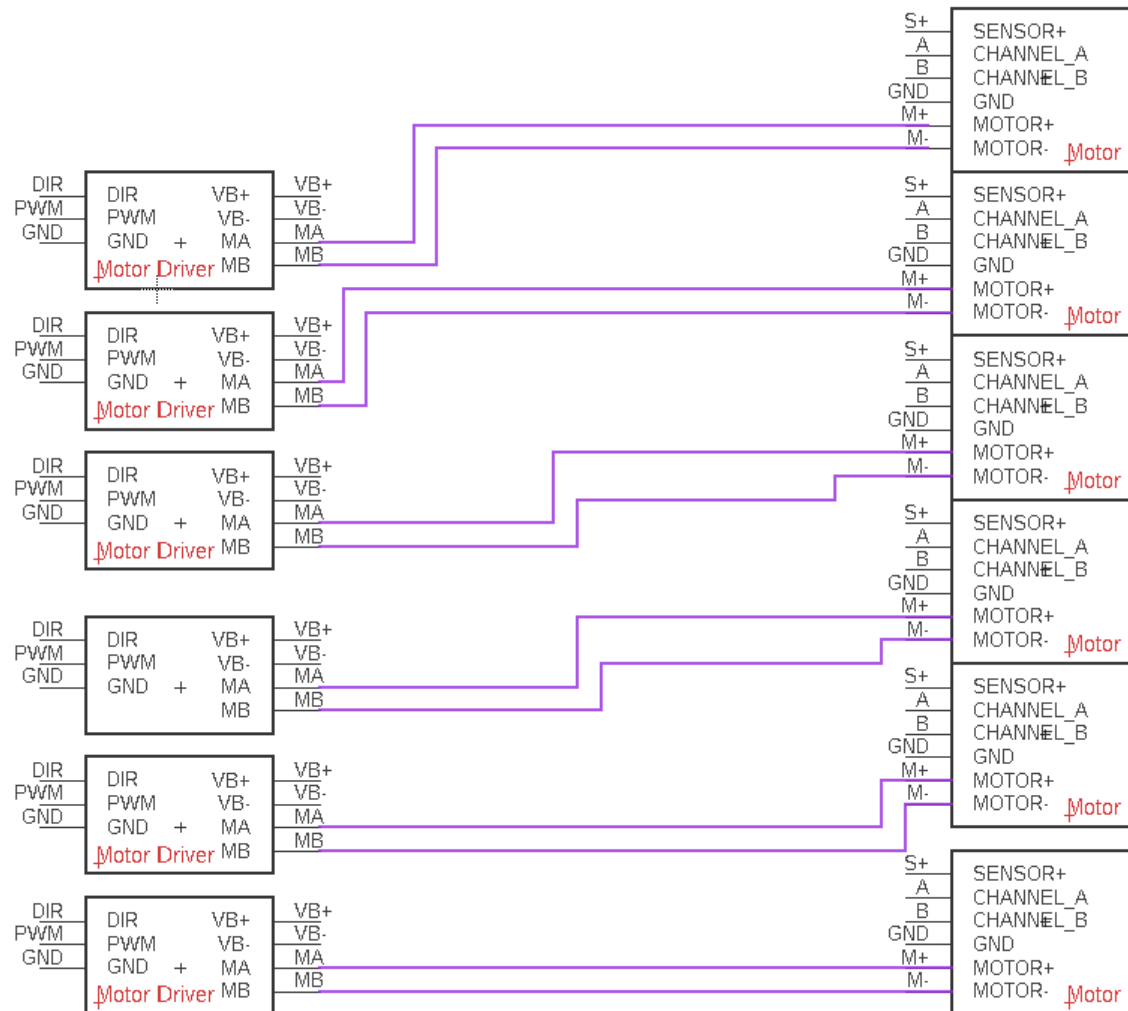


Figure N 9. Motor driver to motor direction digital signal connections.

Table N 5. Motor Direction Combinations.

Output MA	Output MB	Motor
LOW	LOW	Brake
HIGH	LOW	Forward
LOW	HIGH	Backward

## Motor Driver Direction Control Digital Signals

The motor driver DIR (direction) inputs require a digital HIGH or LOW signal to change the rotation direction of the motors. Therefore, each DIR input of the motor controllers is connected to a single digital I/O pin on the Arduino Mega2560.

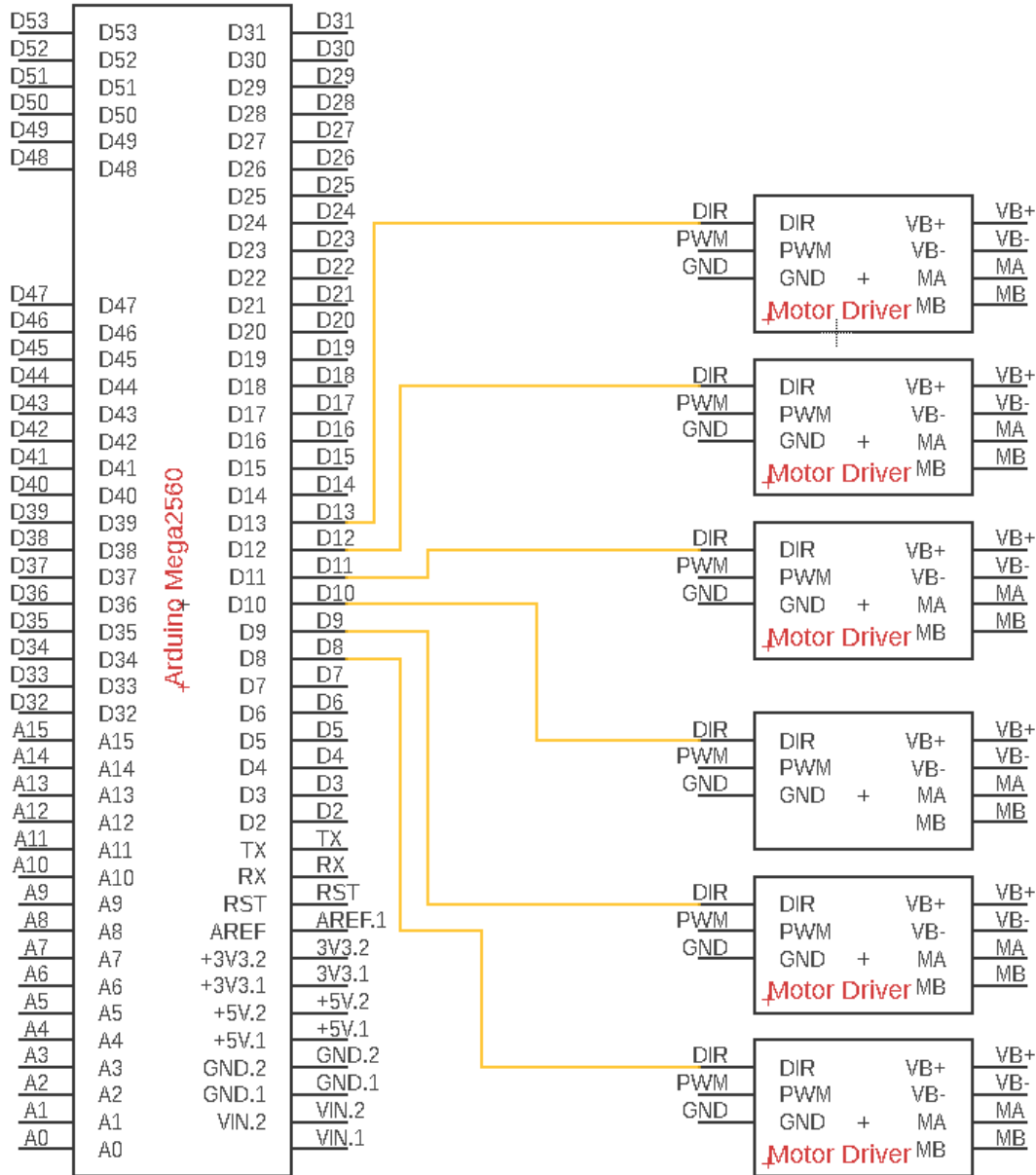


Figure N 10. Motor driver direction control digital connections.

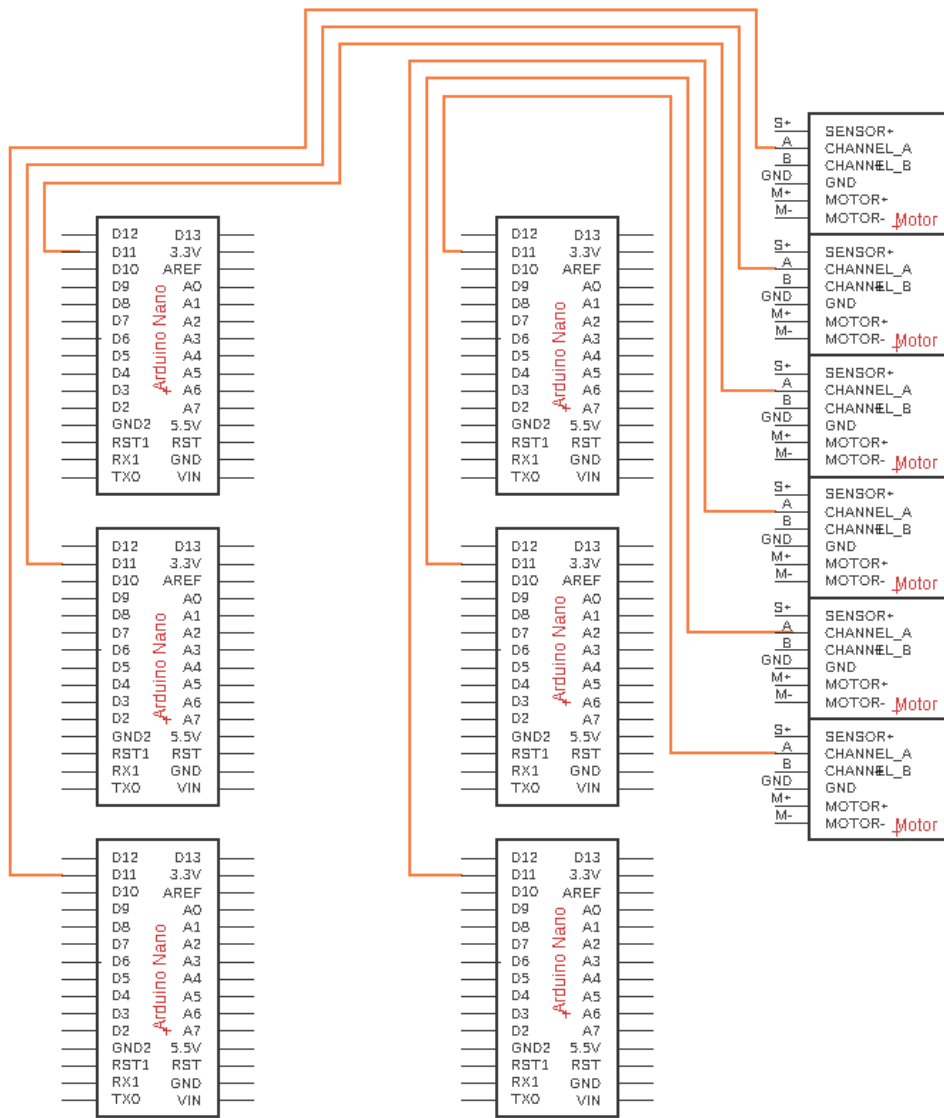


Figure N 11. Sensor pulse digital signal connections.

## Arduino Nano Digital I/O Signals

Each Arduino Nano has one digital I/O pin connected to a digital I/O pin on the Arduino Mega2560. These digital connections deliver a HIGH digital pulse from each Arduino Nano to the Arduino Mega2560, which indicates that the motor rotational position in degrees has been reached. In addition, the same connections deliver a HIGH digital control pulse from the Arduino Mega2560 to command each Arduino Nano when it is time to move to next degree of rotation in the gait cycle.

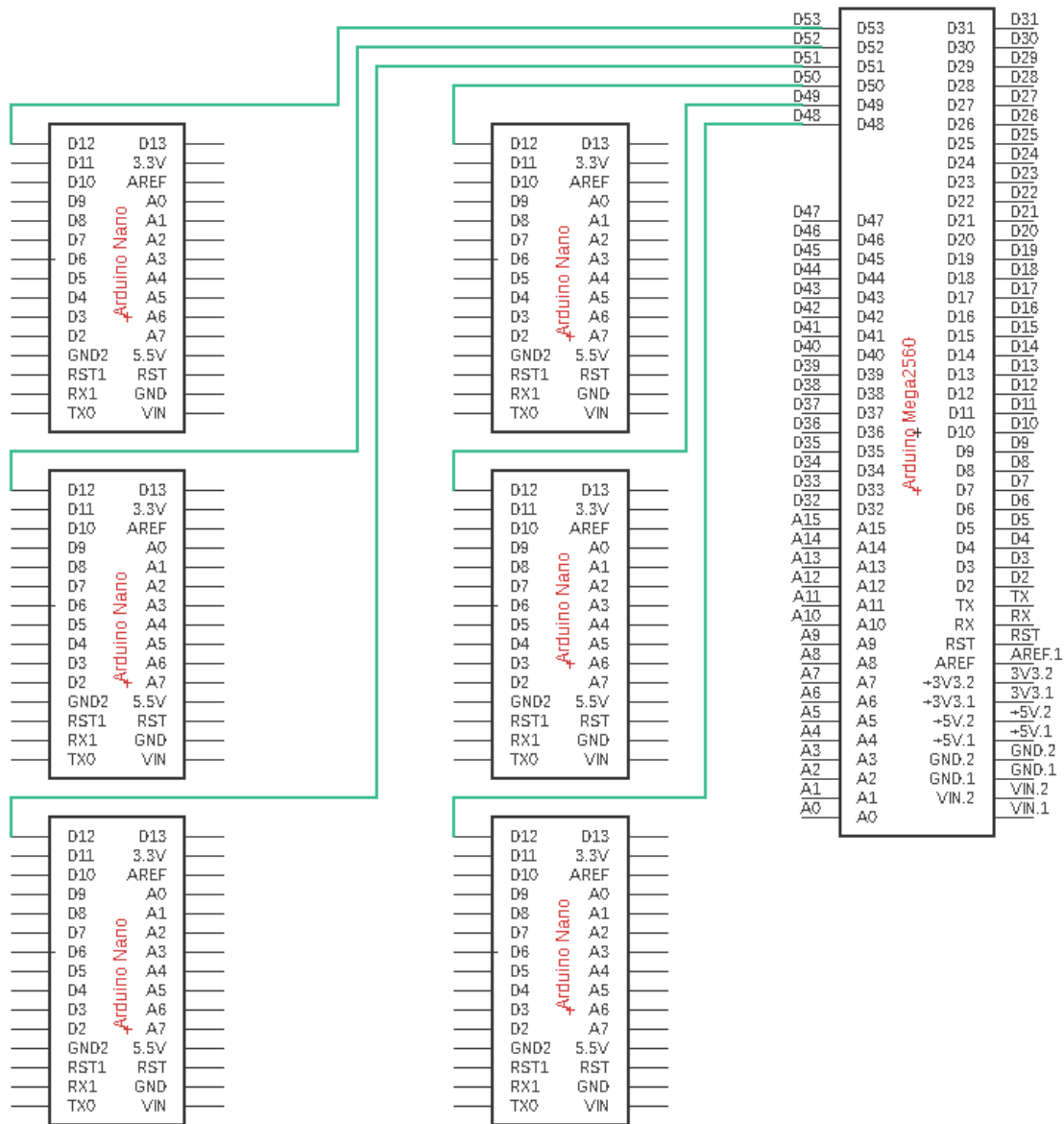


Figure N 12. Arduino Nano digital signal connections.

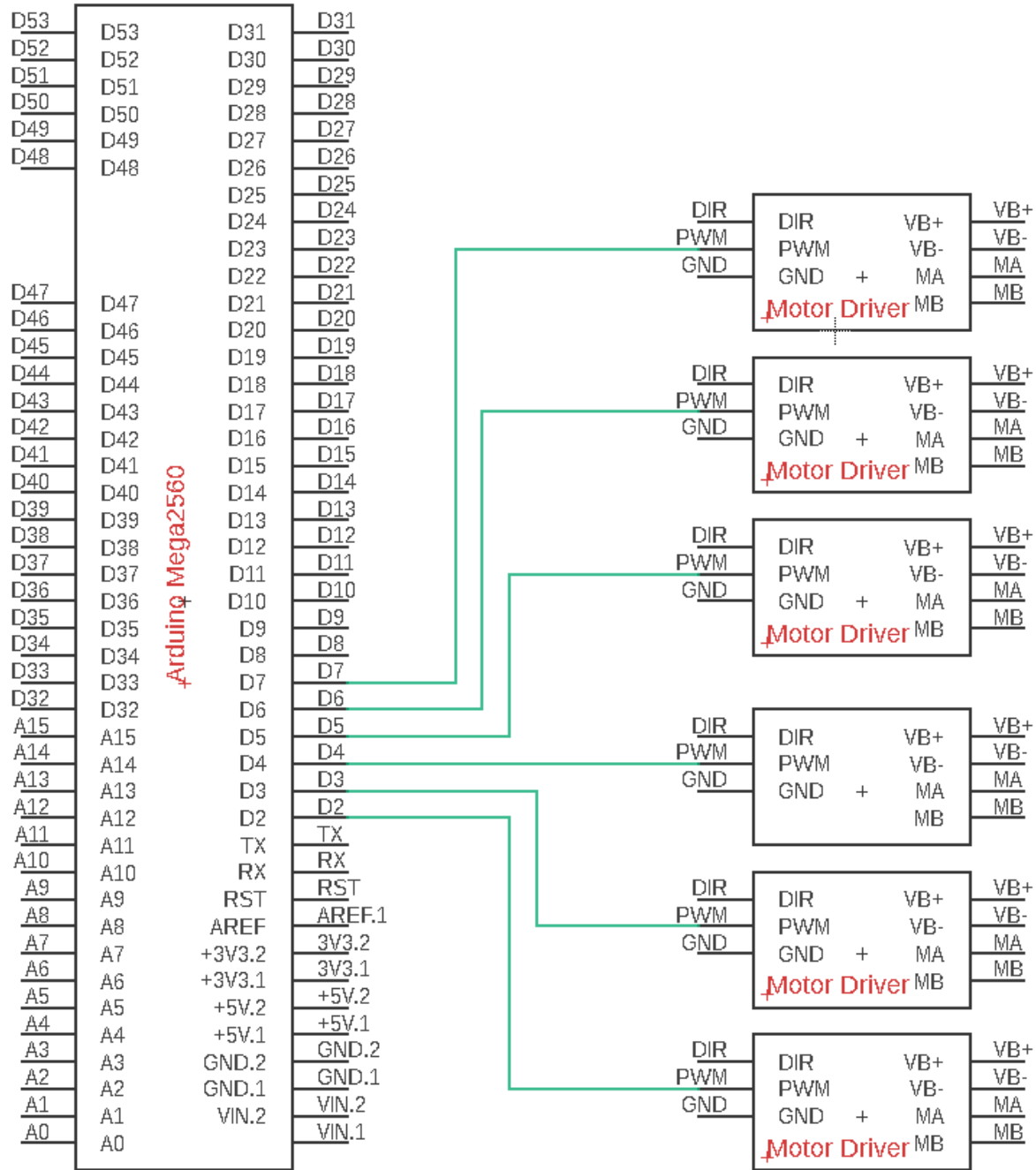


Figure N 13.Motor driver speed control digital connections.

## Appendix N.3

### Measured Hall Sensor Pulse Period

Shown below is the measured pulse period obtained from an oscilloscope to support the pulse period calculations.

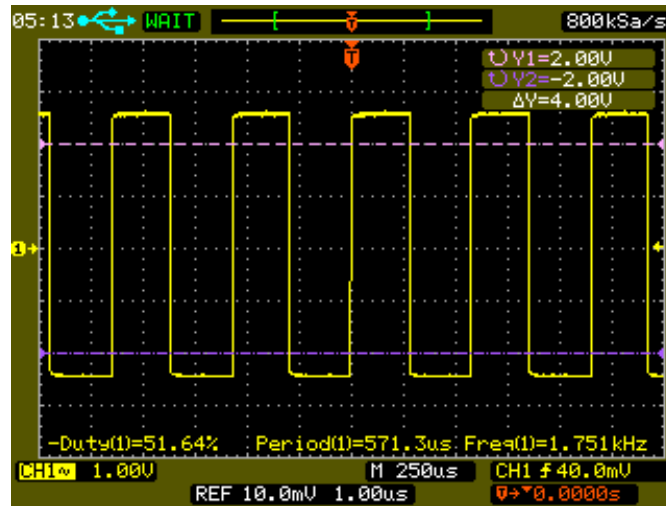


Figure N 14.Oscilloscope reading of sensor pulses at full speed.



## **Encoder Resolution**

Using the calculated pulses per second for one channel (25956 PPS), Equation (1) calculates the encoder resolution, or how many degrees one incoming pulse equals.

$$\frac{360^\circ}{25956} = 0.014^\circ \quad (1)$$

### **Encoder Pulse Digital Signals**

Each motor Hall encoder outputs a quadrature square wave pulse signal using both Channel A and Channel B. The quadrature resolution allows for each incoming encoder pulse to be approximately equivalent to  $0.0035^\circ$  of rotation. In this setup, only the pulse signal from Channel A on each Hall encoder is used as quadrature resolution is not required. Using only Channel A allows a sufficient resolution of each incoming pulse being approximately equivalent to  $0.014^\circ$  of rotation. Each Hall encoder Channel A is connected to each of the six Arduino Nano digital I/O pins. Each Arduino Nano records the number of incoming pulses and calculates the degree of rotation for each motor.

### **Motor Driver Speed Control Digital Signals**

On the Arduino Mega2560, digital I/O pins D2-D13 are PWM (pulse width modulation) pins. As a result, each motor driver's PWM input is connected to one of the D2-D7 pins. The motor driver PWM input is used for controlling the motor output speed from 0% to 100%.

## Appendix N.4

### Left Ankle Code

```
#include <CytronMotorDriver.h>
#include <digitalWriteFast.h>
#include <Wire.h>

int orig[] = {0, -7, 13, -11, 5};
volatile int deg[] = {0, 168, 481, 577, 385};
volatile int firstDeg = 120;
volatile int flagI = 0; // Flag for direction
volatile int flagM = 0; // Flag for motion
int runOnce = 0;
byte aL = 0;

//Pulse counter
volatile int pulse = 0;

void setup() {

  Serial.begin(9600);

  Wire.begin(2);
  pinModeFast(2, INPUT);

  pinModeFast(7, OUTPUT);
  digitalWriteFast(7, HIGH);
  pinModeFast(8, OUTPUT);
  digitalWriteFast(8, LOW);

  //Arduino Nano interrupt pins: 2,3
  attachInterrupt(digitalPinToInterrupt(2), ankleL, RISING);
}

void loop() {
  talk();
}

void ankleL()
{
  pulse = pulse + 1;

  if (pulse == deg[1] && flagM == 0) {
    UDR0 = 'A'; /// Load character into transmit buffer and transmit
                // Used for debugging
    pulse = 0;
    flagM = 1;
    flagI = 1;
    deg[1] = firstDeg;
  }
  if (pulse == deg[2] && flagM == 1) {
    UDR0 = 'B';
  }
}
```

```

    pulse = 0;
    flagM = 2;
    flagI = 0;
}

if (pulse == deg[3] && flagM == 2) {
    UDR0 = 'C';
    pulse = 0;
    flagM = 3;
    flagI = 1;
}

if (pulse == deg[4] && flagM == 3) {
    UDR0 = 'D';
    pulse = 0;
    flagM = 0;
    flagI = 0;
}
}

void talk() {
    if (flagI == 0) {
        UDR0 = 'T';
        aL = 0;
        Wire.write(aL); // Send signal to change direction
        Wire.endTransmission(1);
        flagI = 2;
    }

    if (flagI == 1) {
        aL = 1;
        Wire.beginTransaction(1);
        Wire.write(aL);
        Wire.endTransmission();
        flagI = 2;
    }
}
}

```

## Right Ankle Code

```
#include <CytronMotorDriver.h>
#include <digitalWriteFast.h>
#include <Wire.h>

int orig[] = {0, 5, -11, -13, -7};
volatile int deg[] = {0, 385, 577, 481, 168};
volatile int firstDeg = 168;
volatile int flagI = 0; // Flag for direction
volatile int flagM = 0; // Flag for motion
int runOnce = 0;
byte aR = 0;

//Pulse counter
volatile int pulse = 0;

void setup() {

  Serial.begin(9600);

  Wire.begin(2);
  pinModeFast(2, INPUT);

  pinModeFast(7, OUTPUT);
  digitalWriteFast(7, HIGH);
  pinModeFast(8, OUTPUT);
  digitalWriteFast(8, LOW);

  //Arduino Nano interrupt pins: 2,3
  attachInterrupt(digitalPinToInterrupt(2), ankleR, RISING);
}

void loop() {
  talk();
}

void ankleR()
{
  pulse = pulse + 1;

  if (pulse == deg[1] && flagM == 0) {
    UDR0 = 'A'; // Load character into transmit buffer and transmit
               // Used for debugging
    pulse = 0;
    flagM = 1;
    flagI = 1;
    deg[1] = firstDeg;
  }

  if (pulse == deg[2] && flagM == 1) {
    UDR0 = 'B';
    pulse = 0;
    flagM = 2;
  }
}
```

```

    flagI = 0;
}

if (pulse == deg[3] && flagM == 2) {
    UDR0 = 'C';
    pulse = 0;
    flagM = 3;
    flagI = 1;
}

if (pulse == deg[4] && flagM == 3) {
    UDR0 = 'D';
    pulse = 0;
    flagM = 0;
    flagI = 0;
}
}

void talk() {
    if (flagI == 0) {
        UDR0 = 'T';
        aR = 0;
        Wire.beginTransaction(1); // Open transmission with Mega
        Wire.write(aR); // Send signal to change direction
        Wire.endTransmission(1);
        flagI = 2;
    }

    if (flagI == 1) {
        aR = 1;
        Wire.beginTransaction(1);
        Wire.write(aR);
        Wire.endTransmission();
        flagI = 2;
    }
}
}

```

## Left Knee Code

```
#include <CytronMotorDriver.h>
#include <digitalWriteFast.h>
#include <Wire.h>

int orig[] = {0, 18, 2, 55, 4};
volatile int deg[] = {0, 433, 385, 1274, 1226};
volatile int firstDeg = 337;
volatile int flagI = 0; // Flag for direction
volatile int flagM = 0; // Flag for motion
int runOnce = 0;
byte kL = 0;

volatile int pulse = 0;

void setup() {

  Serial.begin(9600);

  Wire.begin(3);
  pinModeFast(2, INPUT);

  pinModeFast(7, OUTPUT);
  digitalWriteFast(7, HIGH);
  pinModeFast(8, OUTPUT);
  digitalWriteFast(8, LOW);

  //Arduino Nano interrupt pins: 2,3
  attachInterrupt(digitalPinToInterrupt(2), kneeL, RISING);
}

void loop() {
  talk();
}

void kneeL()
{
  pulse = pulse + 1;

  if (pulse == deg[1] && flagM == 0) {
    UDR0 = 'A'; // Load character into transmit buffer and transmit
               // Used for debugging
    pulse = 0;
    flagM = 1;
    flagI = 1;
    deg[1] = firstDeg = 337;
  }

  if (pulse == deg[2] && flagM == 1) {
    UDR0 = 'B';
    pulse = 0;
    flagM = 2;
    flagI = 0;
  }
}
```



```

}

if (pulse == deg[3] && flagM == 2) {
  UDR0 = 'C';
  pulse = 0;
  flagM = 3;
  flagI = 1;
}

if (pulse == deg[4] && flagM == 3) {
  UDR0 = 'D';
  pulse = 0;
  flagM = 0;
  flagI = 0;
}
}

void talk() {
  if (flagI == 0) {
    kL = 0;
    Wire.beginTransaction(1); // Open transmission with Mega
    Wire.write(kL); // Send signal to change direction
    Wire.endTransmission(1);
    flagI = 2;
  }

  if (flagI == 1) {
    kL = 1;
    Wire.beginTransaction(1);
    Wire.write(kL);
    Wire.endTransmission();
    flagI = 2;
  }
}
}

```

## **Right Knee Code**

```
#include <CytronMotorDriver.h>
#include <digitalWriteFast.h>
#include <Wire.h>

int orig[] = {0, 4, 55, 2, 8};
volatile int deg[] = {0, 1226, 1274, 385, 433};
volatile int firstDeg = 192;
volatile int flagI = 0; // Flag for direction
volatile int flagM = 0; // Flag for motion
int runOnce = 0;
byte kR = 0;

volatile int pulse = 0;

void setup() {

    Serial.begin(9600);

    Wire.begin(3);
    pinModeFast(2, INPUT);

    pinModeFast(7, OUTPUT);
    digitalWriteFast(7, HIGH);
    pinModeFast(8, OUTPUT);
    digitalWriteFast(8, LOW);

    //Arduino Nano interrupt pins: 2,3
    attachInterrupt(digitalPinToInterrupt(2), kneeR, RISING);
}

void loop() {
    talk();
}

void kneeR()
{
    pulse = pulse + 1;

    if (pulse == deg[1] && flagM == 0) {
        UDR0 = 'A'; // Load character into transmit buffer and transmit
        // Used for debugging
        pulse = 0;
        flagM = 1;
        flagI = 1;
        deg[1] = firstDeg;
    }

    if (pulse == deg[2] && flagM == 1) {
        UDR0 = 'B';
        pulse = 0;
        flagM = 2;
        flagI = 0;
    }
}
```

```

}

if (pulse == deg[3] && flagM == 2) {
  UDR0 = 'C';
  pulse = 0;
  flagM = 3;
  flagI = 1;
}

if (pulse == deg[4] && flagM == 3) {
  UDR0 = 'D';
  pulse = 0;
  flagM = 0;
  flagI = 0;
}
}

void talk() {
  if (flagI == 0) {
    kR = 0;
    Wire.beginTransaction(1); // Open transmission with Mega
    Wire.write(kR); // Send signal to change direction
    Wire.endTransmission(1);
    flagI = 2;
  }

  if (flagI == 1) {
    kR = 1;
    Wire.beginTransaction(1);
    Wire.write(kR);
    Wire.endTransmission();
    flagI = 2;
  }
}
}

```

## Left Hip Code

```
#include <CytronMotorDriver.h>
#include <digitalWriteFast.h>
#include <Wire.h>

int orig[] = {0, 25, -15, 25, -15};
volatile int deg[] = {0, 601, 961, 961, 961};
volatile int firstDeg = 961;
volatile int flagI = 0; // Flag for direction
volatile int flagM = 0; // Flag for motion
int runOnce = 0;
byte hL = 0;

volatile int pulse = 0;

void setup() {

    Serial.begin(9600);

    Wire.begin(2);
    pinModeFast(2, INPUT);

    pinModeFast(7, OUTPUT);
    digitalWriteFast(7, HIGH);
    pinModeFast(8, OUTPUT);
    digitalWriteFast(8, LOW);

    //Arduino Nano interrupt pins: 2,3
    attachInterrupt(digitalPinToInterrupt(2), hipL, RISING);
}

void loop() {
    talk();
}

void hipL()
{
    pulse = pulse + 1;

    if (pulse == deg[1] && flagM == 0) {
        UDR0 = 'A'; // Load character into transmit buffer and transmit
        // Used for debugging
        pulse = 0;
        flagM = 1;
        flagI = 1;
        deg[1] = firstDeg;
    }

    if (pulse == deg[2] && flagM == 1) {
        UDR0 = 'B';
        pulse = 0;
        flagM = 2;
        flagI = 0;
    }
}
```

```

}

if (pulse == deg[3] && flagM == 2) {
  UDR0 = 'C';
  pulse = 0;
  flagM = 3;
  flagI = 1;
}

if (pulse == deg[4] && flagM == 3) {
  UDR0 = 'D';
  pulse = 0;
  flagM = 0;
  flagI = 0;
}
}

void talk() {
  if (flagI == 0) {
    UDR0 = 'T';
    hL = 0;
    Wire.beginTransaction(1); // Open transmission with Mega
    Wire.write(hL); // Send signal to change direction
    Wire.endTransmission(1);
    flagI = 2;
  }

  if (flagI == 1) {
    hL = 1;
    Wire.beginTransaction(1);
    Wire.write(hL);
    Wire.endTransmission();
    flagI = 2;
  }
}
}

```

## Right Hip Code

```
#include <CytronMotorDriver.h>
#include <digitalWriteFast.h>
#include <Wire.h>

int orig[] = {0, -15, 25, -15, 25};
volatile int deg[] = {0, 361, 961, 961, 961};
volatile int firstDeg = 961;
volatile int flagI = 0; // Flag for direction
volatile int flagM = 0; // Flag for motion
int runOnce = 0;
byte hR = 0;

//Pulse counter for AnkleR
volatile int pulse = 0;

void setup() {

  Serial.begin(9600);

  Wire.begin(2);
  pinModeFast(2, INPUT);

  pinModeFast(7, OUTPUT);
  digitalWriteFast(7, HIGH);
  pinModeFast(8, OUTPUT);
  digitalWriteFast(8, LOW);

  //Arduino Nano interrupt pins: 2,3
  attachInterrupt(digitalPinToInterrupt(2), hipR, RISING);
}

void loop() {
  talk();
}

void hipR()
{
  pulse = pulse + 1;

  if (pulse == deg[1] && flagM == 0) {
    UDR0 = 'A'; // Load character into transmit buffer and transmit
               // Used for debugging
    pulse = 0;
    flagM = 1;
    flagI = 1;
    deg[1] = firstDeg;
  }

  if (pulse == deg[2] && flagM == 1) {
    UDR0 = 'B';
    pulse = 0;
    flagM = 2;
  }
}
```

```

    flagI = 0;
}

if (pulse == deg[3] && flagM == 2) {
    UDR0 = 'C';
    pulse = 0;
    flagM = 3;
    flagI = 1;
}

if (pulse == deg[4] && flagM == 3) {
    UDR0 = 'D';
    pulse = 0;
    flagM = 0;
    flagI = 0;
}
}

void talk() {
    if (flagI == 0) {
        UDR0 = 'T';
        hR = 0;
        Wire.beginTransaction(1); // Open transmission with Mega
        Wire.write(hR); // Send signal to change direction
        Wire.endTransmission(1);
        flagI = 2;
    }

    if (flagI == 1) {
        hR = 1;
        Wire.beginTransaction(1);
        Wire.write(hR);
        Wire.endTransmission();
        flagI = 2;
    }
}
}

```

## Arduino Mega Gait Code

```
#include <CytronMotorDriver.h>
#include <digitalWriteFast.h>
#include <Wire.h>

int orig[] = {0, -15, 25, -15, 25};
volatile int deg[] = {0, 361, 961, 961, 961};
volatile int firstDeg = 961;
volatile int flagI = 0; // Flag for direction
volatile int flagM = 0; // Flag for motion
int runOnce = 0;
byte hR = 0;

//Pulse counter for AnkleR
volatile int pulse = 0;

void setup() {

  Serial.begin(9600);

  Wire.begin(2);
  pinModeFast(2, INPUT);

  pinModeFast(7, OUTPUT);
  digitalWriteFast(7, HIGH);
  pinModeFast(8, OUTPUT);
  digitalWriteFast(8, LOW);

  //Arduino Nano interrupt pins: 2,3
  attachInterrupt(digitalPinToInterrupt(2), hipR, RISING);
}

void loop() {
  talk();
}

void hipR()
{
  pulse = pulse + 1;

  if (pulse == deg[1] && flagM == 0) {
    UDR0 = 'A'; // Load character into transmit buffer and transmit
               // Used for debugging
    pulse = 0;
    flagM = 1;
    flagI = 1;
    deg[1] = firstDeg;
  }

  if (pulse == deg[2] && flagM == 1) {
    UDR0 = 'B';
    pulse = 0;
    flagM = 2;
  }
}
```



```

    flagI = 0;
}

if (pulse == deg[3] && flagM == 2) {
    UDR0 = 'C';
    pulse = 0;
    flagM = 3;
    flagI = 1;
}

if (pulse == deg[4] && flagM == 3) {
    UDR0 = 'D';
    pulse = 0;
    flagM = 0;
    flagI = 0;
}
}

void talk() {
    if (flagI == 0) {
        UDR0 = 'T';
        hR = 0;
        Wire.beginTransaction(1); // Open transmission with Mega
        Wire.write(hR); // Send signal to change direction
        Wire.endTransmission(1);
        flagI = 2;
    }

    if (flagI == 1) {
        hR = 1;
        Wire.beginTransaction(1);
        Wire.write(hR);
        Wire.endTransmission();
        flagI = 2;
    }
}
}

```

## Appendix O

### Senior Design Project II MENG 4216 / EENG 4315 Project RWTD Delivery and Acceptance

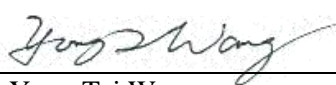
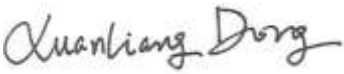

Senior design team Robotic Walking Training Device from UT-Tyler College of Engineering, has worked with a sponsor: Dr. Yong Tai Wang and Dr. X Neil Dong to deliver simulations to demonstrate the functionality and feasibility of the Robotic Walking Training Device part of the senior students' academic work during the academic year of 2019-2020. This document includes the sign-off list and Dr. Yong Tai Wang and Dr. X Neil Dong final approval of the outcome of RWTD delivered by Tyler Team 4, based on the previously set and mutually approved scope and specifications of the project. An authorized signature indicates this approval.

**Table 1: Sponsor Sign OFF list for Deliverables of the Senior Project Robotic Walking Training Device**

<b>Item No.</b>	<b>Description of Deliverable</b>	<b>Comments:</b>	<b>Sponsor Sign Off: Authorized Initials</b>
<i>Motors</i>	12 RPM HD Premium Planetary Gear Motors with Encoder (6x)		TW/ND
<i>Linear Actuator</i>	FA-400-12-2" – P Premium 2" Stroke 400 lb.		TW/ND
<i>T-Slot</i>	T-slots to allow for arm support movement (2x)		TW/ND
<i>Leg assembly</i>	Leg assembly manufactured out of 6061 Aluminum		TW/ND
<i>Base</i>	A36 Steel Plate (1x)		TW/ND
<i>Electrical</i>	Arduino Nanos (6x) Arduino Mega (1x)		TW/ND

<b>Production Model Documentation</b>	<b>Technical Documentation</b>	<b>Comments:</b>	<b>Sponsor Sign Off: Authorized Initials</b>
<i>B.O.M.</i>	Bill of Materials		TW/ND
<i>User Manual</i>	Operations, Safety and Parts List		TW/ND
<i>Mechanical Drawings</i>	Mechanical drawings of manufactured pieces		TW/ND
<i>Electrical Schematic</i>	Electrical Wiring Diagrams		TW/ND
<i>Code</i>	Programming code of the leg motion		TW/ND
<b>Simulations</b>	Simulation of system		TW/ND
<i>FEA of Scissor Lift</i>	FEA of factor of safety, maximum deformation and shear	Final deliverable due to COVID 19	TW/ND
<i>FEA of Pivot Pins</i>	FEA of factor of safety, maximum deformation and shear	Final deliverable due to COVID 19	TW/ND
<i>FEA of Leg Assembly</i>	FEA of factor of safety, maximum deformation and shear	Final deliverable due to COVID 19	TW/ND
<i>Path motion of the leg assembly</i>	Gait path motion of the knee and ankle	Final deliverable due to COVID 19	TW/ND

The following signatures indicate that Dr. Yong Tai Wang and Dr. X Neil Dong approves of the completion of this project and deliverables stated above which included all sponsor changes from original design and any consequent changes in the project, as mutually approved by all signing parties. Also indicated is the acknowledgement by Dr. Yong Tai Wang and Dr. X Neil Dong of reception of the final product of the project.

Dr. Chung Hyun Goh	Date
	04/17/2020
Dr. Yong Tai Wang	Date
	4/17/2020
Dr. X. Neil Dong	Date
	04/17/2020
Senior Project Students' Team: TYL 4 <i>Team Captain: N. Ryley Tharp</i>	Date

## Appendix P

This appendix contains the Gantt charts of both the first and second semester of the project. These Gantt charts were made at the beginning of the first semester for Figure R.2 and the end of the Fall semester for Figure R.3. In Figure R.3 it can be seen that many items are marked with the COVID-19 color key. Due to the pandemic the team was unable to complete many items due to stay-at-home orders and concern for health and safety. Since this was created before the semester started the team deviated from the scheduled plan to meet other specifications agreed upon between the sponsors and the team.

	Done
	IP
	Scheduled
	At Risk
	Failed
	COVID-19

Figure R 1. Color Coded Key for Gantt Charts.

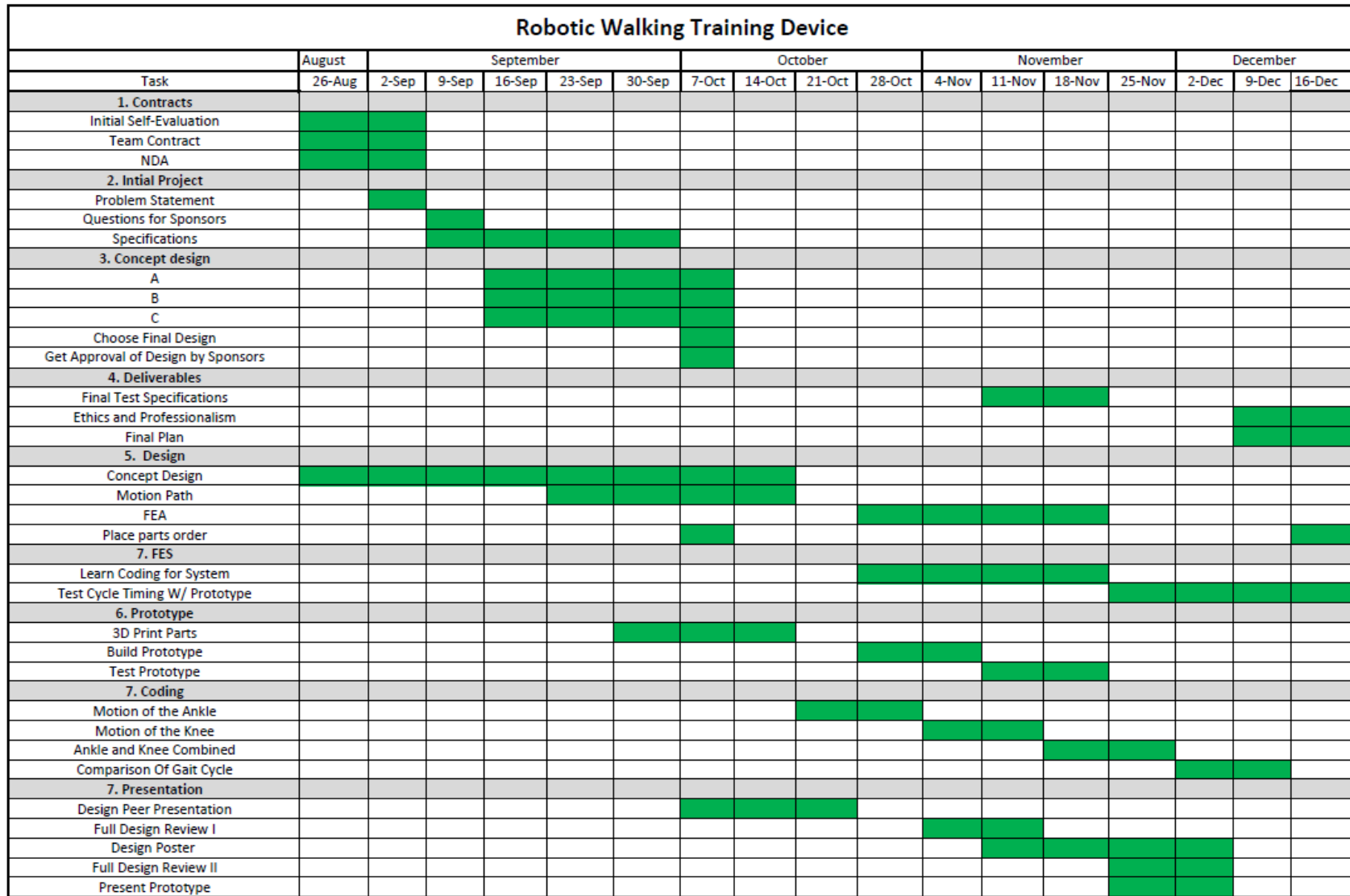


Figure R 2. Gantt Chart for the Fall Semester.

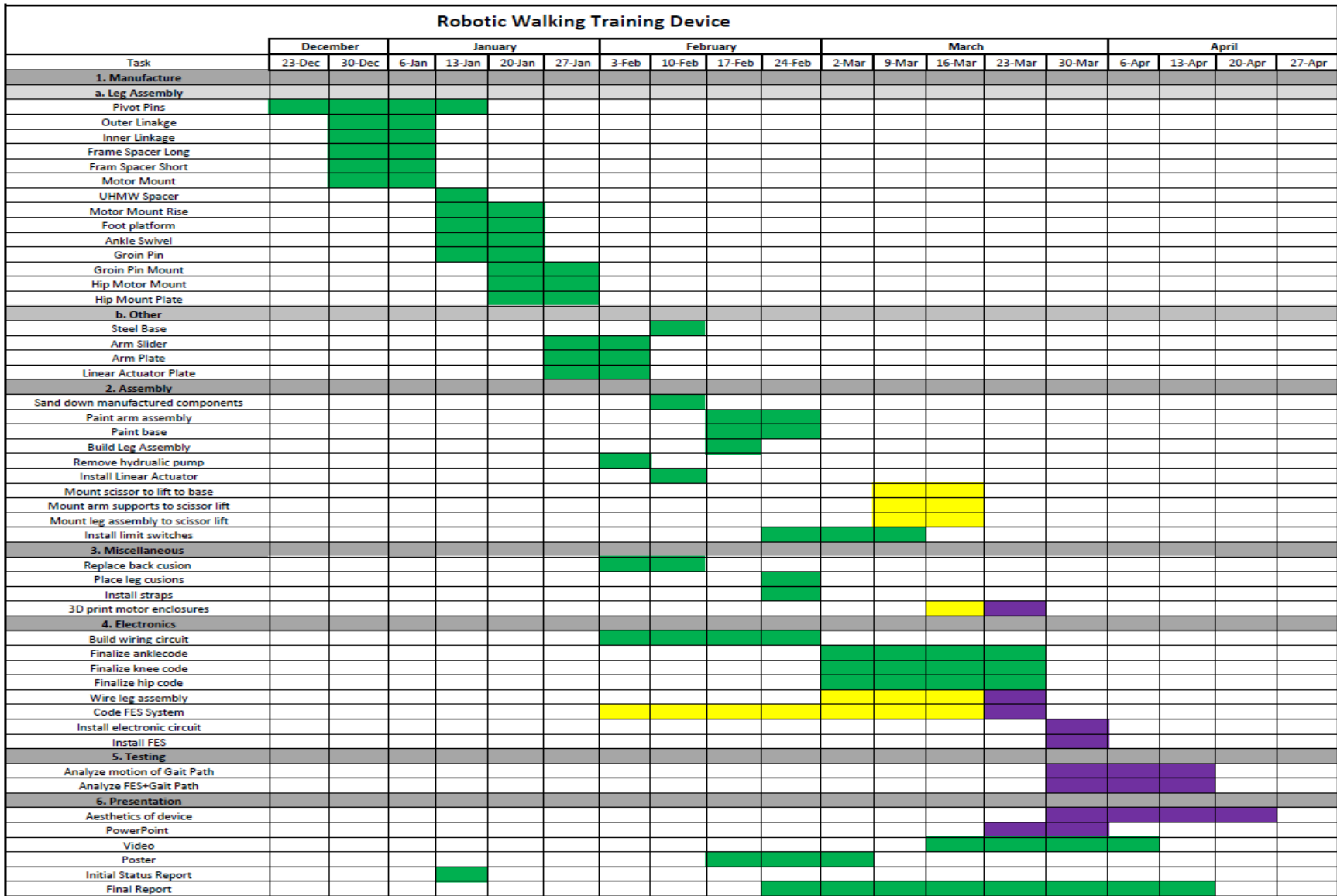


Figure R 3. Gantt Chart for the Spring Semester.

The ARCI Chart was developed to show who was responsible, accountable, consulted and informed.

R=Responsible, A=Accountable, C=Consulted, I=Informed

Table R 1. ARCI Chart for RWTD.

Task	William	Alex	Heather	Ryley	Chris
Problem Statement	C	A	C	R	C
Questions for Sponsors	C	A	C	R	A
Specifications	C	R	C	A	C
Concept Design A	R	I	I	A	I
Concept Design B	A	I	I	I	R
Concept Design C	I	A	I	I	R
Final Design	C	A	C	R	C
Approval of Final Design from Sponsors	A	I	I	R	I
Motion Path generated in Solidworks	I	C	I	A	R
FEA of Key Components	R	C	I	A	C
Place Parts Order	I	A	I	R	I
3D Print parts	C	I	I	R	A
Build Prototype	A	I	I	I	R
Test Prototype	A	C	R	C	C
Code Motion of the Ankle	C	C	R	A	I
Code Motion of the Knee	C	A	R	C	I
Code Motion of the Hip	A	I	R	I	C
Comparison of Gait Cycle	C	R	A	C	C
Manufacture Components	C	C	I	A	R
Sand manufactured components	R	C	I	A	C
Paint Components	C	R	I	A	I
Build Leg Assembly	A	C	I	C	R



Task	William	Alex	Heather	Ryley	Chris
Remove hydraulic pump	A	C	I	R	C
Install linear actuator	A	C	I	R	C
Mount scissor lift to base	A	C	I	C	R
Mount Arm Support to Scissor Lift	C	C	I	R	A
Mount leg assembly to Scissor Lift	R	C	I	A	C
Install Limit Switches	A	C	C	C	R
Replace back cushion	A	C	I	R	I
Place leg cushion	A	I	C	R	I
Install Straps	C	A	I	R	I
3D print motor enclosures	R	A	C	C	C
Build wiring circuit	I	I	R	A	I
Wire leg assembly	C	C	R	A	C
Code FES system	C	C	R	A	I
Install electronic circuit	A	I	R	I	I
Install FES	C	A	R	C	C
Analyze motion gait path	C	A	R	C	C
Analyze FES+Gait Path	C	A	R	C	C

## Appendix Q

The motors were tested to demonstrate that the motors performed to the necessary expectations. The motor was hooked up to oscilloscope and ran at different powers. At 25% the oscilloscope showed that the motor ran at 3 RPM as seen in Figure Q.1 At 50%, 75% and 100% the oscilloscope showed that the motors ran at 6, 9 and 12 RPM as shown in Figure Q.2- Q.4 respectively.

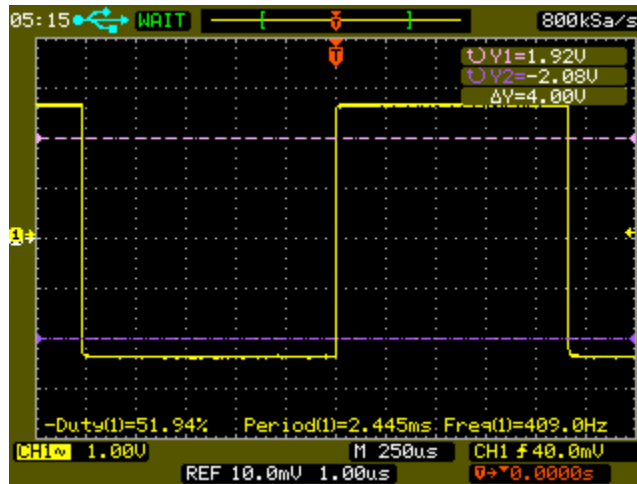


Figure Q 1. Oscilloscope showing the Motor Running at 25%.

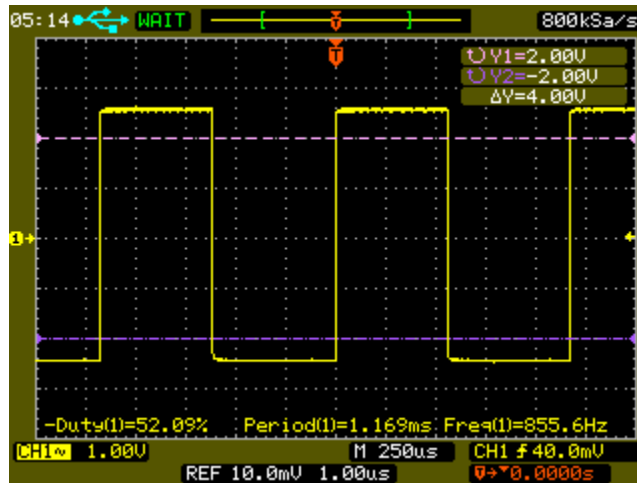


Figure Q 2. Oscilloscope showing the Motor Running at 50%.

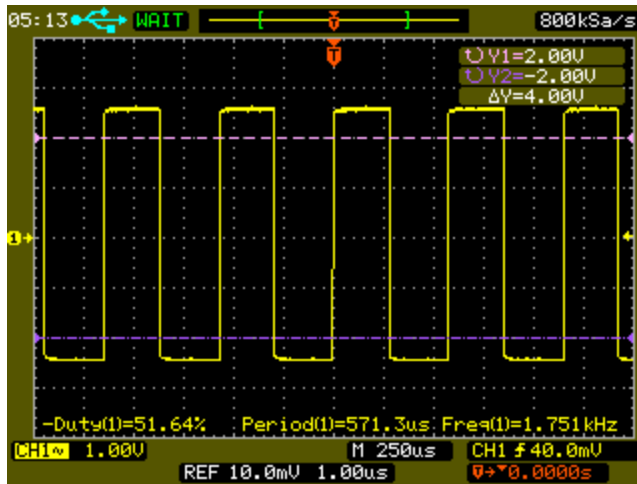


Figure Q 3. Oscpe showing the Motor Running at 75%.

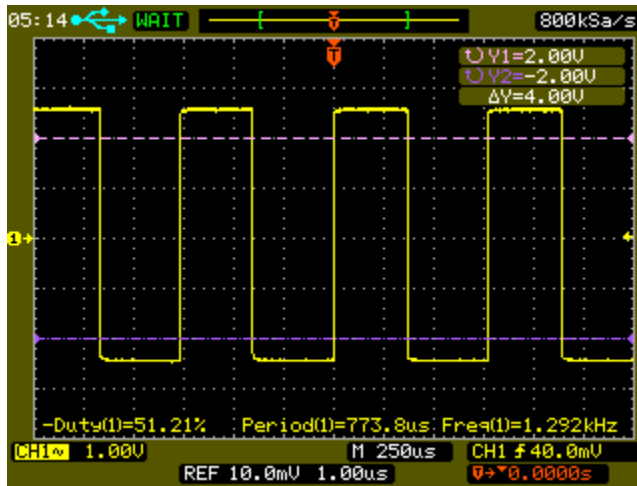


Figure Q 4. Oscpe showing the Motor Running a

# Appendix R

### Robotic Walking Training Device

Team Members: William Clinton, Alex Craig, Heather McIntyre, Ryley Tharp, Chris Whitton  
Sponsor: Department of Nursing and Health Sciences and Department of Health and Kinesiology at UT Tyler  
Advisor: Dr. Chung Hyun Goh

#### Abstract

Partial paralysis caused by spinal cord injury (SCI) or stroke are two of the most prevalent forms of physical disability. It is estimated between 232,000 to 316,000 people have a SCI, and approximately 795,000 people have a new or recurrent stroke annually. More than 50% of stroke victims have difficulty walking, and greater than 90% of SCI patients lose sensory and motor control of their lower limbs. The goal of the Robotic Walking Training device is to build and optimize a training device that can accurately recreate the motion of a gait path. It will also incorporate the use of a Functional Electrical Stimulation to allow for more efficient and effective retraining of neural pathways. To recreate the gait paths, data was collected of a natural walking gait path. The use of FES will be used in sync with the gait cycle to stimulate the muscle at the appropriate timing.

#### Background

Due to patients losing their sensory and motor control when they have injuries, such as SCI or strokes. To help patients who have these disabilities regain the function of walking unassisted, gait rehabilitation is performed.

To also aid in rehabilitation FES device can also be used. A FES is a device that applies small electrical pulses to the muscles in the lower extremities that are affected by injuries to restore or improve muscular function. By applying these small electrical pulses, the pathways that have been disrupted or broken can be re-written allowing for the patient to use their muscles as they did before the injury occurred.

#### Specifications and Design Constraints

##### Specifications

- Reproduce natural gait motion path of knee and ankle.
- Adjustable for varying leg lengths up to 6'4" patients.
- Electro-stimulate thigh muscle in time with the walking motion.
- Able to hold various body types, up to 300 lbs.

##### Design Constraints

- \$2000 budget.
- Fulfill the needs and satisfy the customer.
- Ensure that the required resources, such as tools, materials and parts, are available to construct the RWTD.
- Simulations to prove that specifications are met using the designed system

#### Design and Approach

The RWTD will have 4 main components as seen in Figure 1.

1. Scissor Lift - Provides the vertical motion necessary to raise the patient.
2. Arm Supports - Adjustable for each patient and fold down allowing for the patient to get in the device with ease
3. Leg Assembly - Provides the necessary motion to accurately recreate the gait motion path, using 6 motors, one at each joint: hip, knee and ankle. The leg assembly is adjustable for patients of different heights
4. FES System - Will be used in conjunction with the motion of the legs. The thigh muscle will be stimulated in time with the motion to optimize rehabilitation



Figure 1. RWTD showing the 4 main components of the project.

#### Results and Discussion

The selected concept was the motor driven linkages. Utilizing 6 motors, one at each joint, an accurate gait motion path can be generated. The linkages will be constructed from 6061 Aluminum since it is durable and relatively easy to machine. The pivot pin will be manufactured out of cold-rolled steel since it will need to endure high torque being applied. Lastly, the motors were chosen due to the amount of torque that will need to be applied at both hip motors.

The pulse chosen for the FES was high-voltage pulsed stimulation. This pulse was chosen for its indicators in patients. These include but are not limited to; reeducation of peripheral nerves, delay of denervation, and disuse atrophy by stimulating muscle contractions and restoring range motion. The FES will use 0.500 mA for a treatment duration of 15-30 minutes to aid in the rehabilitation process

#### Upgrades Made to the System

##### Upgrades made from the 2<sup>nd</sup> Generation

- Leg Assembly components machined from Aluminum 6061
- Joint Pins machined from Cold-Rolled 1020 Steel
- Redesigned base fabricated from A36 Steel Plate
- Adjustable arm supports for patient stability and comfort
- Memory foam padding for patient comfort
- Linear actuator that allows smooth transition to upright position
- Planetary gear driven DC motors for each leg joint for customizing degree of motion

#### Conclusion

The goal for this project is to design and optimize a device to assist patients in recreating a natural walking gait while simultaneously applying stimulation with a Functional Electronic Stimulator in order to more efficiently and effectively retrain the neural pathways. The chosen design utilizes 6 motors, located at each joint, to recreate the gait motion path through a programmed pathway. An electrode of the FES will be attached to the thigh muscle to stimulate the muscle while a step is being taken, thus retraining the neural pathways.

Analysis was completed to determine the materials needed to construct the device. Analysis was also performed to determine the stability of the device when in use, the maximum amount of torque and the shearing on the pivot pin in the hip joint.

Lastly, simulations were performed to prove that the design choice for the project would meet specifications if the manufacturing could be completed. Simulations proved that the leg assembly would move in correct path without any interference. The scissor lift could be raised and lowered without failing. The arm supports would not fail during the use of the device.

#### Acknowledgements

The members of the Tyler Team 4 would like to thank Dr. Yong Tai Wang and Dr. X. Neil Dong for their support as sponsors and for their input and ideas on the designing of this project. We would also like to thank Dr. Chung Hyun Goh for being our advisor and guiding us in the right direction, providing valuable feedback and expertise. Lastly, we would like to thank Ed Farina for all the help and advice given when we were working in the Fabrication Lab.

Figure R 4. RWTD Poster.